

UNCLASSIFIED

AD NUMBER
ADB242387
NEW LIMITATION CHANGE
TO Approved for public release, distribution unlimited
FROM Distribution authorized to U.S. Gov't. agencies only; Proprietary Info; Oct 98 Other requests shall be referred to USAMRMC, Fort Detrick, MD 21702-5012
AUTHORITY
USAMRMC ltr, 1 Jun 2001.

THIS PAGE IS UNCLASSIFIED

AD _____

CONTRACT NUMBER DAMD17-95-C-5078

TITLE: A Spine Loading Model of Women in the Military

PRINCIPAL INVESTIGATOR: William S. Marras, Ph.D.

CONTRACTING ORGANIZATION: Ohio State University
Columbus, Ohio 43210-1063

REPORT DATE: October 1998

TYPE OF REPORT: Annual

PREPARED FOR: Commander
U.S. Army Medical Research and Materiel Command
Fort Detrick, Frederick, Maryland 21702-5012

DISTRIBUTION STATEMENT: Distribution authorized to U.S. Government agencies only (proprietary information, Oct 98). Other requests for this document shall be referred to U.S. Army Medical Research and Materiel Command, 504 Scott Street, Fort Detrick, Maryland 21702-5012.

The views, opinions and/or findings contained in this report are those of the author(s) and should not be construed as an official Department of the Army position, policy or decision unless so designated by other documentation.

DTIC QUALITY INSPECTED 4

NOTICE

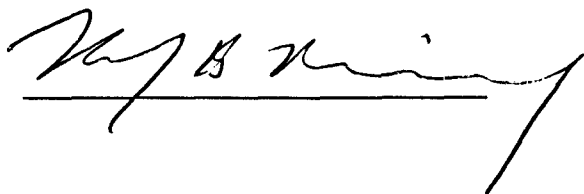
USING GOVERNMENT DRAWINGS, SPECIFICATIONS, OR OTHER DATA INCLUDED IN THIS DOCUMENT FOR ANY PURPOSE OTHER THAN GOVERNMENT PROCUREMENT DOES NOT IN ANY WAY OBLIGATE THE U.S. GOVERNMENT. THE FACT THAT THE GOVERNMENT FORMULATED OR SUPPLIED THE DRAWINGS, SPECIFICATIONS, OR OTHER DATA DOES NOT LICENSE THE HOLDER OR ANY OTHER PERSON OR CORPORATION; OR CONVEY ANY RIGHTS OR PERMISSION TO MANUFACTURE, USE, OR SELL ANY PATENTED INVENTION THAT MAY RELATE TO THEM.

LIMITED RIGHTS LEGEND

Award Number: DAMD17-95-C-5078
Organization: Ohio State University
Location of Limited Rights Data (Pages):

Those portions of the technical data contained in this report marked as limited rights data shall not, without the written permission of the above contractor, be (a) released or disclosed outside the government, (b) used by the Government for manufacture or, in the case of computer software documentation, for preparing the same or similar computer software, or (c) used by a party other than the Government, except that the Government may release or disclose technical data to persons outside the Government, or permit the use of technical data by such persons, if (i) such release, disclosure, or use is necessary for emergency repair or overhaul or (ii) is a release or disclosure of technical data (other than detailed manufacturing or process data) to, or use of such data by, a foreign government that is in the interest of the Government and is required for evaluational or informational purposes, provided in either case that such release, disclosure or use is made subject to a prohibition that the person to whom the data is released or disclosed may not further use, release or disclose such data, and the contractor or subcontractor or subcontractor asserting the restriction is notified of such release, disclosure or use. This legend, together with the indications of the portions of this data which are subject to such limitations, shall be included on any reproduction hereof which includes any part of the portions subject to such limitations.

THIS TECHNICAL REPORT HAS BEEN REVIEWED AND IS APPROVED FOR PUBLICATION.



Public reporting burden for this collection of information is estimated to average 1 hour per response, including the time for reviewing instructions, searching existing data sources, gathering and maintaining the data needed, and completing and reviewing the collection of information. Send comments regarding this burden estimate or any other aspect of this collection of information, including suggestions for reducing this burden, to Washington Headquarters Services, Directorate for Information Operations and Reports, 1215 Jefferson Davis Highway, Suite 1204, Arlington, VA 22202-4302, and to the Office of Management and Budget, Paperwork Reduction Project (0704-0188), Washington, DC 20503.

1. AGENCY USE ONLY (Leave blank)	2. REPORT DATE October 1998	3. REPORT TYPE AND DATES COVERED Annual (25 Sep 97 - 24 Sep 98)	
4. TITLE AND SUBTITLE A Spine Loading Model of Women in the Military		5. FUNDING NUMBERS DAMD17-95-C-5078	
6. AUTHOR(S) William S. Marras, Ph.D.			
7. PERFORMING ORGANIZATION NAME(S) AND ADDRESS(ES) Ohio State University Columbus, Ohio 43210-1063		8. PERFORMING ORGANIZATION REPORT NUMBER	
9. SPONSORING/MONITORING AGENCY NAME(S) AND ADDRESS(ES) Commander U.S. Army Medical Research and Materiel Command Fort Detrick, Frederick, MD 21702-5012		10. SPONSORING/MONITORING AGENCY REPORT NUMBER	
11. SUPPLEMENTARY NOTES		19990318 076	
12a. DISTRIBUTION / AVAILABILITY STATEMENT Distribution authorized to U.S. Government agencies only (proprietary information, Oct 98). Other requests for this document shall be referred to U.S. Army Medical Research and Materiel Command, 504 Scott Street, Fort Detrick, Maryland 21702-5012.		12b. DISTRIBUTION CODE	
13. ABSTRACT (Maximum 200) <p>The risk of low-back disorders (LBD) may be particularly great for women in the military, influencing training effectiveness, costs, and military readiness. The goal of this research is to quantify musculoskeletal loads on the spine of women performing military manual materials handling (MMH) tasks. This will permit assessment of LBD risk factors for military women, and the potential to evaluate tasks and training methods for female military personnel.</p> <p>Our efforts are progressing in general accordance with the proposal and timeline. Magnetic Resonance Images (MRI) have been employed to measure the muscle cross-sectional areas, moment-arms in the coronal and sagittal plane, and muscle vector angles in both healthy females and males. Muscle force-velocity and length-strength relationships have been determined with biomechanical model performance determined, with a few more subjected needed to be collected to solidify the promising results. Validation of the biomechanical model using the relationships determined from muscle geometry and force-velocity and length-strength relationships, as well as comparison of spinal loading between males and females performing the same MMH tasks is almost complete. Validation efforts indicate that the female-specific biomechanical model performs very well in predicting spinal loading on the female spine.</p> <p>After the third year of this research effort, we are progressing well and are confident that an accurate biomechanical model can be developed for the evaluation of spinal loading of women performing military MMH tasks.</p>			
14. SUBJECT TERMS Defense Women's Health Research Program		15. NUMBER 193	
		16. PRICE CODE	
17. SECURITY CLASSIFICATION OF REPORT Unclassified	18. SECURITY CLASSIFICATION OF THIS PAGE Unclassified	19. SECURITY CLASSIFICATION OF ABSTRACT Unclassified	20. LIMITATION OF ABSTRACT Limited

FOREWORD

Opinions, interpretations, conclusions and recommendations are those of the author and are not necessarily endorsed by the U.S. Army.

____ Where copyrighted material is quoted, permission has been obtained to use such material.

____ Where material from documents designated for limited distribution is quoted, permission has been obtained to use the material.

____ Citations of commercial organizations and trade names in this report do not constitute an official Department of Army endorsement or approval of the products or services of these organizations.

____ In conducting research using animals, the investigator(s) adhered to the "Guide for the Care and Use of Laboratory Animals," prepared by the Committee on Care and use of Laboratory Animals of the Institute of Laboratory Resources, national Research Council (NIH Publication No. 86-23, Revised 1985).

✓ ____ For the protection of human subjects, the investigator(s) adhered to policies of applicable Federal Law 45 CFR 46.

____ In conducting research utilizing recombinant DNA technology, the investigator(s) adhered to current guidelines promulgated by the National Institutes of Health.

____ In the conduct of research utilizing recombinant DNA, the investigator(s) adhered to the NIH Guidelines for Research Involving Recombinant DNA Molecules.

____ In the conduct of research involving hazardous organisms, the investigator(s) adhered to the CDC-NIH Guide for Biosafety in Microbiological and Biomedical Laboratories.


PI - Signature

10/22/98
Date

MEMORANDUM OF PROPRIETARY DATA

This progress report contains proprietary and unpublished data for use by the Biodynamics Laboratory, The Ohio State University. Tables 1.2 through 4.4 and equations 1.1 through 2.10 express data describing research results from the Biodynamics Laboratory. These data are still under development, and represent scientific efforts in progress. These data are provided in this annual progress report solely for the demonstration of scientific research progress as per the funding requirements.

We request the distribution of the proprietary portions of this report be limited. We request that the data not be released to the public until these results have been published in the appropriate peer reviewed scientific journals.

William S. Marras,



Director
Biodynamics Laboratory
The Ohio State University

EXECUTIVE SUMMARY

Low back injuries in female military personnel can significantly impact training effectiveness, costs and military readiness. Low back injuries accounted for 75% of compensable military injuries in 1988 through 1991 (Army Safety Center, 1992). When one considers that women have significantly higher incidence of lost time injuries during basic training than men (Jones et al., 1988), it is apparent that the risk of work related low back disorders (LBD) may be particularly great for women in the military. Heavy manual materials handling (MMH) that would challenge the injury tolerance of most industrial workers' spines has been shown to be the most physically demanding task in 90% of all military job specialties (Sharp and Vogel, 1992). As these military occupational specialties (MOSs) are becoming increasingly available to women, the risk of LBD to women will have greater consequences as they fill these roles, particularly when considering a downsizing military. Thus, there is a need to reliably assess the risk of military task related LBD to women, and to identify potential features or training that might mitigate that risk.

The goal of this research is to extend the capability of predicting musculoskeletal loads on the trunk and spine to women performing realistic MMH tasks. Current models of musculoskeletal loading on the spine are based upon male biomechanics, and must be enhanced to account for the anatomical geometry and physiology of the female musculoskeletal torso. This will permit accurate evaluation of the spinal loads in women as they perform military MMH activities, and the potential to assess the relative risk of female military personnel performing MMH tasks in comparison to male personnel.

The first part of this effort is complete. The second, third and fourth part are near completion. The first part consisted of employing Magnetic Resonance Imaging (MRI) techniques to quantitatively describe the internal geometry of the female trunk musculoskeletal system so that the model can accurately represent internal trunk mechanics. The second part consists of the evaluation of the muscle force-velocity and length-strength relationships that are unique to the female trunk musculature and physiology. Validation of the contributions of the internal geometric relationships and the length-strength and force-velocity relationships is currently under way in Part 3. The model performance of the female specific biomechanical

model will be assessed and compared to the model performance from a male biomechanical model used on male subjects performing the same experimental conditions. Part four is now in the process of assessing differences in spinal loading due to gender as well as the experimental conditions using both the male and female specific biomechanical models.

Our efforts in this research is progressing in accordance with the proposed timeline as expected. To date, we have collected and analyzed all the imaging data on healthy women. We have managed to expand this phase of the research, to allow assessment of healthy subjects for improved validity and to collect data of healthy males for direct comparison. The results agree with existing literature, indicating the methods, data, and processing we have been using will lead to valid mechanical representations of the torso. The determination of the female length-strength and force-velocity muscle relationships have progressed to a point where most of the subjects have been collected, and stable and promising results have been obtained. The few additional subjects needed to be collected will serve to enhance promising results to date. The data collection for Part 3 is nearing completion, with both males and females performing asymmetric and sagittally symmetric lifting exertions to validate the biomechanical model developed using the data and relationships found in Part 1 and Part 2. Part 4, which will assess and compare the spinal loading experienced by females and males is currently underway, and should also be nearing completion pending the completion of the data collection on the final few subjects for Part 3.

After the third year of this research effort, we remain confident that we will successfully develop an accurate biomechanical model for the evaluation of spinal loads of women performing MMH tasks. These results may permit assessment of work related LBD, and identification of methods and training techniques that will reduce the risk of low back injury in female military personnel.

TABLE OF CONTENTS

MEMORANDUM OF PROPRIETARY DATA	i
EXECUTIVE SUMMARY.....	ii
TABLE OF CONTENTS.....	iv
LIST OF FIGURES.....	v
LIST OF TABLES.....	vi
 PART 1: ANTHROPOMETRIC MRI MEASUREMENT OF FEMALE MUSCULOSKELETAL TORSO	 1
INTRODUCTION.....	1
BACKGROUND AND OBJECTIVES	3
ADMINISTRATIVE NOTE	3
METHODS	4
RESULTS.....	13
DISCUSSION.....	23
 PART 2: PHYSIOLOGICAL MEASUREMENT OF THE IN-VIVO MUSCULAR LENGTH-STRENGTH AND FORCE-VELOCITY RELATIONSHIPS IN THE FEMALE TRUNK TORSO.	 124
INTRODUCTION.....	124
BACKGROUND AND OBJECTIVES	124
ADMINISTRATIVE NOTE	125
METHODS	126
RESULTS.....	135
DISCUSSION.....	143
CONCLUSIONS	146
 PART 3: IMPLEMENTATION AND VALIDATION OF THE EMG-ASSISTED MODEL FOR FEMALE SUBJECTS.	 147
INTRODUCTION.....	147
BACKGROUND AND OBJECTIVES	147
ADMINISTRATIVE NOTE	147
METHODS	148
RESULTS.....	152

DISCUSSION.....	158
CONCLUSIONS	160

PART 4: ASSESS BIOMECHANICAL LOADS ON THE FEMALE SPINE DURING MILITARY MMH

.....	161
INTRODUCTION.....	161
BACKGROUND AND OBJECTIVES	161
ADMINISTRATIVE NOTE	162
METHODS	162
RESULTS.....	165
DISCUSSION.....	170
CONCLUSIONS	172
REFERENCES.....	173

LIST OF FIGURES

Figure 2.1.	Experimental equipment for the free-dynamic lifting conditions.....	128
Figure 2.2.	Experimental equipment for the lifting trials using the pelvic support structure.....	129
Figure 2.3.	Distribution of the r^2 s for the performance of Model 7a for the lifting trials in the pelvic support structure.....	140
Figure 2.4.	Distribution of the r^2 s for the performance of Model 7a when applied to the lifting trials performed in the controlled velocity free-dynamic exertions.....	140
Figure 2.5.	Female length-strength and male length-strength modulation factor comparison.....	143
Figure 2.6.	Female force-velocity and male force-velocity modulation factor comparison.....	144
Figure 4.1.	Anterior/Posterior shear force (N) on the L ₅ /S ₁ intervertebral disc as a function of gender and asymmetry of the starting lift position.....	167
Figure 4.2.	Compression force (N) on the L ₅ /S ₁ intervertebral disc as a function of gender and weight of the load.....	169
Figure 4.3.	Compression force (N) on the L ₅ /S ₁ intervertebral disc as a function of gender and asymmetry of the starting lift position.....	169
Figure 4.4.	Compression tolerance ratio for the L ₅ /S ₁ intervertebral disc as a function of gender and asymmetry of the starting lift position.....	170

LIST OF TABLES

Table 1.1.	Anthropometric Measurements of Male and Female Subjects	30
Table 1.2.	Right Latissimus Dorsi Physiological Cross-Sectional Areas	31
Table 1.3.	Left Latissimus Dorsi Physiological Cross-Sectional Areas	32
Table 1.4.	Right Erector Spinae Physiological Cross-Sectional Areas.....	33
Table 1.5.	Left Erector Spinae Physiological Cross-Sectional Areas.....	34
Table 1.6.	Right Rectus Abdominis Physiological Cross-Sectional Areas.....	35
Table 1.7.	Left Rectus Abdominis Physiological Cross-Sectional Areas.....	36
Table 1.8.	Right External Oblique Physiological Cross-Sectional Areas.....	37
Table 1.9.	Left External Oblique Physiological Cross-Sectional Areas	38
Table 1.10.	Right Internal Oblique Physiological Cross-Sectional Areas	39
Table 1.11.	Left Internal Oblique Physiological Cross-Sectional Areas	40
Table 1.12.	Right Psoas Major Physiological Cross-Sectional Areas	41
Table 1.13.	Left Psoas Major Physiological Cross-Sectional Areas.....	42
Table 1.14.	Right Quadratus Lumborum Physiological Cross-Sectional Areas.....	43
Table 1.15.	Left Quadratus Lumborum Physiological Cross-Sectional Areas	44
Table 1.16.	Vertebral Body Cross-Sectional Areas	45
Table 1.17.	Trunk Cross-Sectional Areas	46
Table 1.18.	Right Latissimus Dorsi Coronal Plane Moment-Arms.....	47
Table 1.19.	Left Latissimus Dorsi Coronal Plane Moment-Arms	48
Table 1.20.	Right Erector Spinae Coronal Plane Moment-Arms	49
Table 1.21.	Left Erector Spinae Coronal Plane Moment-Arms.....	50
Table 1.22.	Right Rectus Abdominis Coronal Plane Moment-Arms	51
Table 1.23.	Left Rectus Abdominis Coronal Plane Moment-Arms.....	52
Table 1.24.	Right External Oblique Coronal Plane Moment-Arms.....	53
Table 1.25.	Left External Oblique Coronal Plane Moment-Arms	54
Table 1.26.	Right Internal Oblique Coronal Plane Moment-Arms.....	55
Table 1.27.	Left Internal Oblique Coronal Plane Moment-Arms	56
Table 1.27.	Right Psoas Major Coronal Plane Moment-Arms	57
Table 1.29.	Left Psoas Major Coronal Plane Moment-Arms	58
Table 1.30.	Right Quadratus Lumborum Coronal Plane Moment-Arms.....	59
Table 1.31.	Left Quadratus Lumborum Coronal Plane Moment-Arms	60
Table 1.32.	Right Latissimus Dorsi Sagittal Plane Moment-Arms	61
Table 1.33.	Left Latissimus Dorsi Sagittal Plane Moment-Arms.....	62
Table 1.34.	Right Erector Spinae Sagittal Plane Moment-Arms	63
Table 1.35.	Left Erector Spinae Sagittal Plane Moment-Arms	64
Table 1.36.	Right Rectus Abdominis Sagittal Plane Moment-Arms	65
Table 1.37.	Left Rectus Abdominis Sagittal Plane Moment-Arms	66
Table 1.38.	Right External Oblique Sagittal Plane Moment-Arms	67
Table 1.39.	Left External Oblique Sagittal Plane Moment-Arms.....	68
Table 1.40.	Right Internal Oblique Sagittal Plane Moment-Arms	69
Table 1.41.	Left Internal Oblique Sagittal Plane Moment-Arms.....	70
Table 1.42.	Right Psoas Major Sagittal Plane Moment-Arms.....	71

Table 1.43.	Left Psoas Major Sagittal Plane Moment-Arms	71
Table 1.44.	Right Quadratus Lumborum Sagittal Plane Moment-Arms	72
Table 1.45.	Left Quadratus Lumborum Sagittal Plane Moment-Arms.....	73
Table 1.46.	Right Latissimus Dorsi Muscle Vector Directions for Coronal and Sagittal Planes	74
Table 1.47.	Left Latissimus Dorsi Muscle Vector Directions for Coronal and Sagittal Planes	75
Table 1.48.	Right Erector Spinae Muscle Vector Directions for Coronal and Sagittal Planes	76
Table 1.49.	Left Erector Spinae Muscle Vector Directions for Coronal and Sagittal Planes	77
Table 1.50.	Right Rectus Abdominis Muscle Vector Directions for Coronal and Sagittal Planes	78
Table 1.51.	Left Rectus Abdominis Muscle Vector Directions for Coronal and Sagittal Planes	80
Table 1.52.	Right External Obliques Muscle Vector Directions for Coronal and Sagittal Planes	81
Table 1.53.	Left External Obliques Muscle Vector Directions for Coronal and Sagittal Planes	82
Table 1.54.	Right Internal Obliques Muscle Vector Directions for Coronal and Sagittal Planes	83
Table 1.55.	Left Internal Obliques Muscle Vector Directions for Coronal and Sagittal Planes	84
Table 1.56.	Right Psoas Major Muscle Vector Directions for Coronal and Sagittal Planes	85
Table 1.57.	Left Psoas Major Muscle Vector Directions for Coronal and Sagittal Planes	86
Table 1.58.	Right Quadratus Lumborum Muscle Vector Directions for Coronal and Sagittal Planes.....	87
Table 1.59.	Left Quadratus Lumborum Muscle Vector Directions for Coronal and Sagittal Planes.....	88
Table 1.60.	Vertebral Body Vector Directions for Coronal and Sagittal Planes	89
Table 1.61.	Significant Regression Equations Predicting Average of Largest Right and Left Female PCSAs from External Anthropometric Measures	90
Table 1.62.	Significant Regression Equations Predicting the Largest Individual PCSAs from External Anthropometric Measures	90
Table 1.63.	Significant Regression Equations Predicting Average of Largest Right and Left Male PCSAs from External Anthropometric Measures	91
Table 1.64.	Significant Regression Equations Predicting the Largest Male Individual PCSAs from External Anthropometric Measures.....	91
Table 1.65.	Regression Equations Predicting PCSAs for Male and Female Latissimus Dorsi.....	92
Table 1.66.	Regression Equations Predicting PCSAs for Male and Female Erector Spinae.....	93

Table 1.67.	Regression Equations Predicting PCSAs for Male and Female Rectus Abdominis.....	94
Table 1.68.	Regression Equations Predicting PCSAs for Male and Female External Obliques.....	95
Table 1.69.	Regression Equations Predicting PCSAs for Male and Female Internal Obliques.....	96
Table 1.70.	Regression Equations Predicting PCSAs for Male and Female Psoas Major.....	97
Table 1.71.	Regression Equations Predicting PCSAs for Male and Female Quadratus Lumborum.....	98
Table 1.72.	Summary Statistics for Regression Equations Predicting Female Coronal Plane Moment-Arms at the Origin.....	99
Table 1.73.	Summary Statistics for Regression Equations Predicting Female Sagittal Plane Moment-Arms at the Origin.....	99
Table 1.74.	Summary Statistics for Regression Equations Predicting Female Coronal Plane Moment-Arms at the Insertion.....	100
Table 1.75.	Summary Statistics for Regression Equations Predicting Female Sagittal Plane Moment-Arms at the Insertion.....	100
Table 1.76.	Summary Statistics for Regression Equations Predicting Male Coronal Plane Moment-Arms at the Origin.....	101
Table 1.77.	Summary Statistics for Regression Equations Predicting Male Sagittal Plane Moment-Arms at the Origin.....	101
Table 1.78.	Summary Statistics for Regression Equations Predicting Male Coronal Plane Moment-Arms at the Insertion.....	102
Table 1.79.	Summary Statistics for Regression Equations Predicting Male Sagittal Plane Moment-Arms at the Insertion.....	102
Table 1.80.	Regression Equations Predicting Right Latissimus Dorsi Moment-Arms for Males and Females.....	103
Table 1.81.	Regression Equations Predicting Left Latissimus Dorsi Moment Arms for Males and Females.....	104
Table 1.82.	Regression Equations Predicting Right Erector Spinae Moment-Arms for Males and Females.....	105
Table 1.83.	Regression Equations Predicting Left Erector Spinae Moment-Arms for Males and Females.....	106
Table 1.84.	Regression Equations Predicting Right Rectus Abdominis Moment-Arms for Males and Females.....	107
Table 1.85.	Regression Equations Predicting Left Rectus Abdominis Moment-Arms for Males and Females.....	108
Table 1.86.	Regression Equations Predicting Right External Obliques Moment-Arms for Males and Females.....	109
Table 1.87.	Regression Equations Predicting Left External Obliques Moment-Arms for Males and Females.....	110
Table 1.88.	Regression Equations Predicting Right Internal Obliques Moment-Arms for Males and Females.....	111

Table 1.89.	Regression Equations Predicting Left Internal Obliques Moment-Arms for Males and Females	112
Table 1.90.	t-test Results for Differences of Largest Right and Largest Left PCSAs	113
Table 1.91.	ANOVA Table for Differences Between Right and Left Female PCSAs by Vertebral Level	113
Table 1.92.	Post-hoc results of Analysis of Variance of Right versus Left Side PCSAs	113
Table 1.93.	Difference between Female Right and Left Side PCSAs for each Muscle Group, by Vertebral Level	114
Table 1.94.	Difference between Male Right and Left Side PCSAs for each Muscle Group, by Vertebral Level	115
Table 1.95.	Coefficients for Origin Muscle Vector Locations in Coronal and Sagittal Planes using Muscle Centroid Locations.....	116
Table 1.96.	Coefficients for Origin Muscle Vector Locations in Coronal and Sagittal Planes using 45 Degree Anterior/Caudal Vector Angle for External Oblique.....	117
Table 1.97.	Coefficients for Origin Muscle Vector Locations in Coronal and Sagittal Planes using 45 Degree Anterior/Caudal Vector Angle for External Oblique and 45 Degree Posterior/Caudal Vector Angle for Internal Oblique.....	118
Table 1.98.	Coefficients for Insertion Muscle Vector Locations in Coronal and Sagittal Planes, located at most superior level observed.....	119
Table 1.99.	Linear regression equations predicting vertical distance (cm) from the L ₅ vertebral level to different muscle vertebral levels in the coronal direction, as a function of standing height	119
Table 1.100.	Coefficients for Insertion Muscle Vector Locations in Coronal and Sagittal Planes.....	120
Table 1.101.	Distribution of Largest Latissimus Dorsi PCSA by Vertebral Level	121
Table 1.102.	Distribution of Largest Erector Spinae PCSA by Vertebral Level	121
Table 1.103.	Distribution of Largest Rectus Abdominis PCSA by Vertebral Level	121
Table 1.104.	Distribution of Largest External Obliques PCSA by Vertebral Level.....	122
Table 1.105.	Distribution of Largest Internal Obliques PCSA by Vertebral Level.....	122
Table 1.106.	Distribution of Largest Quadratus Lumborum PCSA by Vertebral Level	122
Table 1.107.	Distribution of Largest Psoas Major PCSA by Vertebral Level.....	123
Table 2.1.	Anthropometric data from the female subjects for the lifting in the pelvic support structure and from the free-dynamic lifts.....	126
Table 2.2.	Data sources for maximum physiological cross-sectional muscle areas and muscle vector locations for different biomechanical models used to develop the muscle length-strength (L-S) and force-velocity (F-V) modulation factors.....	134
Table 2.3.	Descriptive results for the normalized muscle activity (percent of maximum muscle activity) occurring at the maximum moment, and maximum sagittal moment (Nm) as a function of velocity and weight, for lifting trials performed in the Pelvic Support Structure.....	136

Table 2.4.	MANOVA and ANOVA results for the normalized muscle activity for the effects of velocity, weight, and the velocity by weight interaction, for lifting trials performed in the Pelvic Support Structure	137
Table 2.5.	Model results as a function of each of the ten models, with different combinations of inputs for the physiological cross-sectional areas, length-strength (L-S) and force-velocity (F-V) modulation factors, vector locations, and lifting trials used	142
Table 2.6.	Model performance results from Model 7a compared to the model performance results when applied to trials from the free-dynamic lifting exertions	143
Table 3.1.	Anthropometric measurements from male and female subjects for Part 3	150
Table 3.2.	Analysis of Variance p-values on the EMG biomechanical model performance parameters as a function of the independent variables for both males and females	154
Table 3.3.	Overall biomechanical model performance parameters for males and females, collapsed across all experimental conditions.....	155
Table 3.4.	Descriptive statistics for the muscle gain, r^2 and AAE (as a percent of measured moment) model performance parameters for the female biomechanical model	156
Table 3.5.	Descriptive statistics for the muscle gain, r^2 and AAE (as a percent of measured moment) model performance parameters for the male biomechanical model	156
Table 3.6.	Model r^2 descriptive statistics for male and female biomechanical models as a function of the experimental conditions	157
Table 3.7.	Model muscle gain descriptive statistics for male and female biomechanical models as a function of the experimental conditions.....	158
Table 4.1	Descriptive statistics for spinal loading as a function of gender and the experimental conditions	166
Table 4.2.	Analysis of Variance p-values on the spinal loading as a function of the experimental conditions.	168
Table 4.3.	Compression tolerance ratio for females and males, as a function of the experimental conditions	171
Table 4.4.	Analysis of Variance p-values for spinal compression tolerance ratio as a function of gender and the experimental conditions	171

PART 1: Anthropometric MRI Measurement of Female Musculoskeletal Torso

Introduction

The control of women's low-back disorder (LBD) risk should be a priority for the military to mitigate escalating injuries and associated costs, and to maintain military readiness and combat effectiveness. Low back injuries accounted for 75% of compensable military injuries and have cost the Army between 46.9 and 61 million dollars per year from 1988 through 1991 (Army Safety Center, 1992). When one considers that women have significantly higher incidence of lost time injuries during basic training than men (Jones et al., 1988), it is apparent that the risk of work related LBD may be particularly great for women in the military. The cost of LBD risk among military women extends beyond medical care expenditures and long term or permanent compensation for the soldier. There is a great cost associated with lost duty time, training and retraining replacement personnel if a soldier must be discharged because of a LBD. Furthermore, military effectiveness and readiness are compromised if the soldier is not able to perform peacetime or combat related tasks because of a LBD.

Many of the military occupational specialties (MOSs) have recently been made available to military women (Army Times, 1994). As of 1995 there were women filling roles as combat engineers, in field artillery, and land combat MOSs. The number of women in these combat related MOSs is expected to increase. As women fill an expanded role in the modern military, the risk of lost female personnel due to LBD will have greater consequences upon military readiness and combat effectiveness than ever before. With military downsizing, the importance of each military women, and the repercussions of LBD will become critical.

Many of the MOSs now being filled by women requires heavy manual material handling and would be expected to challenge the tolerance of most industrial workers' spines. Sharp and Vogel (1992) have shown that "heavy MMH is the most physically demanding task in 90% of all military job specialties." Yet these activities have never been quantitatively evaluated with military women. Thus, there is a need for a biomechanical model that can accurately and reliably assess and evaluate the risk of LBD to women as well as what features or training might mitigate that risk.

The Ohio State University EMG-assisted biomechanical model can be developed to provide a tool to assess and evaluate the risk of LBD to women performing military MMH tasks as part of their MOSs. Our previous efforts have demonstrated that we have been able to build a three-dimensional model of the trunk that is capable of accurately assessing spine loads during free-dynamic trunk motion which accounts for muscle co-contraction (Granata and Marras, 1993; Marras and Granata, 1995; Marras and Sommerich, 1991a,b). However, the modeling efforts to date have been successful in modeling the trunk geometry and subsequent loading imposed upon the spine of only males performing manual materials handling activities.

The geometry of the female trunk is vastly different from that of the male. Women tend to possess greater hip breadth and narrower abdominal depth than men (Pheasant, 1988). The sacroiliac joint is positioned several centimeters anteriorly in the female changing the moment arm associated with the external load as well as affecting the internal moment arm distances between the muscles and the point of rotation of the spine (Tischauer, 1978). In addition, it is suspected that the muscle attachment locations are significantly different between males and females. These changes will dramatically affect the force-length and force-velocity relationships that are vital for the determination of muscle force. In addition, one must understand the differences in the muscle lines of action (attachments) so that the trunk mechanics representation accurately reflects loading of the female trunk.

The ultimate goal of this research is to extend the capability of predicting musculoskeletal loads to that of women performing realistic MMH tasks. This model will be employed to assess the relative risk for musculoskeletal injury due to a MMH task for women relative to men, and to evaluate the proposed changes to those tasks to quantify the change in LBD risk. This EMG-driven biomechanical model will then be available as a tool to assess the risk associated with specific MMH tasks performed as part of MOSs that have recently been made available to military women. In this manner it will be possible to: a) assess risk for a given task, b) evaluate the physical attributes of a potential recruit that would place her at an increased risk of LBD, and c) determine how training or workplace procedures might be changed to minimize risk of LBDs to women (and men) performing the military MMH task.

In order to accomplish these objectives, it will be necessary to accomplish five specific aims. 1.) Quantitatively describe the internal geometry of the female trunk musculoskeletal

system so that the model can accurately represent internal trunk mechanics and lines of muscle action. Magnetic Resonance Imaging (MRI) will be used to collect this information in a safe and accurate manner. 2.) Determine the force-velocity relationship and length-strength relationships that are unique to the female trunk musculature. 3.) Implement female trunk geometry and muscle relationships into the existing OSU EMG-assisted biomechanical model. 4.) Test and validate the model under laboratory conditions. 5.) Use the model to evaluate military MMH tasks of physically demanding MOSs performed by both males and females.

Background and Objectives

The objective of Part 1 was to generate descriptive statistics to describe the relative anthropometric values of muscle cross-sectional areas, origins, and lines of action in the female torso. The EMG-assisted biomechanical model currently accepts regression equations to predict muscle anthropometry of male subjects (Granata and Marras, 1993; Marras and Granata, 1995; Marras and Sommerich, 1991a,b). This is critical for scaling modeled muscle force amplitudes, dynamic behavior and to predict musculoskeletal loads. In order to generate accurate assessments of spinal loading and associated LBD risk of females performing military MMH tasks, it is necessary to generate a biomechanical geometry that accurately describes military age women. Although measures of soft tissue have been reported on elderly females (Chaffin et al., 1990; Kumar, 1988), there have been no studies designed to measure the trunk muscle area and geometry of young active women.

Administrative Note

In the accepted research proposal, the "Statement of Work Addendum" included the collection of anthropometric data describing relative trunk muscle sizes and biomechanical lines of action on 20 women from existing MRI scans. Thus, we were to find torso imaging data of women who had required medical diagnosis of disabilities. The originally proposed "Statement of Work" suggested MRI analyses be performed by scanning 20 healthy women. However, due to budget limitations imposed by USARMC prior to approving the research, it was necessary to revise this part of the research to meet the financial constraints with the "Statement of Work Addendum" as described above.

We have managed to supplement the experimental design of the MRI with alternative funding that will improve the validity and specificity of the research for the purposes of the research goals and objectives. This was achieved by finding the opportunity to support data collection of healthy military age women, a population which more realistically represents active military women. A local hospital with a state-of-the-art MRI facility has agreed to participate in this effort, allowing us the opportunity to scan 20 healthy women and 10 healthy men. This will improve the validity of the data by providing MRI scans of healthy women instead of scans from disabled women, avoiding confounding of musculoskeletal factors.

The alternative funding opportunity also allowed us to collect data for direct comparison of male versus female relative muscle areas, attachment points, and lines of action. To date, there have been no such published analyses of muscular mechanical geometry. This data will allow a direct comparison of the biomechanical loads generated by female versus male soldiers during MMH activities. The comparison will also permit a more valid assessment of LBD risk of women as compared to men, and the influence of task design upon gender related LBD risk.

The results in the tables describing the physiological cross-sectional areas and muscle vector directions have been updated since the last reporting period. These updates also resulted in updates in the statistical analyses performed, as well as changes to the linear regression analysis for the prediction of the physiological cross-sectional areas. Additionally, the prediction of the moment-arms from external anthropometric measures have been updated to include the vertebral levels that are used on the current EMG-assisted biomechanical model.

Methods

Experimental Design

The subjects were placed in the MRI chamber at the Riverside Methodist Hospital, Columbus, OH, where cross-sectional images of the trunk were collected. A Philips GyroScan MRI was set to a spin echo sequence of TR=240 and TE=12, generating slices of 10 mm in thickness. Subjects were placed in a neutral position (supine postures with knees extended and hands lying across their abdomen) on the MRI gantry. The gantry moved the subjects into the center bore of the MRI magnet, aligning the subjects such that the scans could be performed on

the desired region of the torso. A sagittal scout view was first collected to permit vertical quantification of individual transverse planes, and to ensure the cross-sectional scans would be captured in the field-of-view. A single set of 11 torso musculature scans was next performed, which were perpendicular to the gantry table at transverse levels through approximate centers of the vertebral bodies in the lumbar/sacrum and lower thoracic regions of the spine. Specifically, this included transverse scans of the torso through the T₈ through S₁ vertebral levels.

Subjects

Twenty females subjects of military age were recruited from the local community. In order to directly compare the female results with relative male anthropometry, MRI data were also collected on 10 male subjects of military age, also recruited from the local community. None of the subjects had a history of chronic activity limiting chronic back or leg injuries, nor were any experiencing any low back pain at the time of the MRI scan. Upon arrival, anthropometric data were collect from each subject including the age, height and weight, the trunk width and depth measured at the trochanter, iliac crest, and xyphoid process, trunk circumference about the iliac crest, and right and left trochanter height from the floor.

Data Extraction

The MRI scans for each subject were transferred onto a Philips GyroView, where muscle cross-sectional areas could be estimated, as well as muscle centroids located relative to the spinal vertebral body centroid (McGill et al., 1993). The GyroView allows the user to inscribe an object of interest with a computer mouse, which then provides descriptive statistical data including the area of the enclosed region and the three-dimensional location of the area centroids relative to the scan set origin. In this manner, each of the muscles of interest were identified, outlined, and quantified where present for each of the 11 scan levels. The quantified muscles included the right and left pairs of the erector spinae group, quadratus lumborum, latissimus dorsi, internal obliques, external obliques, rectus abdomini, and psoas major. The cross-sectional areas and centroids were also quantified for each vertebral body and the torso at each of the 11 scan levels. Vector component directions for each muscle from level to level were determined in both the coronal plane (*equation 1.2*) and the sagittal plane (*equation 1.3*).

$$\theta_{Lat} = \tan^{-1}\left(\frac{\Delta x}{\Delta z}\right) \quad (Eq\ 1.2)$$

$$\theta_{Sag} = \tan^{-1}\left(\frac{\Delta y}{\Delta z}\right) \quad (Eq\ 1.3)$$

where:

θ_{Lat} = Muscle vector angle in the coronal plane from one vertebral level to the next (caudal direction);

θ_{Sag} = Muscle vector angle in the sagittal plane from one vertebral level to the next (caudal direction);

Δx = Change in the muscle centroid lateral coordinate from one vertebral level to the next (caudal direction);

Δy = Change in the muscle centroid sagittal coordinate from one vertebral level to the next (caudal direction);

Δz = Change in the muscle centroid vertical coordinate from one vertebral level to the next (caudal direction).

To determine the muscle, vertebral body, and trunk cross-sectional areas and centroids at each scan level, each were inscribed several times, with the average of the observation used as the representative values. The coefficient of variation (C.V.) was calculated for the first 15 female subjects, which showed that using three observations resulted in average C.V.'s of 9% or less for each muscle, with most C.V.'s less than 5%. Likewise, the lateral and sagittal moment-arms for each muscle were determined by averaging the three observed distances between the muscle centroid and vertebral centroid. Finally, the muscle vector directions in the lateral plane (Eq. 1.2) and sagittal plane (Eq. 1.3) were also averaged across each of the three observations.

Following the determination of the raw cross-sectional muscle areas, three separate corrections were made to the areas, when necessary. First, to correct for any degree of twisting of the subjects' torso while lying in the MRI machine, the muscle centroid locations were corrected by quantifying the location of the spinous process centroid at each scan level. It was assumed that if the subject was lying flat on the gantry table of the MRI with no twisting of the torso, there would be no difference in the lateral location of the vertebral body centroid and spinous process centroid, relative to the scan origin. Therefore, for any degree of twisting of the torso, the muscle centroid location was adjusted for the angle between vertebral body centroid and spinous process centroid. Secondly, for the muscles that were crescent-shaped in cross-

section, the muscle centroids lied outside of the muscle. Specifically, at certain levels of the spine, the muscle centroids for the latissimus dorsi, external obliques, and the internal obliques lied medial to the medial border of the muscle. Therefore, to obtain more realistic centroid locations for the calculation of the corrected cross-sectional areas of these muscles (described in the next step), a line was drawn from the vertebral body centroid, through the muscle centroid, to the estimated midpoint of the muscle. This estimated midpoint was then used as the vector location for the muscle for determination of the physiological cross-sectional area (described next). Finally, the raw muscle cross-sectional area was adjusted so that the plane of the cross-sectional muscle area was perpendicular to the muscle vector direction. Since the MRI scan slices were perpendicular to the gantry table, and the muscles may not necessarily run parallel to the table, the resulting estimated cross-sectional areas of the muscles may be larger than the true cross-sectional area which would be perpendicular to the muscle vector direction. Therefore, the raw muscle cross-sectional areas at each scan level were converted to the physiological cross-sectional area (PCSA) using a general form of *equation 1.4*. For the muscles where the area centroid lied outside the muscle (i.e., latissimus dorsi, internal and external obliques), the adjusted vector directions (θ_{Cor} and θ_{Sag}) which were determined from the estimated midpoints of the muscles, were used to calculate the corrected cross-sectional areas.

$$Area_{Corr} = Area_{Raw} \cos(\theta_{Lat}) \cos(\theta_{Sag}) \quad (Eq. 1.4)$$

where:

$PCSA$ = Physiological cross-sectional muscle area;

$Area_{Raw}$ = Raw cross-sectional area determined by outline from GyroView.

θ_{Lat} = Muscle vector angle in the lateral plane from one vertebral level to the next;

θ_{Sag} = Muscle vector angle in the sagittal plane from one vertebral level to the next;

The raw cross-sectional area, however, was multiplied by different vector values, depending on where in the spine the muscle is present. For the first level that the muscle was present (the most superior level), the raw cross-sectional area was multiplied by cosines of the sagittal and lateral vector for that level, using *equation 1.4*. For example, in some subjects, the most superior level where the rectus abdominis was first present was at the T_{12} level; therefore, the corrected cross-sectional area for the rectus abdominis at T_{12} was determined by:

$$Area_{Corr-T_{12}} = Area_{Raw-T_{12}} \cos(\theta_{Lat-T_{12}}) \cos(\theta_{Sag-T_{12}}) \quad (Eq. 1.5)$$

where:

- $Area_{Corr-T_{12}}$ = Corrected cross-sectional area at the T_{12} vertebral level;
- $Area_{Raw-T_{12}}$ = Raw cross-sectional area at the T_{12} vertebral level, determined by the GyroView;
- $\theta_{Lat-T_{12}}$ = Lateral muscle vector angle between the T_{12} and L_1 vertebral level;
- $\theta_{Sag-T_{12}}$ = Sagittal muscle vector angle between the T_{12} and L_1 vertebral level.

For the same subjects, the second most superior level where the rectus abdominis was present would then have been L_1 ; however, to determine the corrected cross-sectional area of the rectus abdominis for the second level it was present, the raw cross-sectional area was multiplied by the cosines of the average of the muscle vector angles at the T_{12} and L_1 levels, for both the sagittal and lateral components:

$$Area_{Corr-L_1} = Area_{Raw-L_1} \cos\left(\frac{\theta_{Lat-T_{12}} + \theta_{Lat-L_1}}{2}\right) \cos\left(\frac{\theta_{Sag-T_{12}} + \theta_{Sag-L_1}}{2}\right) \quad (Eq. 1.6)$$

where:

- $Area_{Corr-L_1}$ = Corrected cross-sectional area at the L_1 vertebral level;
- $Area_{Raw-L_1}$ = Raw cross-sectional area at the L_1 vertebral level, from the GyroView;
- $\theta_{Lat-T_{12}}$ = Lateral muscle vector angle from the T_{12} to L_1 vertebral level;
- θ_{Lat-L_1} = Lateral muscle vector angle from the L_1 to L_2 vertebral level;
- $\theta_{Sag-T_{12}}$ = Sagittal muscle vector angle from the T_{12} to L_1 vertebral level;
- θ_{Sag-L_1} = Sagittal muscle vector angle from the L_1 to L_2 vertebral level.

Likewise, the corrected cross-sectional area for the rectus abdominis when present at the next level (L_2), given that the muscle was present at L_1 , was determined in the following manner:

$$Area_{Corr-L_2} = Area_{Raw-L_2} \cos\left(\frac{\theta_{Lat-L_1} + \theta_{Lat-L_2}}{2}\right) \cos\left(\frac{\theta_{Sag-L_1} + \theta_{Sag-L_2}}{2}\right) \quad (Eq. 1.7)$$

where:

- $Area_{Corr-L_2}$ = Corrected cross-sectional area at the L_2 vertebral level;
- $Area_{Raw-L_2}$ = Raw cross-sectional area at the L_2 vertebral level, from the GyroView;
- θ_{Lat-L_1} = Lateral muscle vector angle from the L_1 to L_2 vertebral level;

θ_{Lat-L_2} = Lateral muscle vector angle from the L_2 to L_3 vertebral level;

θ_{Sag-L_1} = Sagittal muscle vector angle from the L_1 to L_2 vertebral level;

θ_{Sag-L_2} = Sagittal muscle vector angle from the L_2 to L_3 vertebral level.

Finally, to calculate the corrected cross-sectional area for the lowest level where the muscle was present (the most inferior level), using the example where the lowest level that the rectus abdominis was present was at S_1 , the following equation was used:

$$Area_{Corr-S_1} = Area_{Raw-S_1} \cos(\theta_{Lat-L_5}) \cos(\theta_{Sag-L_5}) \quad (Eq. 3.8)$$

where:

$Area_{Corr-S_1}$ = Corrected cross-sectional area at the S_1 vertebral level;

$Area_{Raw-S_1}$ = Raw cross-sectional area at the S_1 vertebral level, determined by the GyroView;

θ_{Lat-L_5} = Lateral muscle vector angle between the L_5 and S_1 vertebral level;

θ_{Sag-L_5} = Sagittal muscle vector angle between the L_5 and S_1 vertebral level.

Although the rectus abdominis was used as an example of how the corrected cross-sectional areas were calculated as a function of where it was present, *equations 1.5 through 1.8* were used for all the muscles to determine the corrected cross-sectional muscle areas perpendicular to the muscle vectors. Generally, the first level where a muscle was present (starting at the most superior level and working down), *equation 1.5* was used; the last level that the muscle was present (the most inferior level), *equation 1.8* was used to calculate the corrected cross-sectional area. Finally, for all other levels in between the first and last level where the muscle was present, *equations 1.6 or 1.7* were used to calculate the corrected cross-sectional areas.

The moment-arms of the muscles at each level were determined by calculating the absolute difference between the muscle centroid and the vertebral body centroid, in both the sagittal plane and the lateral plane. The muscle centroids used for the calculation of the moment-arms were corrected for any torso twisting in the MRI machine, but were not corrected for those muscles where the centroids lied outside the inscribed muscle. Sign designations were given to the moment-arms, such that positive and negative values for the sagittal moment-arms

represented anterior and posterior to the vertebral body centroid, respectively, and positive and negative values for the lateral moment-arms represent right and left sides of the vertebral body centroid, respectively.

Descriptive Statistics

Descriptive statistics (means and standard deviations at each vertebral level) were first generated for the PCSAs, as well as for the cross-sectional areas for the vertebral bodies corrected for the spine vector directions and the trunk cross-sectional areas. Descriptive statistics were also generated for the corrected moment-arms for each muscle, both in the coronal and sagittal planes, as well as the muscle vector directions from level to level, in both the coronal and sagittal planes.

In the current EMG-assisted biomechanical model (Granata and Marras, 1993; Marras and Granata, 1995; Marras and Sommerich, 1991a,b), the muscle vector locations for the muscle origins and insertions are identified as a percentage of the trunk width for the coronal plane location, and the sagittal plane location is calculated as a percentage of the trunk depth, both measured at the iliac crest. The current database of 20 females and 10 males, however, allows other anthropometric measures to be explored; therefore, in addition to the vector locations being calculated as a function of trunk measurements about the iliac crest, the vector locations as a function of the trunk width and depth measured at the xyphoid process were also calculated, as well as a function of the body mass index (BMI).

Finally, since individual differences may dictate where the largest PCSA exists along the spine, the distribution of the largest PCSA for each muscle by vertebral level for both males and females were determined.

As a benchmark, the results of the PCSAs and moment-arms in the coronal and sagittal plane were then compared with data from Chaffin et al. (1990) who examined elderly women, and McGill et al. (1993) who examined young males. These comparisons consisted of the magnitude of the difference of similar measures, as well as the percent difference. Difficulty arose when comparing cross-sectional areas from level to level, since in both the Chaffin et al. (1990) and the McGill et al. (1993) study, the scan slices were set through the middle of the intervertebral disc, whereas in the current study, the scan slices were set through the estimated

midpoint of the vertebral body. Therefore, the comparisons of muscle cross-sectional areas and moment-arms were off by one-half of a level. To account for the difference in the location of the slices, the area and moment-arm midpoint between adjacent slices of the data in the current study were determined, thus creating a more comparable area value to the Chaffin et al. (1990) and the McGill et al. study (1993). For example, averaging the muscle cross-sectional area at T₈ and T₉ of the current study, would allow a more logical comparison to the muscle cross-sectional areas of the T₈/T₉ scan slice from McGill et al. (1993).

Statistical Analyses

Linear regression techniques were used to predict the largest PCSA for each muscle, for both males and females independently. The dependent variable consisted of the largest PCSA, irrespective of the vertebral level. The individual independent variables for each regression equation consisted of the product of trunk width and trunk depth (cm²) measured at the xyphoid process, the iliac crest and the trochanter, as well as the body mass index (kg/m²). Statistical differences between the regression equations predicting the PCSA for males versus females were also investigated using a hierarchical multiple linear regression approach (Neter et al., 1985). First, the combined male and female data were used to generate one regression equation using the individual independent variables of the trunk width multiplied by the trunk depth at the xyphoid process, the trochanter, and the iliac crest, as well as the BMI. Then, a single regression equation was developed to predict the male and female PCSA independently, using a gender indicator variable. Finally, the effect of including a gender indicator variable was examined by testing to see if there was a significant increase in the multiple coefficient of variation (R²). If there was a significant difference, then the male and female regression equations were statistically different, which indicates that the male regression equation could not be used to predict the female PCSA.

Regression equations were also developed to predict the moment-arms of the muscles at the muscle origin and insertion points, for both the sagittal and coronal planes. In the EMG-assisted biomechanical model for males (Granata and Marras, 1993; Marras and Granata, 1995; Marras and Sommerich, 1991a,b), the origin was defined to exist at the L₅, where the specific insertion point for each muscle pair was a function of the magnitude of forward sagittal bending.

The dependent variable consisted of either the coronal or sagittal plane moment-arm. The independent variables were the trunk width measured at the xyphoid process and the iliac crest when the coronal plane moment-arm was used as the dependent variable, whereas the trunk depth measured at the xyphoid process and the iliac crest was used for the independent variable when the dependent variable was the sagittal plane moment-arm. Additionally, the body mass index (kg/m^2) was also used as an independent variable for the moment-arm regression equations.

Differences between the right and left side PCSAs were statistically analyzed in two different ways. First, differences between the right and left side largest PCSA (irrespective of which level it was located) for each muscle was assessed by using dependent sample *t*-tests, performed independently for each gender. Secondly, differences between the right and left sides at each specific vertebral level were assessed by performing an Analysis of Variance (ANOVA). The dependent variable consisted of the muscle PCSA, and the independent variables included the subject, vertebral level, side (right or left), and a vertebral level by side interaction. Since each muscle was not always present at the same level for each subject, the data set was restricted to the levels where complete data existed, and where each subject had the muscle present between the two vertebral level endpoints. Thus, the latissimus dorsi muscle was restricted between T₈ and L₃, the erector spinae between T₈ and S₁, the rectus abdominis between L₁ and S₁, the external obliques between L₁ and L₄, the internal obliques between L₃ and L₄, the quadratus lumborum between L₂ and L₄, and the psoas major between L₂ and S₁. For subjects who did not have muscle areas present between the vertebral level endpoints listed above, they were excluded from the ANOVA. Post-hoc analyses consisted of Tukey pairwise comparisons on significant effects.

Finally, statistical differences between males and females for the PCSA, the coronal and sagittal plane moment-arms, as well as the muscle vector component directions at each vertebral level were determined by using *t*-tests with independent observations, with equal or unequal variances where appropriate, with a significant difference indicated when $p \leq 0.05$.

Results

Anthropometric Measurements

The anthropometric data from the males and females are shown in Table 1.1. As expected, the mean value of each variable for the males were greater in magnitude than those of the females, although this difference was not tested statistically. When compared to other studies, the females in this study were much younger (25.0 vs 49.6 yrs), slightly taller (165.5 vs 163.1 cm), and lighter (57.9 vs 67.6 kg) than those females in the study by Chaffin et al. (11). The males in this study were slightly older (26.4 vs 25.3 yrs), were virtually the same height (175.9 vs 176.1 cm), and slightly lighter (79.8 vs 81.5 kg) than the males in the study by McGill et al. (15).

Physiological Cross-Sectional Muscle Areas

The PCSAs for each of the muscles are shown in Tables 1.2 through 1.15. These tables list the mean and standard deviation of the PCSA for each muscle, by vertebral level. Also included in these tables are comparisons between the female PCSA from this study and the data from the females in the Chaffin et al. (11) study, comparisons between the male PCSAs of this study and the data from males in a study by McGill et al. (15), as well as comparisons between the female and male PCSAs of this study. The comparison between the different data sets consist of the magnitude of the difference, as well as the percent difference, where the shaded cells represent significant differences between the male and female PCSA.

As expected, the cross-sectional areas of the females were smaller than those of the males, however, this difference differed as a function of the muscle of interest. The female latissimus dorsi areas (Tables 1.2 and 1.3) ranged from 37% to 49% smaller than that of the males, with an average of 40.7%, and were all significantly smaller than the male muscle areas. Similarly, the female erector spinae areas (Tables 1.4 and 1.5) ranged from 37% to 48% smaller than that of the males, with an average of 39.5%, again with the female PCSAs significantly smaller at every level. The female rectus abdominis areas (Tables 1.6 and 1.7) ranged from 22% to 41% smaller than the males, with an average of 30.3%. All levels except for the left rectus abdominis at T₁₂ were significantly smaller than the male PCSA. The female external obliques

(Tables 1.8 and 1.9) ranged from 22% to 39% smaller than the males external obliques, with an average of 29.9% across all levels. All but the right and left female PCSA at L₅ were significantly smaller than the male PCSA. The internal obliques (Tables 1.10 and 1.11) of the females showed a wide range of area in comparison to the males, ranging from 10% larger to 47% smaller than the males, with the female areas at L₃ and L₄ significantly smaller than the males for both right and left sides. The largest difference between the female and male PCSA existed for the psoas major muscle (Tables 1.12 and 1.13), where the female PCSA ranged from 43% to 51%, averaging 47.3% smaller than the male psoas major PCSA. Finally, the female quadratus lumborum (Tables 1.14 and 1.15) ranged from 33% to 61% smaller than the male area, with an average of 43.3% smaller. The female PCSA were significantly smaller than the male PCSA at all levels except L₁, which had very few observations.

The cross-sectional area of the female vertebral body (Table 1.16) was consistently smaller than that of the males, ranging from 20% to 27% smaller, averaging 24.4% smaller than that of the males. The trunk cross-sectional areas for the females (Table 1.17) ranged from 34% smaller to 6% smaller. The largest difference was at T₈ (34% smaller than the male trunk area), and the difference consistently decreased while descending the spine caudally to the smallest difference (6% smaller) at the S₁ level.

Comparisons between the results of this study and similar studies from the literature are also shown in Tables 1.2 through 1.17. Comparisons between the corrected cross-sectional areas by level between the males of this study and the male subjects from McGill et al. (15) found that across all muscles and levels, the absolute difference averaged 25.7%. After making the one-half vertebral level adjustment to the current dataset, the absolute percent difference dropped to 12.7%. Thus, adjusting for the difference in the scan levels between the two studies resulted in fairly good comparability for most of the muscle PCSAs between the two studies.

The study on elderly females by Chaffin et al. (1990) also set the scan slices through the intervertebral disc, at the L₂/L₃, L₃/L₄, and L₄/L₅ levels. When comparing the cross-sectional muscle area of the current study from the L₂, L₃, and L₄ levels with the muscle areas at the L₂/L₃, L₃/L₄, and L₄/L₅ levels, respectively, from the Chaffin et al. study (1990), the absolute percent difference was 31%. When using the midpoint adjusted area data for the current study, the absolute percent difference dropped only to 23.3%. Generally, the PCSAs for the latissimus

dorsi, rectus abdominis, and the external obliques for the current study were larger in comparison to the data from Chaffin et al. (1990), whereas, the PCSAs for the erector spinae, internal obliques, psoas major and quadratus lumborum were smaller than the cross-sectional areas of the females in Chaffin et al. (1990).

Coronal Plane Moment-Arms

The coronal plane moment-arms for the males and females, as well as those documented in other studies for comparison purposes are shown in Tables 1.18 through 1.31. The male moment-arms were significantly greater than the females at all levels for the latissimus dorsi and left erector spinae, and all but the lower three levels for the right erector spinae. Only the right rectus abdominis resulted in significant differences between males and females, whereas none of the levels were different on the left side. Five of the six levels resulted in significantly larger male moment-arms for the external obliques and the psoas major, and three of the four levels resulted in significantly larger male lateral moment-arms for the quadratus lumborum. Three of the four levels for the right internal oblique and two of the for levels for the left internal oblique resulted in larger male moment-arms.

The male coronal plane moment-arms of this study were very consistent with those reported in McGill et al. (1993), with an average absolute difference of 8.0%, which decreased to 5.5% when adjusting for the one-half vertebral level difference. The absolute percent difference between the coronal plane moment-arms were slightly larger when comparing the female data of the current study to those of the Chaffin et al. (1990) study. Without adjusting for the one-half vertebral level difference, the absolute percent difference was 11.2%, where the difference dropped to 8.6% when adjusting for the vertebral level difference. Generally, the moment-arms were smaller for all muscles except for the erector spinae, which were very similar to those of the elderly female population in the Chaffin et al. (1990) study.

Sagittal Plane Moment-Arms

The sagittal plane moment-arms for the males and females, as well as those documented in other studies for comparison purposes are shown in Tables 1.32 through 1.45. Compared to the coronal plane moment-arms, there were fewer significant differences between males and

females. For the latissimus dorsi, only the moment-arm at L₃ was significantly larger for the males; the remaining levels resulted in no significant differences. The majority of levels, however, for both sides of the erector spinae showed the males to have significantly larger sagittal plane moment-arms than the females. Only the moment-arm at the S₁ level was not significantly different between males and females for both right and left rectus abdominis. The results were mixed for the external and internal obliques as well as the psoas major; the left side of each muscle, however, did result in more significant differences than the right side, with the males exhibiting larger moment-arms than the females, except for the psoas major. Finally, there were no significant difference between the moment-arms for both the right and left quadratus lumborum.

The absolute percent differences between the sagittal plane moment-arms for the males of the current study and those of McGill et al. (1993) were much larger than the differences of the coronal plane moment-arms. Generally, the absolute percent difference between the two studies was 32.8%, which dropped to 23.6% when adjusting the data of the current study for the one-half vertebral level difference. Extremely large percent differences exist for the external obliques and the internal obliques, with the upper levels of the males in the current study having larger moment-arms and the lowest level having smaller moment-arms. Large average percent differences also resulted for the psoas major (75.2% and 52.2% for the right and left side, respectively), with the moment-arms for the males in the current study being smaller at each level (Tables 1.42 and 1.43). Aside from the left latissimus dorsi, (Table 1.33), the rest of the muscles resulted in absolute percent differences between 6.6% and 11.4% (5.6% and 6.3% when adjusting for the one-half vertebral difference).

The absolute percent difference between the females of the current study and those from Chaffin et al. (1990) was fairly large (32.0%), although this large difference was primarily driven by large percent differences between the psoas major. When accounting for the one-half vertebral difference, the absolute percent difference drops to 16.7%, where the difference between the sagittal plane moment-arms of the external and internal obliques increases the percent difference.

Muscle Vector Directions

The muscle vector directions for both males and females, in both the coronal and sagittal plane are shown in Tables 1.46 through 1.59. Additionally, the results of the *t*-tests for the statistical difference between the males and females by muscle and vertebral level are also shown. For the right latissimus dorsi (Tables 1.46), the sagittal plane vector angle was greater for the females than the males at T₁₂, whereas the males exhibited a greater anterior muscle vector at T₈ for the left latissimus dorsi (Table 1.47). For the erector spinae (Tables 1.48 and 1.49), there were significant differences between males and females at L₂ and L₃ for the left and right muscles for the coronal plane vector, and only at L₂ for the left erector spinae for the sagittal plane vector. Several differences existed between males and females for the rectus abdominis (Tables 1.50 and 1.51). The vector angle differences at L₁ and L₂ ranged from 1.8 to 9.4 degrees, with the male vector angles being more posterior in the sagittal plane than the females. For the right side, L₂ and L₄ showed significant differences for coronal plane vectors; for the left rectus abdominis, T₁₂, L₃ and L₅ were significantly different in the coronal plane between the genders. For the external obliques (Tables 1.52 and 1.53), the coronal plane vector at L₃ was significant for both the right and left sides, with the females exhibiting a larger lateral angle than the males. Additionally, the coronal plane vector at T₁₂ was significant for only the left external oblique. For the sagittal plane vectors, males exhibited greater posterior angles at T₁₂ for both right and left external oblique, as well as at L₂ and L₃ for the right external oblique. There were no gender differences for vectors in the sagittal plane for the internal obliques (Tables 1.54 and 1.55), however, the coronal plane vector at L₃ was significantly different for the right and left internal obliques, and at L₄ for the right internal oblique, with the females exhibiting a greater lateral angle of the muscle vector than the males. There were no significant differences for the right psoas major (Table 1.56), however, the vector at L₅ was significant in the coronal plane for the left psoas major (Table 1.57) as well as L₂ for the sagittal plane vector. For the quadratus lumborum (Tables 1.58 and 1.59), there was no difference between the genders in either plane for the right side, and the females exhibited a greater anterior sagittal plane vector for the left side at L₃. Finally, the females exhibited greater anterior angles than males between the T₁₀ and T₁₁, and the T₁₁ and T₁₂ vertebral levels (Table 1.60), although the differences were only 4.3 and 3.2 degrees, respectively. The females had a significantly larger posterior vector

angle between L₅ and S₁ than the males, with the females angle being 6.7 degrees greater in the posterior direction than the males.

Prediction of Largest Muscle Areas

Summary tables of significant regression equations for predicting largest cross-sectional areas, by muscle and gender are shown in Tables 1.61 through 1.64. The regression equations predicting cross-sectional area for the muscles are shown in Tables 1.65 through 1.71, with each table documenting a separate muscle. For the latissimus dorsi, use of the anthropometric measurements at the xyphoid process resulted in significant regression equations for females, with 33.5% to 37.2% of the variability in the PCSA explained. Similarly, for the males, the xyphoid process resulted in a significant regression equation predicting the left latissimus dorsi PCSA and the average of the largest of the right and left PCSA. None of the other anthropometric variables (i.e., iliac crest, trochanter, and BMI) resulted in significant regression equations predicting latissimus dorsi cross-sectional PCSA. When comparing the male and female regression equations, there were no significant differences between the male and female regression equations for those gender specific equations which significantly predicted muscle PCSAs.

The use of BMI and the xyphoid process measurements resulted in significant equations for the female erector spinae PCSA (Table 1.66), with R²'s between 0.423 and 0.443 for the xyphoid process, and between 0.424 and 0.468 for the BMI. For the male erector spinae PCSAs, use of the BMI and measurements about the trochanter resulted in significant regression equations, with R²'s between 0.409 and 0.451 for the trochanter, and 0.443 and 0.452 for the BMI. When comparing the gender specific regression equations, each regression equation (by anthropometric variable) for the females was significantly different than the regression equations for the males, thus indicating that the regression equations cannot be used interchangeably to predict male or female muscle erector spinae PCSA.

For prediction of the rectus abdominis PCSA (Table 1.67), the use of the BMI and measurements about the xyphoid process resulted in significant regression equations for the females, with R²'s ranging from 0.353 to 0.405 using the xyphoid process measurements and 0.251 and 0.258 for the BMI. The use of the BMI resulted in significant regression equations for

predicting male rectus abdominis PCSA (including the right and left side, as well as the average of the largest right and left side), with R^2 's ranging from 0.472 to 0.476. Investigation of differences between regression equations predicting male and female muscle PCSA resulted in no significant differences between the gender specific equations.

The use of the measurements about the xyphoid process resulted in significant regression equations predicting the right, left, and average of the right and left largest external oblique PCSA, for both females and males (Table 1.68). The R^2 's ranged from 0.194 to 0.228 for females, and 0.466 to 0.508 for males. The male and female regression equations were significantly different from each other when predicting the left cross-sectional area, and also the average of the right and left largest cross-sectional areas, and was marginally significant when predicting the right external oblique area ($p=0.0534$). Thus, the individual regression equations for the males and females are not interchangeable for predicting the largest PCSAs of the external obliques.

The use of the BMI and measurements about the xyphoid process resulted in significant regression equations predicting the PCSA of the internal obliques for the females (Table 1.69), with R^2 's ranging from 0.505 to 0.591 when using the xyphoid process, and ranging from 0.415 to 0.590 when using the BMI. The xyphoid process measurements resulted in significant regression equations for predicting male internal obliques PCSA for the right ($R^2=0.470$) and the average of the right and left side ($R^2=0.493$), whereas the BMI significantly predicted the left internal oblique PCSA. When comparing the gender specific regression equations, there were no significant differences between the gender specific equations when using measurements about the xyphoid process, however, the use of the BMI did result in significant differences in gender specific equations for the left and average of the right and left PCSA.

As shown in Table 1.70, none of the anthropometric variables used to predict the psoas major PCSA resulted in significant regressions for females, and only the measures about the xyphoid process significantly predicted PCSAs for males. The use of measurements about the xyphoid process resulted in significant regression equations predicting the PCSA of the quadratus lumborum (Table 1.71) for the right and left sides, as well as the average of the largest right and left areas for the females only (R^2 's ranged from 0.269 to 0.329). The measurements about the trochanter resulted in significant regression equations predicting the right and left

PCSAs as well as the average of the right and left PCSA for males (R^2 's ranged from 0.453 to 0.561). Finally, the male and female regression equations were significantly different from each other for PCSA predicted, as well as for each anthropometric variable used to predict the PCSAs.

Prediction of Muscle Moment-Arms

Summary statistics (p-values) for the prediction of female moment-arms at the origin and insertion in both the coronal and sagittal plane, from external anthropometric measurements are shown in Table 1.72 to 1.75. Generally, there were no significant prediction equations of the moment-arms at the origin (L_5) in the sagittal plane for females, and only the right external oblique was predicted by any external anthropometric measure (trunk width at the xyphoid process). Summary statistics for prediction of male moment-arms at the origin and insertion in both the coronal and sagittal plane, from external anthropometric measurements are shown in Table 1.76 to 1.79. The resulting regression equations for each muscle, plane, and gender are shown in Table 1.80 to 1.89. For the latissimus dorsi (Tables 1.80 and 1.81), the trunk depth and width measures at the iliac crest did not result in any significant associations for females. Generally, the xyphoid process and BMI resulted in significant predictions of the coronal plane moment-arm for both sides for females. The BMI was significant for the coronal plane male moment-arm at the origin of the right latissimus dorsi, and also for the coronal plane moment-arm of the left latissimus dorsi at the insertion. For the erector spinae (Tables 1.82 and 1.83), there were no significant regression equations for moment-arms for either gender for the left erector spinae, and only the sagittal plane moment-arm at the insertion for females and coronal plane moment-arm for males at the insertion resulted in significant predictions. The regression equations predicting coronal and sagittal plane moment-arms for the rectus abdominis (Tables 1.84 and 1.85) resulted in several significant associations. The most consistent predictions occurred for the moment-arms in the sagittal plane at the insertion, for both males and females, for both the right and left side. The trunk depth measured at the xyphoid process and the BMI significant for both sides. Prediction of right and left external oblique moment-arms in the coronal plane at the origin and insertion for males resulted in several significant anthropometric variables, including the trunk depth measured at the xyphoid process and iliac crest, as well as the BMI (Tables 1.86 and 1.87). Essentially, only the coronal plane female moment-arms at the

insertion were significant, with the trunk width measured at the xyphoid process and the BMI resulting in significant regression equations (Tables 1.86 and 1.87). Finally, the trunk width and depth measures at the xyphoid process and the BMI were significant predictors of both coronal and sagittal plane moment-arms for the right and left internal obliques for the females at the insertion level (Tables 1.88 and 1.89).

Differences between Right and Left Muscle Areas

The mean difference between the largest right and left muscle PCSAs, for both males and females are shown in Table 1.90. Both males and females exhibited significantly larger right side than left side for the latissimus dorsi. The external obliques were significantly larger on the right side than the left for the females, where the left side was significantly larger for the psoas major and quadratus lumborum. No other significant differences between the sides existed for the males. The Analysis of Variance on the differences between the right and left side cross-sectional areas by vertebral level for both females and males are shown in Table 1.91. There were significant differences between the right and left cross-sectional areas for the latissimus dorsi for both the females and males, and the quadratus lumborum for only the females. Post-hoc tests found that these differences occurred at the T₈ through T₁₀ levels for both males and females for the latissimus dorsi, with the right side being larger than the left side (Table 1.87). For the quadratus lumborum muscle, post-hoc tests found that the left side was significantly larger than the right side for levels L₃ and L₄ for the females. The magnitude and percent difference between the right and left sides for each muscle group are shown in Table 1.93 for the females, and 1.94 for the males. Significant differences found from the Tukey pairwise comparisons are also shown, which correspond to the significant levels and sides shown in Table 1.92.

Muscle Vector Locations

The locations of the components of the muscle vectors in the coronal and sagittal plane at the origin specified by the EMG-assisted model (L₅) for each of the five pairs of muscles are shown in Tables 1.95 to 1.97. Each of the values in these tables represents the coefficient in which the external anthropometric measure is multiplied by to estimate the distance of the vector from the vertebral body centroid in the coronal plane. In Tables 1.95 through 1.97, the

coefficients for the latissimus dorsi, erector spinae, and rectus abdominis are all the same, however, the vector locations at the origin for the external and internal obliques were determined differently. In Table 1.95, the vectors were projected through L₅ using the vector at the angle between L₁ and L₄ for the external obliques, and L₃ and L₄ for the internal obliques. In Table 1.96, the internal obliques are the same as in Table 1.95, however, the external obliques were projected at a anterior/caudal 45 degree angle from the centroid at L₄ to L₅. In Table 1.97, the internal obliques were projected from the L₄ centroid to L₅ at a posterior/caudal 45 degree angle. These angles for the external and internal oblique represent estimates of the muscle fiber angle rather than the vectors determined from the centroid. The vector coefficients for the origins (Tables 1.95 to 1.97) are all very similar, for both males and females, whether using the iliac crest or the xyphoid process external anthropometric measures. Inspection of differences between males and females indicate that the female centroid for the external and internal obliques lies relatively more lateral from the spine centroid than for males. Similarly, the centroid locations for the latissimus dorsi and erector spinae lie relatively more posterior to the spine centroid for females than males, as a function of the trunk depth measured at the xyphoid process. The effect of using different vector directions for the external and internal obliques are evident when observing the resulting coefficients in Tables 1.95 to 1.97. When the 45 degree angle was used for the external oblique, the vector location at the origin is further in the anterior direction than when using the vector direction determined from the muscle centroids. In Table 1.97, using the 45 degree angle for the internal vector direction, the coefficients indicate they lie posterior to the vertebral centroid, rather than anterior to the vertebral centroid when using the muscle centroid method. The posterior location of the vector at the origin is consistent with the assumption that the internal oblique functions as an extensor of the spine (Marras and Granata, 1997). Viewing the insertion vector locations for both the iliac crest and xyphoid process (Table 1.98), the coefficients are all very similar between the iliac crest and xyphoid process, for both males and females. Slight differences exist between the male and female insertion vector locations, where the largest differences occur between the iliac crest coefficients for the rectus abdominis in the sagittal plane (females exhibiting a smaller ratio of A/P moment-arm to trunk depth than males).

Distribution of the Largest Muscle Area

The distribution of the largest muscle PCSA for both the right and left pairs of each muscle, as a function of vertebral level are shown in Tables 1.99 through 1.105. Although there was some variability between the right and left pairs of each muscle as far as which vertebral levels had the highest percentage of the largest PCSAs, as well as which levels had the largest PCSA present, general trends did exist. For the latissimus dorsi (Table 1.99), the largest PCSA occurred mostly at the T₈ level, with very few at T₉. The largest PCSA for the erector spinae were generally split between L₃ and L₄, with a few located at L₂ and L₅ (Table 1.100). The largest PCSA location for the rectus abdominis indicated a large variability for both males and females (Table 1.101). For the females, the largest PCSA generally occurred at S₁ for the right side, and L₅ and S₁ for the left side, with a few at several other levels. For the males, 60% of the largest PCSAs were at S₁ for the right side, and was evenly distributed between the L₃, L₅ and S₁ levels for the left side. For both male and females, the largest external oblique PCSA for the right and left sides were generally located at L₃ and L₄ (Table 1.102). The largest internal obliques PCSA (Table 1.103) generally were located at L₄, with a few also located at L₂ and L₃. The largest PCSA for the quadratus lumborum (Table 1.104) was typically found at L₄, with a few distributed across L₂, L₃ and L₅. Finally, the largest PCSA for the psoas major (Table 1.105) were found between L₄ and L₅, with a few also found at the S₁ level. major.

Discussion

Female Data

The database of muscle cross-sectional areas, moment-arms from the vertebral centroid, and muscle vector angles represent the largest and most complete database for the females to date, as well as for male to female comparisons. The female areas for the latissimus dorsi, rectus abdominis and external obliques are larger than those quantified by Chaffin et al. (1990), whereas the areas were smaller for the erector spinae, internal obliques, psoas major and quadratus lumborum were smaller than Chaffin et al. (1990), even after adjusting the areas by one-half of a vertebral level. The scans in Chaffin et al. (1990) were taken by computed tomography (CT), and the separation between muscles or the muscle borders may not have been

as clear as when using MRI technology. Additionally, the female subjects in Chaffin et al (1990) were elderly females, with a mean age of 49 yrs, compared to 25.3 yrs in the current study, which may show up as muscle atrophy in the elderly population for some of the muscles.

Differences also existed for the moment-arms in both planes between the females from Chaffin et al. (1990) and the current study. Generally, all the coronal plane moment-arms in the current study were smaller than from Chaffin et al. (1990), with the one-half level adjustment making better comparisons only for the psoas major and quadratus lumborum. The sagittal plane moment-arms for the current study showed no apparent patterns. The erector spinae moment-arms of the current study were slightly smaller than those in Chaffin et al. (1990), with the one-half level adjustment not making much difference for comparability, and the rectus abdominis were smaller at the lower two levels of comparison for the current study, again the one-half level adjustment not making much difference. The external and internal obliques, as well as the psoas major were both smaller and larger, depending on the level of comparison, with the one-half level of adjustment decreasing the differences between the two studies. The differences between the moment-arm distances between the two studies may have been influenced by the different scan techniques, with Chaffin et al (1990) using CT technology versus MRI in the current study. The use of MRI technology, again, may increase the clarity of the muscle border and spine border locations, which can affect the resulting distances between the centroids of the objects of interest.

Differences in the moment-arm distances may also exist due to possible age-related differences such as increases in body mass. The females in Chaffin et al. (1990) average 49.6 years compared to 25.0 yrs for the current study, with the elderly females being shorter (163.1 cm vs 165.5 cm) and heavier (67.6 kg vs 57.9 kg) than the females of the current study. This indicates that the elderly females had a higher BMI, or more soft tissue, which may increase the distance between the spine and certain muscles, depending on the deposit locations of adipose tissue. The larger BMI of the elderly female populations is also consistent with observation that the trunk cross-sectional areas at the three levels of comparison, with the females of the current study averaging 23% less cross-sectional area at the levels of comparison than the older females in the Chaffin et al. (1990) study.

Male Data

The largest database for comparison purposes to the male data in the current study was from McGill et al. (1993), which quantified the muscle cross-sectional areas and moment-arms from T₅/T₆ through L₅/S₁, also with the use of MRI technology. Generally, when correcting for the one-half of a level difference of the location of the scan slices, the cross-sectional areas of similar muscles were fairly consistent between the two studies for the latissimus dorsi, erector spinae, rectus abdominis (Tables 1.2 through 1.7), and the psoas major (Tables 1.12 and 1.13), with average percent differences ranging from 6% to 12.8% between similar muscles at similar levels. Larger differences existed between the external and internal obliques (Tables 1.8 through 1.11), as well as the quadratus lumborum (Tables 1.14 and 1.15), between the two studies.

Comparisons of the lateral moment-arms between the males of the current study and those of McGill et al. (1993) found that the moment-arm distances were all very comparable, with most of the differences ranging from an average of 2.8% difference (left psoas major) to a 6.2% difference (left rectus abdominis). Only the right rectus abdominis and left quadratus lumborum resulted in larger differences between the two studies (15.5% and 9.0%, respectively). The differences between the sagittal moment-arms, however, were much higher between similar muscles and scan levels between the males from the current study and those of McGill et al. (1993). The erector spinae and rectus abdominis sagittal moment-arms were very similar between the two studies. However, the left latissimus dorsi (30.8%), the external obliques (14.3% and 25.2%, for right and left, respectively), internal obliques (26.7% and 30%, for right and left, respectively), and the psoas major (81.8% and 53.8%, for right and left, respectively), had fairly large absolute percent differences. The large percent differences between the psoas major can be attributed to the small moment-arms, where slight differences would result in large percent differences.

The differences between the internal and external obliques, and the quadratus lumborum for the PCSAs and some of the moment-arms, however, may have resulted from the differences in the vector directions used to obtain the PCSA. In the current study, the centroid method was used to represent the vector direction of muscle force. However, McGill et al. (1993) utilized muscle fiber directions rather than the centroids. These resulted in different angles used for the

adjustment from raw CSAs to PCSAs between the two studies, and thus result in different PCSAs and moment-arms.

Females vs. Males

As expected, the comparisons of the PCSAs, coronal and sagittal plane moment-arms, as well as the muscle vector directions in both the coronal and sagittal planes resulted in many significant differences between the two genders. The importance of these differences may, however, be illuminated when trying to predict the PCSAs of the males and females based upon external anthropometry, or in other words, normalizing the PCSAs, as well as the moment-arms in both the coronal and sagittal planes, to measurable external anthropometry variables. The current EMG-assisted biomechanical model (Granata and Marras, 1993; Marras and Granata, 1995; Marras and Sommerich, 1991a,b) uses coefficients which are multiplied by the trunk width to estimate the coronal plane moment-arms, and trunk depth to estimate the sagittal plane moment-arm, where the trunk width and depth are measured at the iliac crest. Additionally, the product of the trunk width and trunk depth measured at the iliac crest is used to predict the cross-sectional areas of the trunk muscles. However, the use of trunk width and trunk measurements at the iliac crest to predict the PCSA of each of the 10 trunk muscles, as well as the average of the right and left muscles for each of the five pairs of muscles resulted in no significant regression equations for females (Tables 1.61 and 1.62), nor for the males (Tables 1.63 and 1.64). Typically, the measures about the xyphoid process did much better at predicting the largest PCSAs, for both males and females. As shown in Table 1.63, use of the male xyphoid process measures resulted in significant prediction equations of the PCSAs ($p \leq 0.05$) for all but the erector spinae, rectus abdominis and quadratus lumborum, with the erector spinae and rectus abdominis equations approaching significance ($p = 0.0871$ and $p = 0.0742$, respectively). For the females (Table 1.61), the measures about the xyphoid process resulted in significant prediction equations for PCSAs for all but the psoas major. When using measures about the xyphoid process, the percent of the variance of the PCSA explained were somewhat modest, however, ranging from 22.8% to 50.5% for the average of the right and left muscles for the females, and 19.4% to 59.1% for each of the individual muscles for the females. These values, however, are much higher than when using the measures about the iliac crest, where 1.1% to 14.3% of the

variance of the PCSA was explained when predicting the average of the largest right and left muscles; when predicting the individual muscle PCSAs, only 0.4% to 14.3% of the variance was explained for females using the measures about the iliac crest. Thus, the use of measures about the xyphoid process provided better prediction of the largest PCSA for both the females and the males than when using the iliac crest anthropometric measurements.

The use of measures about the iliac crest to predict moment-arms in the coronal and sagittal plane showed very poor results for females and males. For the females, only the right external oblique resulted in a significant predicted moment-arm at the origin, which was based on the trunk width in the coronal plane (Table 1.72). The use of trunk depth and width measures about the xyphoid process resulted in more significant prediction equations for moment-arms at the insertion. Both anthropometric measures significantly predicted the moment-arms in the coronal plane for the latissimus dorsi, and external and internal obliques (Table 1.74), and also for the rectus abdominis and internal obliques for the moment-arms in the sagittal plane (Table 1.75). For the males, the measures about the iliac crest and xyphoid process resulted in no significant prediction equations for the right and left pairs of the latissimus dorsi and erector spinae for the sagittal moment-arms at both the origin and insertion levels, as well as no significant regression equations for the internal and external obliques at the insertion levels (L_3 for internal obliques, and L_1 for external obliques). The rest of the muscles showed inconsistent associations or no associations to trunk width or trunk depth measurements either at the iliac crest or the xyphoid process. Therefore, the use of measures about the xyphoid process to predict moment-arms, although not consistent across all muscles, performs better at predicting moment-arms than using measures about the iliac crest, for females as well as males.

Most of the male PCSAs were significantly larger than those of the females. However, when normalizing the PCSAs to external anthropometric measures of the trunk width multiplied by the trunk depth, fewer differences resulted. Specifically, the separate regression equations predicting the PCSAs were significantly different for the erector spinae, external and internal obliques, and the psoas major and quadratus lumborum, but not for the rectus abdominis or latissimus dorsi muscles. Given that the erector spinae are the major extensor muscles which raise the torso during lifting activities, and that the external and internal obliques are involved during twisting activities, it is necessary that the development of the EMG-assisted

biomechanical model for females be developed using the female specific regression equations predicting cross-sectional muscle areas.

The external obliques exhibited greater lateral angles for the females than the males between the L_3 and L_4 vertebral levels, with differences of about 7 degrees (Tables 1.52 and 1.53). The internal obliques also showed larger differences in the lateral vector angles for the lower levels as well (L_3 and L_4), with differences ranging from 5.6 to 14.3 degrees, with the females exhibiting vector angles more lateral from the L_3 to L_5 vertebral levels than the males (Tables 1.54 and 1.55). Thus, these differences in vector angles between males and females near the L_5 vertebral level indicates that the contribution of the external and internal obliques to the loading on the spine may be different between the males and females for similar motions and exertion levels.

Right and Left Side Symmetry

Results of the statistical analysis revealed several differences between the PCSAs for both the males and females. Both males and females exhibited significantly larger right side latissimus dorsi muscle area when considering just the largest PCSAs (Table 1.90). Additionally, there existed statistically larger right side than left side PCSAs for both males and females for the more superior levels scanned (1.91 and 1.92). The findings of McGill et al. (1993) also support the existence of larger right than left side cross-sectional areas, although this difference was not tested statistically, and this was only for males. Thus, the influence of the force generating capability of the muscles may be influenced by the direction of the exertion (right or left side), as well as the type of exertion which would have an influence on the muscle groups recruited.

Muscle Vector Locations

As shown in Tables 1.95 to 1.98, the muscle vector locations for males and females, as a function of external anthropometric measurements are given for each of the ten muscles used in the EMG-assisted biomechanical model, as a function of external anthropometric measurements. Generally, there were very small differences between the coefficients determined from the iliac crest and from the xyphoid process at the muscle origins (L_5). Differences between the

coefficients for males and females were very small, generally in the 1 to 3% range. However, a large difference existed at the origin for the external and internal obliques, with the females vector location lying more lateral than the males vector location when the xyphoid process trunk width measurement was used. This is consistent with the observation of females possessing greater hip breadth than men (9), as well as the observation of the females in this study exhibiting larger lateral vector angles in the lower lumbar area than males (Tables 1.54 to 1.57).

Additionally, the female coefficients at the insertion level were smaller than the males for the rectus abdominis in the sagittal plane when using the trunk depth measured at the iliac crest as a reference (Table 1.98). This is consistent with the findings of Reid and Costigan (1987) who found the females exhibited smaller sagittal moment-arm to trunk depth ratios than males, with the trunk depth measured at the L₅ level. Thus, these gender differences in muscle vector location indicates that the loading directions may be different depending on the direction of the exertion (e.g., flexion for the rectus abdominis or twisting or extension for the internal obliques), or as increases in coactivity occur, which would influence the loading on the spine (Granata and Marras, 1995).

Table 1.1. Female and Male Subject mean (s.d.) anthropometric measurements.

Gender	Age (yrs)	Height (cm)	Weight (kg)	Trunk Depth at Trochanter (cm)	Trunk Width at Trochanter (cm)	Trunk Depth at Iliac Crest (cm)	Trunk Width at Iliac Crest (cm)	Trunk Depth at Xyphoid Process (cm)	Trunk Width at Xyphoid Process (cm)	Trunk Circumference at Iliac Crest (cm)	Right Trochanter Height (cm)	Left Trochanter Height (cm)	Body Mass Index (kg/m ²)
Female (N=20)	25.0 (7.2)	165.5 (5.9)	57.9 (6.4)	23.1 (2.1)	33.7 (1.9)	19.8 (2.1)	28.0 (2.4)	18.4 (1.8)	27.0 (1.9)	76.0 (5.7)	85.3 (9.0)	86.7 (5.0)	21.2 (2.5)
Male (N=10)	26.4 (5.5)	175.9 (9.1)	79.8 (13.3)	25.4 (2.1)	34.8 (2.4)	22.3 (2.2)	30.3 (2.2)	22.9 (2.2)	32.4 (2.0)	86.8 (7.5)	89.0 (6.8)	88.8 (6.6)	25.7 (2.3)

Table 1.2. Mean (s.d.) trunk muscle physiological cross-sectional area of the Right Latissimus Dorsi. Data collected (OSU) are compared with literature values for males and females. Differences between literature values and the current data are described in terms of area and as a percent of the literature values []. Absolute and percent differences in muscle areas between male and female subjects are also shown.

Right Latissimus Dorsi - Physiological Cross-Sectional Area

Level	OSU Male mean ^A (s.d.)	McGill et al., (1993) mean ^A (s.d.)	Difference ^A [% Diff.]	Difference ^D [% Diff.]	OSU Female mean ^A (s.d.)	Chaffin et al., (1990) mean ^A (s.d.)	Difference ^A [% Diff.]	Difference ^D [% Diff.]	Female vs Male ^{B,C} [% Diff.]
T8	2205 (520)	1581 (159)	624 [39]	522 [33]	1350 (472)				-855 [-39]
T9	2000 (465)	1458 (269)	542 [27]	388 [27]	1181 (550)				-819 [-41]
T10	1692 (487)	1368 (330)	324 [19]	221 [16]	1020 (534)				-672 [-40]
T11	1486 (454)	1254 (281)	232 [19]	124 [10]	903 (522)				-583 [-39]
T12	1269 (396)	1014 (264)	255 [25]	87 [9]	772 (455)				-497 [-39]
L1	932 (260)	717 (260)	215 [30]	72 [10]	546 (307)				-386 [-41]
L2	646 (206)	429 (202)	217 [51]	35 [8]	345 (193)	120 (40)	225 [188]	125 [104]	-301 [-47]
L3	282 (153)	232 (192)	50 [22]		144 (68)	130 (40)	14 [11]		-138 [-49]
L4						130 (50)			
L5									
S1									

A: Square mm;

B: Female minus Male (Square mm);

C: Shaded cells represent significant difference between females and males ($p \leq 0.05$);

D: Comparisons based on data adjusted one-half of a vertebral level.

Table 1.3. Mean (s.d.) trunk muscle physiological cross-sectional area of the Left Latissimus Dorsi. Data collected (OSU) are compared with literature values for males and females. Differences between literature values and the current data are described in terms of area and as a percent of the literature values []. Absolute and percent differences in muscle areas between male and female subjects are also shown.

Left Latissimus Dorsi - Physiological Cross-Sectional Area

Level	OSU Male mean ^A (s.d.)	McGill et al., (1993) mean ^A (s.d.)	Difference ^A [% Diff.]	Difference ^B [% Diff.]	OSU Female mean ^A (s.d.)	Chaffin et al., (1990) mean ^A (s.d.)	Difference ^A [% Diff.]	Difference ^B [% Diff.]	Female vs Male ^{B,C} [%Diff.]
T8	1988 (608)	1582 (281)	406 [26]	314 [20]	1210 (496)				-778 [-39]
T9	1804 (462)	1417 (293)	387 [27]	253 [18]	1080 (530)				-724 [-40]
T10	1535 (484)	1239 (257)	296 [24]	245 [20]	939 (512)				-596 [-39]
T11	1433 (476)	1102 (316)	331 [30]	202 [18]	863 (494)				-570 [-40]
T12	1175 (421)	960 (310)	215 [22]	83 [9]	729 (441)				-446 [-38]
L1	910 (294)	682 (260)	228 [33]	84 [12]	572 (312)				-338 [-37]
L2	621 (243)	372 (161)	249 [67]	81 [22]	365 (252)	140 (60)	225 [161]	126 [90]	-256 [-41]
L3	284 (158)	256 (217)	28 [11]		166 (75)	130 (50)	36 [28]		-118 [-42]
L4						150 (60)			
L5									
S1									

A: Square mm;

B: Female minus Male (Square mm);

C: Shaded cells represent significant difference between females and males ($p \leq 0.05$);

D: Comparisons based on data adjusted one-half of a vertebral level.

Table 1.4. Mean (s.d.) trunk muscle physiological cross-sectional area of the Right Erector Spinae. Data collected (OSU) are compared with literature values for males and females. Differences between literature values and the current data are described in terms of area and as a percent of the literature values []. Absolute and percent differences in muscle areas between male and female subjects are also shown.

Right Erector Spinae - Physiological Cross-Sectional Area

Level	OSU Male mean ^A (s.d.)	McGill et al., (1993) mean ^A (s.d.)	Difference ^A [% Diff.]	Difference ^B [% Diff.]	OSU Female mean ^A (s.d.)	Chaffin et al., (1990) mean ^A (s.d.)	Difference ^A [% Diff.]	Difference ^B [% Diff.]	Female vs Male ^{B,C} [%Diff.]
T8	1291 (216)	1049 (201)	242 [23]	283 [27]	760 (166)				-531 [-41]
T9	1372 (248)	1413 (304)	-41 [-3]	26 [2]	834 (169)				-538 [-39]
T10	1506 (281)	1690 (210)	-184 [-11]	-92 [-5]	944 (183)				-562 [-37]
T11	1713 (275)	1832 (282)	-119 [-7]	-6 [0]	1076 (238)				-637 [-37]
T12	1938 (293)	2614 (584)	-676 [-26]	-511 [-20]	1151 (248)				-787 [-41]
L1	2267 (362)	2615 (405)	-348 [-13]	-156 [-6]	1370 (325)				-897 [-40]
L2	2651 (435)	2854 (547)	-203 [-7]	-125 [-4]	1601 (373)	1820 (270)	-219 [-12]	-157 [-9]	-1050 [-40]
L3	2807 (412)	2831 (458)	-24 [-1]	-48 [-2]	1725 (411)	1850 (300)	-125 [-7]	-144 [-8]	-1082 [-39]
L4	2758 (321)	2151 (539)	607 [28]	98 [5]	1687 (332)	1740 (300)	-53 [-3]	-411 [-24]	-1071 [-39]
L5	1740 (625)	905 (331)	835 [92]	361 [40]	972 (391)				-768 [-44]
S1	792 (144)				493 (98)				-299 [-38]

A: Square mm;

B: Female minus Male (Square mm);

C: Shaded cells represent significant difference between females and males ($p \leq 0.05$);

D: Comparisons based on data adjusted one-half of a vertebral level.

Table 1.5. Mean (s.d.) trunk muscle physiological cross-sectional area of the Left Erector Spinae. Data collected (OSU) are compared with literature values for males and females. Differences between literature values and the current data are described in terms of area and as a percent of the literature values []. Absolute and percent differences in muscle areas between male and female subjects are also shown.

Left Erector Spinae - Cross-Sectional Area

Level	OSU Male mean ^A (s.d.)	McGill et al., (1993) mean ^A (s.d.)	Difference ^A [% Diff.]	Difference ^B [% Diff.]	OSU Female mean ^A (s.d.)	Chaffin et al., (1990) mean ^A (s.d.)	Difference ^A [% Diff.]	Difference ^B [% Diff.]	Female vs Male ^{B,C} [%Diff.]
T8	1301 (225)	1129 (100)	172 [15]	214 [19]	781 (160)				-520 [-40]
T9	1384 (238)	1471 (351)	-87 [-6]	8 [1]	836 (188)				-548 [-40]
T10	1574 (303)	1722 (279)	-148 [-9]	-44 [-3]	957 (230)				-617 [-39]
T11	1782 (352)	2041 (285)	-259 [-13]	-167 [-8]	1082 (250)				-700 [-39]
T12	1966 (345)	2601 (559)	-635 [-24]	-480 [-18]	1184 (264)				-782 [-40]
L1	2275 (374)	2723 (428)	-448 [-16]	-269 [-10]	1400 (299)				-875 [-38]
L2	2633 (420)	2833 (456)	-200 [-7]	-100 [-4]	1614 (362)	1790 (310)	-176 [-10]	-111 [-6]	-1019 [-39]
L3	2833 (455)	2933 (382)	-100 [-3]	-136 [-5]	1743 (357)	1850 (300)	-107 [-6]	-112 [-6]	-1090 [-38]
L4	2760 (381)	2234 (476)	526 [24]	43 [2]	1732 (322)	1730 (300)	-2 [0]	-387 [-22]	-1028 [-37]
L5	1793 (585)	986 (338)	807 [82]	321 [33]	954 (377)				-839 [-48]
S1	821 (129)				518 (114)				-303 [-37]

A: Square mm;

B: Female minus Male (Square mm);

C: Shaded cells represent significant difference between females and males ($p \leq 0.05$);

D: Comparisons based on data adjusted one-half of a vertebral level.

Table 1.6. Mean (s.d.) trunk muscle physiological cross-sectional area of the Right Rectus Abdominis. Data collected (OSU) are compared with literature values for males and females. Differences between literature values and the current data are described in terms of area and as a percent of the literature values []. Absolute and percent differences in muscle areas between male and female subjects are also shown.

Right Rectus Abdominis - Physiological Cross-Sectional Area

Level	OSU Male mean ^A (s.d.)	McGill et al., (1993) mean ^A (s.d.)	Difference ^A [% Diff.]	Difference ^B [% Diff.]	OSU Female mean ^A (s.d.)	Chaffin et al., (1990) mean ^A (s.d.)	Difference ^A [% Diff.]	Difference ^B [% Diff.]	Female vs Male ^{B,C} [%Diff.]
T8									
T9									
T10									
T11									
T12	555 (171)				409 (78)				-146 [-26]
L1	614 (160)	576 (151)	38 [7]	20 [3]	478 (103)				-136 [-22]
L2	577 (102)	712 (239)	-135 [-19]	-69 [-10]	418 (118)	330 (160)	88 [27]	99 [30]	-159 [-28]
L3	709 (266)	670 (133)	39 [6]	37 [6]	439 (131)	370 (110)	69 [19]	93 [25]	-270 [-38]
L4	704 (223)	750 (207)	-46 [-6]	24 [3]	487 (173)	400 (100)	87 [22]	110 [28]	-217 [-31]
L5	843 (206)	787 (250)	56 [7]	72 [9]	532 (150)				-311 [-37]
S1	874 (241)				587 (216)				-287 [-33]

A: Square mm;

B: Female minus Male (Square mm);

C: Shaded cells represent significant difference between females and males ($p \leq 0.05$);

D: Comparisons based on data adjusted one-half of spine level.

Table 1.7. Mean (s.d.) trunk muscle physiological cross-sectional area of the Left Rectus Abdominis. Data collected (OSU) are compared with literature values for males and females. Differences between literature values and the current data are described in terms of area and as a percent of the literature values []. Absolute and percent differences in muscle areas between male and female subjects are also shown.

Left Rectus Abdominis - Physiological Cross-Sectional Area

Level	OSU Male mean ^A (s.d.)	McGill et al., (1993) mean ^A (s.d.)	Difference ^A [% Diff.]	Difference ^D [% Diff.]	OSU Female mean ^A (s.d.)	Chaffin et al., (1990) mean ^A (s.d.)	Difference ^A [% Diff.]	Difference ^D [% Diff.]	Female vs Male ^{B,C} [%Diff.]
T8									
T9									
T10									
T11									
T12	591 (188)				450 (92)				-141 [-24]
L1	641 (206)	514 (99)	127 [25]	105 [20]	484 (108)				-157 [-24]
L2	597 (134)	748 (240)	-151 [-20]	-70 [-9]	434 (131)	340 (120)	94 [28]	100 [29]	-163 [-27]
L3	758 (267)	693 (177)	65 [9]	27 [4]	446 (126)	370 (120)	76 [21]	105 [28]	-312 [-41]
L4	682 (236)	746 (181)	-64 [-9]	26 [3]	503 (221)	410 (120)	93 [23]	47 [11]	-179 [-26]
L5	861 (232)	802 (247)	59 [57]	60 [7]	539 (129)				-322 [-37]
S1	863 (225)				605 (238)				-258 [-30]

A: Square mm;

B: Female minus Male (Square mm);

C: Shaded cells represent significant difference between females and males ($p \leq 0.05$);

D: Comparisons based on data adjusted one-half of spine level.

Table 1.8. Mean (s.d.) trunk muscle physiological cross-sectional area of the Right External Obliques. Data collected (OSU) are compared with literature values for males and females. Differences between literature values and the current data are described in terms of area and as a percent of the literature values []. Absolute and percent differences in muscle areas between male and female subjects are also shown.

Right External Obliques - Physiological Cross-Sectional Area

Level	OSU Male mean ^A (s.d.)	McGill et al., (1993) mean ^{A,E} (s.d.)	Difference ^A [% Diff.]	Difference ^D [% Diff.]	OSU Female mean ^A (s.d.)	Chaffin et al., (1990) mean ^A (s.d.)	Difference ^A [% Diff.]	Difference ^D [% Diff.]	Female vs Male ^{B,C} [%Diff.]
T8									
T9									
T10									
T11									
T12	622 (159)				486 (110)				-136 [-22]
L1	797 (178)				539 (112)				-258 [-32]
L2	849 (179)	1158 (222)	-309 [-27]	-220 [-19]	619 (133)	370 (120)	249 [67]	291 [79]	-230 [-27]
L3	1026 (210)	1121	-95 [-8]	-69 [-6]	702 (100)	440 (140)	262 [60]	258 [59]	-324 [-32]
L4	1078 (201)	915 (199)	163 [18]	5 [1]	693 (115)	460 (140)	233 [51]	179 [39]	-385 [-36]
L5	761 (301)				585 (185)				-176 [-23]
S1									

A: Square mm;

B: Female minus Male (Square mm);

C: Shaded cells represent significant difference between females and males ($p \leq 0.05$);

D: Comparisons based on data adjusted one-half of spine level.

E: Cross-sectional area at L3/L4 (shown as L3 in the table) corrected for muscle fiber direction.

Table 1.9. Mean (s.d.) trunk muscle physiological cross-sectional area of the Left External Obliques. Data collected (OSU) are compared with literature values for males and females. Differences between literature values and the current data are described in terms of area and as a percent of the literature values []. Absolute and percent differences in muscle areas between male and female subjects are also shown.

Left External Obliques - Physiological Cross-Sectional Area

Level	OSU Male mean ^A (s.d.)	McGill et al., (1993) mean ^{A,E} (s.d.)	Difference ^A [% Diff.]	Difference ^D [% Diff.]	OSU Female mean ^A (s.d.)	Chaffin et al., (1990) mean ^A (s.d.)	Difference ^A [% Diff.]	Difference ^D [% Diff.]	Female vs Male ^{B,C} [%Diff.]
T8									
T9									
T10									
T11									
T12	584 (119)				448 (66)				-136 [-23]
L1	751 (157)				499 (104)				-252 [-34]
L2	841 (197)	1351 (282)	-510 [-38]	-417 [-31]	597 (117)	550 (160)	47 [9]	87 [16]	-244 [-29]
L3	1026 (254)	1121	-95 [-8]	-55 [-5]	676 (120)	600 (140)	76 [13]	76 [13]	-350 [-34]
L4	1106 (226)	992 (278)	114 [11]	-26 [-3]	675 (103)	600 (160)	75 [13]	35 [6]	-431 [-39]
L5	826 (237)				594 (143)				-232 [-28]
S1									

A: Square mm;

B: Female minus Male (Square mm);

C: Shaded cells represent significant difference between females and males ($p \leq 0.05$);

D: Comparisons based on data adjusted one-half of spine level.

E: Cross-sectional area at L3/L4 (shown as L3 in the table) corrected for muscle fiber direction.

Table 1.10. Mean (s.d.) trunk muscle physiological cross-sectional area of the Right Internal Obliques. Data collected (OSU) are compared with literature values for males and females. Differences between literature values and the current data are described in terms of area and as a percent of the literature values []. Absolute and percent differences in muscle areas between male and female subjects are also shown.

Right Internal Obliques - Physiological Cross-Sectional Area

Level	OSU Male mean ^A (s.d.)	McGill et al., (1993) mean ^{A,E} (s.d.)	Difference ^A [% Diff.]	Difference ^D [% Diff.]	OSU Female mean ^A (s.d.)	Chaffin et al., (1990) mean ^A (s.d.)	Difference ^A [% Diff.]	Difference ^D [% Diff.]	Female vs Male ^{B,C} [%Diff.]
T8									
T9									
T10									
T11									
T12									
L1									
L2	279 (158)	1055 (173)	-776 [-74]	-549 [-52]	308 (185)	400 (140)	-92 [-23]	-37 [-9]	29 [10]
L3	733 (316)	1154	-421 [-36]	-287 [-25]	418 (193)	530 (130)	-112 [-21]	-21 [-4]	-315 [-43]
L4	1002 (269)	903 (83)	99 [11]	-186 [-21]	599 (160)	530 (180)	69 [13]	-14 [-3]	-403 [40]
L5	432 (575)				432 (138)				0 [0]
S1									

A: Square mm;

B: Female minus Male (Square mm);

C: Shaded cells represent significant difference between females and males ($p \leq 0.05$);

D: Comparisons based on data adjusted one-half of spine level.

E: Cross-sectional area at L3/L4 (shown as L3 in the table) corrected for muscle fiber direction.

Table 1.11. Mean (s.d.) trunk muscle physiological cross-sectional area of the Left Internal Obliques. Data collected (OSU) are compared with literature values for males and females. Differences between literature values and the current data are described in terms of area and as a percent of the literature values []. Absolute and percent differences in muscle areas between male and female subjects are also shown.

Left Internal Obliques - Physiological Cross-Sectional Area

Level	OSU Male mean ^A (s.d.)	McGill et al., (1993) mean ^{A,E} (s.d.)	Difference ^A [% Diff.]	Difference ^D [% Diff.]	OSU Female mean ^A (s.d.)	Chaffin et al., (1990) mean ^A (s.d.)	Difference ^A [% Diff.]	Difference ^D [% Diff.]	Female vs Male ^{B,C} [%Diff.]
T8									
T9									
T10									
T11									
T12									
L1									
L2	356 (177)	1027 (342)	-671 [-65]	-473 [-46]	297 (170)	430 (150)	-133 [-31]	-81 [-19]	-59 [-17]
L3	751 (305)	1154	-403 [-35]	-256 [-22]	401 (192)	580 (150)	-179 [-31]	-73 [-13]	-350 [-47]
L4	1046 (279)	900 (115)	146 [16]	-68 [-8]	612 (130)	520 (150)	92 [17]	32 [6]	434 [-41]
L5	618 (167)				492 (177)				-126 [-20]
S1									

A: Square mm;

B: Female minus Male (Square mm);

C: Shaded cells represent significant difference between females and males ($p \leq 0.05$);

D: Comparisons based on data adjusted one-half of spine level.

E: Cross-sectional area at L3/L4 (shown as L3 in the table) corrected for muscle fiber direction.

Table 1.12. Mean (s.d.) trunk muscle physiological cross-sectional area of the Right Psoas Major. Data collected (OSU) are compared with literature values for males and females. Differences between literature values and the current data are described in terms of area and as a percent of the literature values []. Absolute and percent differences in muscle areas between male and female subjects are also shown.

Right Psoas Major - Physiological Cross-Sectional Area

Level	OSU Male mean ^A (s.d.)	McGill et al., (1993) mean ^A (s.d.)	Difference ^A [% Diff.]	Difference ^D [% Diff.]	OSU Female mean ^A (s.d.)	Chaffin et al., (1990) mean ^A (s.d.)	Difference ^A [% Diff.]	Difference ^D [% Diff.]	Female vs Male ^{B,C} [%Diff.]
T8									
T9									
T10									
T11									
T12		330 (210)							
L1	255 (--)	513 (329)			217 (126)				-38 [-15]
L2	676 (234)	1177 (285)	-501 [-43]	-199 [-17]	328 (83)	580 (150)	-252 [-43]	-96 [-17]	-348 [-51]
L3	1279 (302)	1594 (369)	-315 [-20]	-75 [-5]	640 (172)	830 (190)	-190 [-23]	-52 [-6]	-639 [-50]
L4	1758 (348)	1861 (347)	-103 [-6]	-80 [-4]	916 (157)	980 (200)	-64 [-7]	-39 [-4]	-842 [-48]
L5	1804 (361)	1606 (198)	198 [12]	79 [5]	965 (171)				-839 [-47]
S1	1566 (270)				887 (157)				-679 [-43]

A: Square mm;

B: Female minus Male (Square mm);

C: Shaded cells represent significant difference between females and males ($p \leq 0.05$);

D: Comparisons based on data adjusted one-half of spine level.

Table 1.13. Mean (s.d.) trunk muscle physiological cross-sectional area of the Left Psoas Major. Data collected (OSU) are compared with literature values for males and females. Differences between literature values and the current data are described in terms of area and as a percent of the literature values []. Absolute and percent differences in muscle areas between male and female subjects are also shown.

Left Psoas Major - Physiological Cross-Sectional Area

Level	OSU Male mean ^A (s.d.)	McGill et al., (1993) mean ^A (s.d.)	Difference ^A [% Diff.]	Difference ^D [% Diff.]	OSU Female mean ^A (s.d.)	Chaffin et al., (1990) mean ^A (s.d.)	Difference ^A [% Diff.]	Difference ^D [% Diff.]	Female vs Male ^{B,C} [%Diff.]
T8									
T9									
T10									
T11									
T12		462 (190)							
L1	309 (133)	488 (250)	-179 [-37]	51 [10]	222 (42)				-87 [-28]
L2	768 (242)	1211 (298)	-443 [-37]	-165 [-14]	354 (83)	590 (170)	-236 [-40]	-84 [-14]	-414 [-54]
L3	1324 (253)	1593 (291)	-269 [-17]	-21 [-1]	657 (163)	830 (190)	-173 [-21]	-20 [-2]	-667 [-50]
L4	1819 (291)	1820 (272)	-1 [0]	12 [1]	962 (168)	980 (220)	-18 [-2]	21 [2]	-854 [-47]
L5	1845 (268)	1590 (244)	255 [16]	134 [8]	1039 (173)				-806 [-44]
S1	1602 (275)				895 (176)				-707 [-44]

A: Square mm;

B: Female minus Male (Square mm);

C: Shaded cells represent significant difference between females and males ($p \leq 0.05$);

D: Comparisons based on data adjusted one-half of spine level.

Table 1.14. Mean (s.d.) trunk muscle physiological cross-sectional area of the Right Quadratus Lumborum. Data collected (OSU) are compared with literature values for males and females. Differences between literature values and the current data are described in terms of area and as a percent of the literature values []. Absolute and percent differences in muscle areas between male and female subjects are also shown.

Right Quadratus Lumborum - Physiological Cross-Sectional Area

Level	OSU Male mean ^A (s.d.)	McGill et al., (1993) mean ^{A,E} (s.d.)	Difference ^A [% Diff.]	Difference ^D [% Diff.]	OSU Female mean ^A (s.d.)	Chaffin et al., (1990) mean ^A (s.d.)	Difference ^A [% Diff.]	Difference ^D [% Diff.]	Female vs Male ^{B,C} [%Diff.]
T8									
T9									
T10									
T11									
T12		320 (197)							
L1	270 (--)	358	-88 [-25]	-64 [-18]	182 (57)				-88 [-33]
L2	319 (138)	507	-188 [-37]	-50 [-10]	196 (48)	300 (70)	-104 [-35]	-85 [-28]	-123 [-39]
L3	595 (211)	582	13 [2]	50 [9]	234 (52)	410 (120)	-176 [-43]	-116 [-28]	-361 [-61]
L4	669 (189)	328	-341 [103]		353 (54)	460 (100)	-107 [-23]		-316 [-47]
L5									
S1									

A: Square mm;

B: Female minus Male (Square mm);

C: Shaded cells represent significant difference between females and males ($p \leq 0.05$);

D: Comparisons based on data adjusted one-half of spine level.

E: Cross-sectional area between L1/L2 and L4/L5 (shown as L1 through L4 in the table) are corrected for muscle fiber direction.

Table 1.15. Mean (s.d.) trunk muscle physiological cross-sectional area of the Left Quadratus Lumborum. Data collected (OSU) are compared with literature values for males and females. Differences between literature values and the current data are described in terms of area and as a percent of the literature values []. Absolute and percent differences in muscle areas between male and female subjects are also shown.

Left Quadratus Lumborum - Physiological Cross-Sectional Area

Level	OSU Male mean ^A (s.d.)	McGill et al., (1993) mean ^{A,E} (s.d.)	Difference ^A [% Diff.]	Difference ^D [% Diff.]	OSU Female mean ^A (s.d.)	Chaffin et al., (1990) mean ^A (s.d.)	Difference ^A [% Diff.]	Difference ^D [% Diff.]	Female vs Male ^{B,C} [%Diff.]
T8									
T9									
T10									
T11									
T12		326 (5)							
L1	281 (128)	358	-77 [-22]	-66 [-18]	183 (45)				-98 [-35]
L2	303 (121)	507	-204 [-40]	-45 [-9]	196 (44)	330 (160)	-134 [-41]	-98 [-30]	-107 [-35]
L3	622 (222)	582	40 [7]	76 [13]	268 (72)	450 (140)	-182 [-40]	-103 [-23]	-354 [-57]
L4	693 (198)	328	365 [111]		425 (75)	450 (130)	-25 [-6]		-268 [-39]
L5									
S1									

A: Square mm;

B: Female minus Male (Square mm);

C: Shaded cells represent significant difference between females and males ($p \leq 0.05$);

D: Comparisons based on data adjusted one-half of spine level.

E: Cross-sectional area between L1/L2 and L4/L5 (shown as L1 through L4 in the table) are corrected for muscle fiber direction.

Table 1.16. Vertebral body mean (s.d.) cross-sectional area. Data collected (OSU) are compared with literature values for males and females. Differences between literature values and the current data are described in terms of area and as a percent of the literature values []. Absolute and percent differences in muscle areas between male and female subjects are also shown.

Vertebral Body - Cross-Sectional Area

Level	OSU Male mean ^A (s.d.)	McGill et al., (1993) mean ^A (s.d.)	Difference ^A [% Diff.]	OSU Female mean ^A (s.d.)	Chaffin et al., (1990) mean ^A (s.d.)	Difference ^A [% Diff.]	Female vs Male ^B [% Diff.]
T8	983 (181)	798 (91)	185 [23]	728 (107)			-255 [-26]
T9	1041 (205)	933 (112)	108 [12]	780 (90)			-261 [-25]
T10	1087 (166)	1015 (125)	72 [7]	843 (82)			-244 [-22]
T11	1225 (177)	1133 (124)	92 [8]	893 (97)			-332 [-27]
T12	1287 (189)	1241 (166)	46 [4]	937 (115)			-350 [-27]
L1	1249 (207)	1334 (285)	-85 [-6]	949 (95)			-300 [-24]
L2	1311 (240)	1332 (294)	-21 [-2]	1011 (115)	1420 (240)	-409 [-29]	-300 [-23]
L3	1413 (197)	1415 (249)	-2 [0]	1089 (114)	1520 (230)	-431 [-28]	-324 [-23]
L4	1478 (244)	1459 (270)	19 [1]	1125 (124)	1530 (220)	-405 [-26]	-353 [-24]
L5	1466 (222)	1360 (276)	106 [8]	1180 (219)			-286 [-20]
S1	1742 (261)			1275 (253)			-468 [-27]

A: Square mm;

B: Female minus Male (Square mm).

Table 1.17. Trunk mass mean (s.d.) cross-sectional area. Data collected (OSU) are compared with literature values for males and females. Differences between literature values and the current data are described in terms of area and as a percent of the literature values []. Absolute and percent differences in muscle areas between male and female subjects are also shown.

Trunk - Cross-Sectional Area

Level	OSU Male mean ^A (s.d.)	McGill et al., (1993) mean ^A (s.d.)	Difference ^A [% Diff.]	OSU Female mean ^A (s.d.)	Chaffin et al., (1990) mean ^A (s.d.)	Difference ^A [% Diff.]	Female vs Male ^B [% Diff.]
T8	73338 (11078)	65794 (5254)	7544 [11]	48230 (6569)			-25108 [-34]
T9	68831 (9016)	61732 (6960)	7099 [11]	46605 (6328)			-22226 [-32]
T10	64559 (8261)	61051 (7570)	3508 [6]	44405 (6122)			-20154 [-31]
T11	61648 (8553)	59249 (7272)	2399 [4]	43092 (5991)			-18556 [-30]
T12	59441 (8461)	63287 (9153)	-3846 [-6]	42551 (6003)			-16890 [-28]
L1	57478 (7934)	59091 (6899)	-1613 [-3]	41598 (6156)			-15880 [-28]
L2	54435 (8114)	55834 (8112)	-1399 [-3]	39913 (6135)	44300 (12200)	-4387 [-10]	-14522 [-27]
L3	52543 (8769)	54286 (8702)	-1743 [-3]	37756 (5791)	50900 (16800)	-13146 [-26]	-14789 [-28]
L4	51432 (10184)	51813 (9845)	-382 [-1]	38882 (7169)	57600 (15900)	-18718 [-33]	-12550 [-24]
L5	52481 (8823)	52912 (9123)	-431 [-1]	47166 (7766)			-5315 [-10]
S1	56547 (7701)			53320 (7958)			-3277 [-6]

A: Square mm;

B: Female minus Male (Square mm).

Table 1.18. Right Latissimus Dorsi mean (s.d.) lateral moment-arm distance from the center of the vertebral body to the area centroid of the muscle cross-sectional area. Negative values represent right lateral and positive represent left lateral. Data collected (OSU) are compared with literature values for males and females. Differences between literature values and the current data are described in terms of the magnitude (mm) and as a percent of the literature values []. Magnitude and percent difference in lateral moment-arms between male and female subjects are also shown.

Right Latissimus Dorsi - Corrected Lateral Moment Arms

Level	OSU Male mean ^A (s.d.)	McGill et al., (1993) mean ^A (s.d.)	Difference ^A [% Diff.]	OSU Female mean ^A (s.d.)	Chaffin et al., (1990) mean ^A (s.d.)	Difference ^A [% Diff.]	Female vs Male ^{B,C} [% Diff.]
T8	-153 (10)	-145 (7)	8 [4]	-132 (10)			-21 [-14]
T9	-145 (9)	-141 (8)	4 [3]	-124 (9)			-21 [-14]
T10	-135 (10)	-140 (9)	-5 [-4]	-114 (9)			-21 [-16]
T11	-128 (9)	-129 (9)	-1 [-1]	-109 (9)			-19 [-15]
T12	-122 (8)	-129 (10)	-7 [-5]	-104 (9)			-18 [-15]
L1	-116 (6)	-122 (12)	-6 [-5]	-99 (9)			-17 [-15]
L2	-109 (7)	-108 (8)	1 [1]	-93 (10)	-100 (11)	-7 [-7]	-16 [-15]
L3	-103 (8)	-102 (8)	1 [1]	-90 (11)	-106 (16)	-16 [-15]	-13 [-13]
L4	-110 (2)				-119 (11)		
L5							
S1							

A = millimeters (mm)

B = Female minus Male (mm)

C = Shaded cells represent significant difference between females and males ($p \leq 0.05$).

Table 1.19. Left Latissimus Dorsi mean (s.d.) lateral moment-arm distance from the center of the vertebral body to the area centroid of the muscle cross-sectional area. Negative values represent right lateral and positive represent left lateral. Data collected (OSU) are compared with literature values for males and females. Differences between literature values and the current data are described in terms of the magnitude (mm) and as a percent of the literature values []. Magnitude and percent difference in lateral moment-arms between male and female subjects are also shown.

Left Latissimus Dorsi - Corrected Lateral Moment Arms

Level	OSU Male mean ^A (s. d.)	McGill et al., (1993) mean ^A (s.d.)	Difference ^A [% Diff.]	OSU Female mean ^A (s.d.)	Chaffin et al., (1990) mean ^A (s.d.)	Difference ^A [% Diff.]	Female vs Male ^{B,C} [% Diff.]
T8	150 (7)	143 (6)	7 [5]	131 (9)			-19 [-13]
T9	140 (8)	139 (8)	1 [1]	122 (9)			-18 [-13]
T10	132 (9)	137 (9)	-5 [-4]	114 (10)			-18 [-14]
T11	126 (9)	129 (10)	-3 [-2]	108 (10)			-18 [-14]
T12	121 (9)	128 (7)	-7 [-5]	104 (9)			-17 [-14]
L1	116 (9)	117 (11)	-1 [-1]	101 (9)			-15 [-13]
L2	110 (7)	107 (9)	3 [3]	94 (11)	99 (12)	-5 [-5]	-16 [-15]
L3	105 (8)	104 (15)	1 [1]	92 (11)	107 (14)	-15 [-14]	-13 [-12]
L4	108 (8)				118 (15)		
L5							
S1							

A = millimeters (mm)

B = Female minus Male (mm)

C = Shaded cells represent significant difference between females and males ($p \leq 0.05$).

Table 1.20. Right Erector Spinae mean (s.d.) lateral moment-arm distance from the center of the vertebral body to the area centroid of the muscle cross-sectional area. Negative values represent right lateral and positive represent left lateral. Data collected (OSU) are compared with literature values for males and females. Differences between literature values and the current data are described in terms of the magnitude (mm) and as a percent of the literature values []. Magnitude and percent difference in lateral moment-arms between male and female subjects are also shown.

Right Erector Spinae - Corrected Lateral Moment Arms

Level	OSU Male mean ^A (s.d.)	McGill et al., (1993) mean ^A (s.d.)	Difference ^A [% Diff.]	OSU Female mean ^A (s.d.)	Chaffin et al., (1990) mean ^A (s.d.)	Difference ^A [% Diff.]	Female vs Male ^{B,C} [% Diff.]
T8	-31 (2)	-31 (7)	0 [0]	-26 (3)			-5 [-16]
T9	-32 (3)	-32 (4)	0 [0]	-28 (3)			-4 [-13]
T10	-34 (3)	-34 (4)	0 [0]	-29 (3)			-5 [-15]
T11	-36 (3)	-34 (4)	2 [6]	-31 (3)			-5 [-14]
T12	-36 (3)	-42 (3)	-6 [-14]	-32 (3)			-4 [-11]
L1	-40 (4)	-44 (5)	-4 [-9]	-34 (3)			-6 [-15]
L2	-41 (3)	-42 (4)	-1 [-2]	-35 (3)	-34 (4)	1 [3]	-6 [-15]
L3	-38 (3)	-40 (4)	-2 [-5]	-34 (3)	-34 (4)	0 [0]	-4 [-11]
L4	-36 (3)	-34 (7)	2 [6]	-34 (3)	-35 (4)	-1 [3]	-2 [-6]
L5	-30 (7)	-22 (6)	8 [36]	-26 (6)			-4 [-13]
S1	-19 (3)			-19 (3)			-0 [-0]

A = millimeters (mm)

B = Female minus Male (mm)

C = Shaded cells represent significant difference between females and males ($p \leq 0.05$).

Table 1.21. Left Erector Spinae mean (s.d.) lateral moment-arm distance from the center of the vertebral body to the area centroid of the muscle cross-sectional area. Negative values represent right lateral and positive represent left lateral. Data collected (OSU) are compared with literature values for males and females. Differences between literature values and the current data are described in terms of the magnitude (mm) and as a percent of the literature values []. Magnitude and percent difference in lateral moment-arms between male and female subjects are also shown.

Left Erector Spinae - Corrected Lateral Moment Arms

Level	OSU Male mean ^A (s.d.)	McGill et al., (1993) mean ^A (s.d.)	Difference ^A [% Diff.]	OSU Female mean ^A (s.d.)	Chaffin et al., (1990) mean ^A (s.d.)	Difference ^A [% Diff.]	Female vs Male ^{B,C} [% Diff.]
T8	33 (4)	33 (6)	0 [0]	27 (4)			-6 [-18]
T9	34 (4)	35 (4)	-1 [-3]	28 (3)			-6 [-18]
T10	36 (3)	36 (3)	0 [0]	31 (2)			-5 [-14]
T11	38 (3)	40 (3)	-2 [-5]	32 (3)			-6 [-16]
T12	38 (3)	40 (4)	-2 [-5]	34 (4)			-4 [-11]
L1	42 (3)	41 (7)	1 [2]	35 (3)			-7 [-17]
L2	43 (4)	41 (6)	2 [5]	35 (3)	33 (4)	2 [6]	-8 [-19]
L3	40 (2)	38 (5)	2 [5]	35 (3)	34 (4)	1 [3]	-5 [-13]
L4	38 (3)	33 (6)	5 [15]	35 (3)	35 (4)	0 [0]	-3 [-8]
L5	32 (5)	21 (5)	11 [52]	27 (5)			-5 [-16]
S1	22 (2)			19 (2)			-3 [-14]

A = millimeters (mm)

B = Female minus Male (mm)

C = Shaded cells represent significant difference between females and males ($p \leq 0.05$).

Table 1.22. Right Rectus Abdominis mean (s.d.) lateral moment-arm distance from the center of the vertebral body to the area centroid of the muscle cross-sectional area. Negative values represent right lateral and positive represent left lateral. Data collected (OSU) are compared with literature values for males and females. Differences between literature values and the current data are described in terms of the magnitude (mm) and as a percent of the literature values []. Magnitude and percent difference in lateral moment-arms between male and female subjects are also shown.

Right Rectus Abdominis - Corrected Lateral Moment Arms

Level	OSU Male mean ^A (s.d.)	McGill et al., (1993) mean ^A (s.d.)	Difference ^A [% Diff.]	OSU Female mean ^A (s.d.)	Chaffin et al., (1990) mean ^A (s.d.)	Difference ^A [% Diff.]	Female vs Male ^{B,C} [% Diff.]
T8							
T9							
T10							
T11							
T12	-39 (6)			-29 (8)			-10 [-26]
L1	-46 (11)	-37 (8)	9 [24]	-34 (9)			-12 [-26]
L2	-49 (11)	-46 (8)	3 [7]	-36 (8)	-44 (12)	-8 [-18]	-13 [-27]
L3	-47 (7)	-43 (7)	4 [9]	-39 (8)	-43 (11)	-4 [-9]	-8 [-17]
L4	-46 (5)	-38 (7)	8 [21]	-40 (8)	-42 (11)	-2 [-5]	-6 [-13]
L5	-41 (5)	-32 (5)	9 [28]	-38 (9)			-3 [-7]
S1	-38 (5)			-33 (7)			-5 [-13]

A = millimeters (mm)

B = Female minus Male (mm)

C = Shaded cells represent significant difference between females and males ($p \leq 0.05$).

Table 1.23. Left Rectus Abdominis mean (s.d.) lateral moment-arm distance from the center of the vertebral body to the area centroid of the muscle cross-sectional area. Negative values represent right lateral and positive represent left lateral. Data collected (OSU) are compared with literature values for males and females. Differences between literature values and the current data are described in terms of the magnitude (mm) and as a percent of the literature values []. Magnitude and percent difference in lateral moment-arms between male and female subjects are also shown.

Left Rectus Abdominis - Corrected Lateral Moment Arms

Level	OSU Male mean ^A (s.d.)	McGill et al., (1993) mean ^A (s.d.)	Difference ^A [% Diff.]	OSU Female mean ^A (s.d.)	Chaffin et al., (1990) mean ^A (s.d.)	Difference ^A [% Diff.]	Female vs Male ^{B,C} [% Diff.]
T8							
T9							
T10							
T11							
T12	35 (7)			35 (5)			0 [0]
L1	41 (8)	35 (17)	6 [17]	37 (7)			-4 [-10]
L2	39 (8)	43 (7)	-4 [-9]	34 (8)	42 (10)	-8 [-19]	-5 [-13]
L3	40 (7)	38 (8)	2 [5]	33 (9)	43 (12)	-10 [-23]	-7 [-18]
L4	36 (8)	36 (7)	0 [0]	35 (8)	41 (11)	-6 [-15]	-1 [-3]
L5	33 (8)	33 (5)	0 [0]	32 (8)			-1 [-3]
S1	29 (5)			33 (6)			4 [14]

A = millimeters (mm)

B = Female minus Male (mm)

C = Shaded cells represent significant difference between females and males ($p \leq 0.05$).

Table 1.24. Right External Obliques mean (s.d.) lateral moment-arm distance from the center of the vertebral body to the area centroid of the muscle cross-sectional area. Negative values represent right lateral and positive represent left lateral. Data collected (OSU) are compared with literature values for males and females. Differences between literature values and the current data are described in terms of the magnitude (mm) and as a percent of the literature values []. Magnitude and percent difference in lateral moment-arms between male and female subjects are also shown.

Right External Obliques - Corrected Lateral Moment Arms

Level	OSU Male mean ^A (s.d.)	McGill et al., (1993) mean ^A (s.d.)	Difference ^A [% Diff.]	OSU Female mean ^A (s.d.)	Chaffin et al., (1990) mean ^A (s.d.)	Difference ^A [% Diff.]	Female vs Male ^{B,C} [% Diff.]
T8							
T9							
T10							
T11							
T12	-129 (10)			-108 (8)			-21 [-16]
L1	-130 (12)			-109 (10)			-21 [-16]
L2	-132 (10)	-140 (5)	-8 [-6]	-109 (8)	-117 (15)	-8 [-7]	-21 [-16]
L3	-128 (7)	-130 (10)	-2 [-2]	-108 (7)	-120 (16)	-12 [-10]	-20 [-16]
L4	-128 (7)	-125 (13)	3 [2]	-112 (8)	-121 (14)	-9 [-7]	-16 [-13]
L5	-126 (6)			-116 (3)			-10 [-8]
S1				-106 (-)			

A = millimeters (mm)

B = Female minus Male (mm)

C = Shaded cells represent significant difference between females and males ($p \leq 0.05$).

Table 1.25. Left External Obliques mean (s.d.) lateral moment-arm distance from the center of the vertebral body to the area centroid of the muscle cross-sectional area. Negative values represent right lateral and positive represent left lateral. Data collected (OSU) are compared with literature values for males and females. Differences between literature values and the current data are described in terms of the magnitude (mm) and as a percent of the literature values []. Magnitude and percent difference in lateral moment-arms between male and female subjects are also shown.

Left External Obliques - Corrected Lateral Moment Arms

Level	OSU Male mean ^A (s.d.)	McGill et al., (1993) mean ^A (s.d.)	Difference ^A [% Diff.]	OSU Fe male mean ^A (s.d.)	Chaffin et al., (1990) mean ^A (s.d.)	Difference ^A [% Diff.]	Female vs Male ^{B,C} [% Diff.]
T8							
T9							
T10							
T11							
T12	124 (9)			112 (10)			-12 [-10]
L1	126 (9)			110 (9)			-16 [-13]
L2	124 (11)	133 (7)	-9 [-7]	108 (10)	117 (14)	-9 [-8]	-16 [-13]
L3	124 (10)	125 (9)	-1 [-1]	106 (9)	122 (16)	-16 [-13]	-18 [-15]
L4	122 (9)	120 (9)	2 [2]	108 (9)	123 (20)	-15 [-12]	-14 [-11]
L5	125 (11)			113 (11)			-12 [-10]
S1				107 (-)			

A = millimeters (mm)

B = Female minus Male (mm)

C = Shaded cells represent significant difference between females and males ($p \leq 0.05$).

Table 1.26. Right Internal Obliques mean (s.d.) lateral moment-arm distance from the center of the vertebral body to the area centroid of the muscle cross-sectional area. Negative values represent right lateral and positive represent left lateral. Data collected (OSU) are compared with literature values for males and females. Differences between literature values and the current data are described in terms of the magnitude (mm) and as a percent of the literature values []. Magnitude and percent difference in lateral moment-arms between male and female subjects are also shown.

Right Internal Obliques - Corrected Lateral Moment Arms

Level	OSU Male mean ^A (s.d.)	McGill et al., (1993) mean ^A (s.d.)	Difference ^A [% Diff.]	OSU Female mean ^A (s.d.)	Chaffin et al., (1990) mean ^A (s.d.)	Difference ^A [% Diff.]	Female vs Male ^{B,C} [% Diff.]
T8							
T9							
T10							
T11							
T12							
L1				-83 (-)			
L2	-114 (16)	-123 (9)	-9 [-2]	-99 (14)	-109 (15)	-10 [-9]	-15 [-13]
L3	-115 (8)	-116 (8)	-1 [-1]	-97 (11)	-113 (16)	-16 [-14]	-18 [-16]
L4	-114 (6)	-109 (11)	5 [5]	-101 (8)	-115 (20)	-14 [-12]	-13 [-11]
L5	-109 (3)			-104 (3)			-5 [-5]
S1				-92 (-)			

A = millimeters (mm)

B = Female minus Male (mm)

C = Shaded cells represent significant difference between females and males ($p \leq 0.05$).

Table 1.27. Left Internal Obliques mean (s.d.) lateral moment-arm distance from the center of the vertebral body to the area centroid of the muscle cross-sectional area. Negative values represent right lateral and positive represent left lateral. Data collected (OSU) are compared with literature values for males and females. Differences between literature values and the current data are described in terms of the magnitude (mm) and as a percent of the literature values []. Magnitude and percent difference in lateral moment-arms between male and female subjects are also shown.

Left Internal Obliques - Corrected Lateral Moment Arms

Level	OSU Male mean ^A (s.d.)	McGill et al., (1993) mean ^A (s.d.)	Difference ^A [% Diff.]	OSU Female mean ^A (s.d.)	Chaffin et al., (1990) mean ^A (s.d.)	Difference ^A [% Diff.]	Female vs Male ^{B,C} [% Diff.]
T8							
T9							
T10							
T11							
T12							
L1				93 (-)			
L2	107 (13)	121 (11)	-14 [-12]	102 (15)	109 (15)	-7 [-6]	-5 [-5]
L3	111 (14)	112 (8)	-1 [-1]	94 (14)	114 (16)	-20 [-18]	-17 [-15]
L4	107 (8)	103 (9)	4 [4]	98 (8)	114 (20)	-16 [-14]	-9 [-8]
L5	106 (9)			103 (10)			-3 [-3]
S1				94 (-)			

A = millimeters (mm)

B = Female minus Male (mm)

C = Shaded cells represent significant difference between females and males ($p \leq 0.05$).

Table 1.28. Right Psoas Major mean (s.d.) lateral moment-arm distance from the center of the vertebral body to the area centroid of the muscle cross-sectional area. Negative values represent right lateral and positive represent left lateral. Data collected (OSU) are compared with literature values for males and females. Differences between literature values and the current data are described in terms of the magnitude (mm) and as a percent of the literature values []. Magnitude and percent difference in lateral moment-arms between male and female subjects are also shown.

Right Psoas Major - Corrected Lateral Moment Arms

Level	OSU Male mean ^A (s.d.)	McGill et al., (1993) mean ^A (s.d.)	Difference ^A [% Diff.]	OSU Female mean ^A (s.d.)	Chaffin et al., (1990) mean ^A (s.d.)	Difference ^A [% Diff.]	Female vs Male ^{B,C} [% Diff.]
T8							
T9							
T10							
T11							
T12		-32 (3)					
L1	-26 (-)	-32 (3)	-6 [-19]	-23 (2)			-3 [-12]
L2	-33 (3)	-39 (2)	-6 [-15]	-27 (2)	-33 (4)	-6 [-18]	-6 [-18]
L3	-39 (3)	-44 (3)	-5 [-11]	-33 (2)	-37 (4)	-4 [-11]	-6 [-15]
L4	-47 (3)	-50 (3)	-3 [-6]	-40 (3)	-44 (4)	-4 [-9]	-7 [-15]
L5	-53 (3)	-54 (4)	-1 [-2]	-47 (4)			-6 [-11]
S1	-56 (4)			-50 (4)			-6 [-11]

A = millimeters (mm)

B = Female minus Male (mm)

C = Shaded cells represent significant difference between females and males ($p \leq 0.05$).

Table 1.29. Left Psoas Major mean (s.d.) lateral moment-arm distance from the center of the vertebral body to the area centroid of the muscle cross-sectional area. Negative values represent right lateral and positive represent left lateral. Data collected (OSU) are compared with literature values for males and females. Differences between literature values and the current data are described in terms of the magnitude (mm) and as a percent of the literature values []. Magnitude and percent difference in lateral moment-arms between male and female subjects are also shown.

Left Psoas Major - Corrected Lateral Moment Arms

Level	OSU Male mean ^A (s.d.)	McGill et al., (1993) mean ^A (s.d.)	Difference ^A [% Diff.]	OSU Female mean ^A (s.d.)	Chaffin et al., (1990) mean ^A (s.d.)	Difference ^A [% Diff.]	Female vs Male ^{B,C} [% Diff.]
T8							
T9							
T10							
T11							
T12		32 (2)					
L1	28 (2)	31 (3)	-3 [-10]	23 (1)			-5 [-18]
L2	33 (3)	38 (3)	-5 [-13]	27 (1)	32 (4)	-5 [-16]	-6 [-18]
L3	39 (3)	42 (3)	-3 [-7]	32 (2)	38 (4)	-5 [-13]	-7 [-18]
L4	44 (4)	48 (4)	-4 [-8]	38 (3)	43 (4)	-5 [-12]	-6 [-14]
L5	50 (5)	54 (5)	-4 [-7]	45 (3)			-5 [-10]
S1	54 (5)			51 (3)			-3 [-6]

A = millimeters (mm)

B = Female minus Male (mm)

C = Shaded cells represent significant difference between females and males ($p \leq 0.05$).

Table 1.30. Right Quadratus Lumborum mean (s.d.) lateral moment-arm distance from the center of the vertebral body to the area centroid of the muscle cross-sectional area. Negative values represent right lateral and positive represent left lateral. Data collected (OSU) are compared with literature values for males and females. Differences between literature values and the current data are described in terms of the magnitude (mm) and as a percent of the literature values []. Magnitude and percent difference in lateral moment-arms between male and female subjects are also shown.

Right Quadratus Lumborum - Corrected Lateral Moment Arms

Level	OSU Male mean ^A (s.d.)	McGill et al., (1993) mean ^A (s.d.)	Difference ^A [% Diff.]	OSU Female mean ^A (s.d.)	Chaffin et al., (1990) mean ^A (s.d.)	Difference ^A [% Diff.]	Female vs Male ^{B,C} [% Diff.]
T8							
T9							
T10							
T11							
T12		-46 (11)					
L1	-38 (-)	-46 (6)	-8 [-17]	-38 (6)			0 [0]
L2	-50 (6)	-63 (5)	-13 [-21]	-41 (4)	-56 (8)	-15 [-27]	-9 [-18]
L3	-64 (6)	-75 (6)	-11 [-15]	-55 (7)	-65 (7)	-10 [-15]	-9 [-14]
L4	-75 (5)	-81 (5)	-6 [-7]	-68 (5)	-74 (8)	-6 [-8]	-7 [-9]
L5				-74 (-)			
S1							

A = millimeters (mm)

B = Female minus Male (mm)

C = Shaded cells represent significant difference between females and males ($p \leq 0.05$).

Table 1.31. Left Quadratus Lumborum mean (s.d.) lateral moment-arm distance from the center of the vertebral body to the area centroid of the muscle cross-sectional area. Negative values represent right lateral and positive represent left lateral. Data collected (OSU) are compared with literature values for males and females. Differences between literature values and the current data are described in terms of the magnitude (mm) and as a percent of the literature values []. Magnitude and percent difference in lateral moment-arms between male and female subjects are also shown.

Left Quadratus Lumborum - Corrected Lateral Moment Arms

Level	OSU Male mean ^A (s.d.)	McGill et al., (1993) mean ^A (s.d.)	Difference ^A [% Diff.]	OSU Female mean ^A (s.d.)	Chaffin et al., (1990) mean ^A (s.d.)	Difference ^A [% Diff.]	Female vs Male ^{B,C} [% Diff.]
T8							
T9							
T10							
T11							
T12		47 (5)					
L1	44 (4)	50 (6)	-6 [-12]	37 (3)			-7 [-16]
L2	47 (10)	64 (5)	-17 [-27]	42 (3)	55 (7)	-13 [-24]	-5 [-11]
L3	65 (7)	73 (4)	-8 [-11]	57 (7)	65 (7)	-8 [-12]	-8 [-12]
L4	73 (6)	78 (12)	-5 [-6]	68 (7)	75 (10)	-7 [-9]	-5 [-7]
L5				79 (-)			
S1							

A = millimeters (mm)

B = Female minus Male (mm)

C = Shaded cells represent significant difference between females and males ($p \leq 0.05$).

Table 1.32. Right Latissimus Dorsi mean (s.d.) anterior-posterior moment-arm distance from the center of the vertebral body to the area centroid of the muscle cross-sectional area. Negative values represent right lateral and positive represent left lateral. Data collected (OSU) are compared with literature values for males and females. Differences between literature values and the current data are described in terms of the magnitude (mm) and as a percent of the literature values []. Magnitude and percent difference in lateral moment-arms between male and female subjects are also shown.

Right Latissimus Dorsi - Corrected Anterior-Posterior Moment Arms

Level	OSU Male mean ^A (s.d.)	McGill et al., (1993) mean ^A (s.d.)	Difference ^A [% Diff.]	OSU Female mean ^A (s.d.)	Chaffin et al., (1990) mean ^A (s.d.)	Difference ^A [% Diff.]	Female vs Male ^{B,C} [% Diff.]
T8	-18 (9)	-18 (9)	0 [0]	-16 (12)			-2 [-11]
T9	-22 (10)	-22 (7)	0 [0]	-19 (11)			-3 [-14]
T10	-24 (9)	-24 (7)	0 [0]	-23 (9)			-1 [-4]
T11	-27 (8)	-32 (7)	-5 [-16]	-26 (8)			-1 [-4]
T12	-29 (7)	-39 (8)	-10 [-26]	-29 (8)			0 [0]
L1	-38 (9)	-47 (10)	-9 [-19]	-32 (10)			-6 [-16]
L2	-41 (7)	-47 (12)	-6 [-13]	-34 (11)	-36 (9)	-2 [-6]	-7 [-17]
L3	-42 (8)	-45 (16)	-3 [-7]	-31 (12)	-30 (10)	1 [3]	-11 [-26]
L4	-40 (13)				-17 (11)		
L5							
S1							

A = millimeters (mm)

B = Female minus Male (mm)

C = Shaded cells represent significant difference between females and males ($p \leq 0.05$).

Table 1.33. Left Latissimus Dorsi mean (s.d.) anterior-posterior moment-arm distance from the center of the vertebral body to the area centroid of the muscle cross-sectional area. Negative values represent right lateral and positive represent left lateral. Data collected (OSU) are compared with literature values for males and females. Differences between literature values and the current data are described in terms of the magnitude (mm) and as a percent of the literature values []. Magnitude and percent difference in lateral moment-arms between male and female subjects are also shown.

Left Latissimus Dorsi - Corrected Anterior-Posterior Moment Arms

Level	OSU Male mean ^A (s.d.)	McGill et al., (1993) mean ^A (s.d.)	Difference ^A [% Diff.]	OSU Female mean ^A (s.d.)	Chaffin et al., (1990) mean ^A (s.d.)	Difference ^A [% Diff.]	Female vs Male ^{B,C} [% Diff.]
T8	-7 (11)	-17 (7)	-10 [-59]	-7 (10)			0 [0]
T9	-9 (11)	-19 (7)	-10 [-53]	-11 (9)			2 [22]
T10	-13 (11)	-23 (7)	-10 [-43]	-16 (9)			3 [23]
T11	-16 (10)	-28 (9)	-12 [-43]	-20 (8)			4 [25]
T12	-22 (10)	-37 (8)	-15 [-41]	-26 (8)			4 [18]
L1	-30 (12)	-46 (7)	-16 [-35]	-31 (10)			1 [3]
L2	-40 (11)	-46 (10)	-6 [-13]	-39 (11)	-34 (11)	5 [15]	-1 [-3]
L3	-39 (11)	-43 (17)	-4 [-9]	-40 (12)	-30 (10)	10 [33]	1 [3]
L4	-37 (11)				-14 (13)		
L5							
S1							

A = millimeters (mm)

B = Female minus Male (mm)

C = Shaded cells represent significant difference between females and males ($p \leq 0.05$).

Table 1.34. Right Erector Spinae mean (s.d.) anterior-posterior moment-arm distance from the center of the vertebral body to the area centroid of the muscle cross-sectional area. Negative values represent right lateral and positive represent left lateral. Data collected (OSU) are compared with literature values for males and females. Differences between literature values and the current data are described in terms of the magnitude (mm) and as a percent of the literature values []. Magnitude and percent difference in lateral moment-arms between male and female subjects are also shown.

Right Erector Spinae - Corrected Anterior-Posterior Moment Arms

Level	OSU Male mean ^A (s.d.)	McGill et al., (1993) mean ^A (s.d.)	Difference ^A [% Diff.]	OSU Female mean ^A (s.d.)	Chaffin et al., (1990) mean ^A (s.d.)	Difference ^A [% Diff.]	Female vs Male ^{B,C} [% Diff.]
T8	-52 (4)	-52 (3)	0 [0]	-44 (3)			-8 [-15]
T9	-53 (4)	-52 (4)	1 [2]	-45 (4)			-8 [-15]
T10	-52 (4)	-54 (4)	-2 [-4]	-44 (4)			-8 [-15]
T11	-51 (4)	-54 (4)	-3 [-6]	-44 (4)			-7 [-14]
T12	-50 (4)	-56 (5)	-6 [-11]	-44 (4)			-6 [-12]
L1	-52 (5)	-59 (5)	-7 [-12]	-47 (5)			-5 [-10]
L2	-54 (7)	-61 (5)	-7 [-11]	-48 (4)	-54 (4)	-6 [-11]	-6 [-11]
L3	-57 (7)	-61 (5)	-4 [-7]	-50 (5)	-52 (4)	-2 [-4]	-7 [-12]
L4	-56 (6)	-61 (5)	-5 [-8]	-49 (4)	-52 (3)	-3 [-6]	-7 [-13]
L5	-61 (7)	-64 (6)	-3 [-5]	-54 (5)			-7 [-11]
S1	-62 (7)			-54 (5)			-8 [-13]

A = millimeters (mm)

B = Female minus Male (mm)

C = Shaded cells represent significant difference between females and males ($p \leq 0.05$).

Table 1.35. Left Erector Spinae mean (s.d.) anterior-posterior moment-arm distance from the center of the vertebral body to the area centroid of the muscle cross-sectional area. Negative values represent right lateral and positive represent left lateral. Data collected (OSU) are compared with literature values for males and females. Differences between literature values and the current data are described in terms of the magnitude (mm) and as a percent of the literature values []. Magnitude and percent difference in lateral moment-arms between male and female subjects are also shown.

Left Erector Spinae - Corrected Anterior-Posterior Moment Arms

Level	OSU Male mean ^A (s.d.)	McGill et al., (1993) mean ^A (s.d.)	Difference ^A [% Diff.]	OSU Female mean ^A (s.d.)	Chaffin et al., (1990) mean ^A (s.d.)	Difference ^A [% Diff.]	Female vs Male ^{B,C} [% Diff.]
T8	-49 (5)	-51 (3)	-2 [-4]	-42 (3)			-7 [-14]
T9	-49 (6)	-51 (4)	-2 [-4]	-43 (3)			-6 [-12]
T10	-48 (5)	-52 (4)	-4 [-8]	-42 (3)			-6 [-13]
T11	-47 (5)	-52 (4)	-5 [-10]	-42 (4)			-5 [-11]
T12	-48 (5)	-57 (5)	-9 [-16]	-43 (4)			-5 [-10]
L1	-50 (6)	-60 (4)	-10 [-17]	-47 (5)			-3 [-6]
L2	-54 (6)	-62 (5)	-8 [-13]	-51 (6)	-54 (4)	-3 [-6]	-3 [-6]
L3	-56 (6)	-61 (5)	-5 [-8]	-53 (6)	-53 (2)	0 [0]	-3 [-5]
L4	-57 (5)	-61 (5)	-4 [-7]	-53 (5)	-54 (4)	-1 [-2]	-4 [-7]
L5	-61 (7)	-63 (5)	-2 [-3]	-57 (6)			-4 [-7]
S1	-63 (8)			-56 (5)			-7 [-11]

A = millimeters (mm)

B = Female minus Male (mm)

C = Shaded cells represent significant difference between females and males ($p \leq 0.05$).

Table 1.36. Right Rectus Abdominis mean (s.d.) anterior-posterior moment-arm distance from the center of the vertebral body to the area centroid of the muscle cross-sectional area. Negative values represent right lateral and positive represent left lateral. Data collected (OSU) are compared with literature values for males and females. Differences between literature values and the current data are described in terms of the magnitude (mm) and as a percent of the literature values []. Magnitude and percent difference in lateral moment-arms between male and female subjects are also shown.

Right Rectus Abdominis - Corrected Anterior-Posterior Moment Arms

Level	OSU Male mean ^A (s.d.)	McGill et al., (1993) mean ^A (s.d.)	Difference ^A [% Diff.]	OSU Female mean ^A (s.d.)	Chaffin et al., (1990) mean ^A (s.d.)	Difference ^A [% Diff.]	Female vs. Male ^{B,C} [% Diff.]
T8							
T9							
T10							
T11							
T12	135 (17)			104 (9)			-31 [-23]
L1	124 (12)	109 (8)	15 [14]	96 (10)			-28 [-23]
L2	107 (12)	90 (14)	17 [19]	85 (9)	70 (15)	15 [21]	-24 [-22]
L3	89 (13)	79 (13)	10 [13]	70 (9)	70 (19)	0 [0]	-19 [-21]
L4	77 (15)	73 (14)	4 [5]	61 (9)	69 (20)	-8 [-12]	-16 [-21]
L5	76 (14)	81 (16)	-5 [-6]	65 (10)			-11 [-14]
S1	84 (12)			75 (13)			-9 [-11]

A = millimeters (mm)

B = Female minus Male (mm)

C = Shaded cells represent significant difference between females and males ($p \leq 0.05$).

Table 1.37. Left Rectus Abdominis mean (s.d.) anterior-posterior moment-arm distance from the center of the vertebral body to the area centroid of the muscle cross-sectional area. Negative values represent right lateral and positive represent left lateral. Data collected (OSU) are compared with literature values for males and females. Differences between literature values and the current data are described in terms of the magnitude (mm) and as a percent of the literature values []. Magnitude and percent difference in lateral moment-arms between male and female subjects are also shown.

Left Rectus Abdominis - Corrected Anterior-Posterior Moment Arms

Level	OSU Male mean ^A (s.d.)	McGill et al., (1993) mean ^A (s.d.)	Difference ^A [% Diff.]	OSU Female mean ^A (s.d.)	Chaffin et al., (1990) mean ^A (s.d.)	Difference ^A [% Diff.]	Female vs. Male ^{B,C} [% Diff]
T8							
T9							
T10							
T11							
T12	137 (17)			105 (10)			-32 [-23]
L1	127 (11)	112 (6)	15 [13]	97 (11)			-30 [-24]
L2	108 (13)	92 (14)	16 [17]	85 (11)	72 (16)	13 [18]	-23 [-21]
L3	92 (13)	80 (14)	12 [15]	69 (11)	72 (19)	-3 [-4]	-23 [-25]
L4	78 (14)	73 (14)	5 [7]	60 (9)	70 (20)	-10 [-14]	-18 [-23]
L5	76 (15)	80 (15)	-4 [-5]	61 (10)			-15 [-20]
S1	82 (12)			73 (12)			-9 [-11]

A = millimeters (mm)

B = Female minus Male (mm)

C = Shaded cells represent significant difference between females and males ($p \leq 0.05$).

Table 1.38. Right External Obliques mean (s.d.) anterior-posterior moment-arm distance from the center of the vertebral body to the area centroid of the muscle cross-sectional area. Negative values represent right lateral and positive represent left lateral. Data collected (OSU) are compared with literature values for males and females. Differences between literature values and the current data are described in terms of the magnitude (mm) and as a percent of the literature values []. Magnitude and percent difference in lateral moment-arms between male and female subjects are also shown.

Right External Obliques - Corrected Anterior-Posterior Moment Arms

Level	OSU Male mean ^A (s.d.)	McGill et al., (1993) mean ^A (s.d.)	Difference ^A [% Diff.]	OSU Female mean ^A (s.d.)	Chaffin et al., (1990) mean ^A (s.d.)	Difference ^A [% Diff.]	Female vs Male ^{B,C} [% Diff.]
T8							
T9							
T10							
T11							
T12	85 (12)			68 (7)			-17 [-20]
L1	67 (10)			56 (12)			-11 [-16]
L2	46 (6)	28 (12)	18 [64]	40 (11)	22 (13)	18 [82]	-6 [-13]
L3	22 (10)	20 (14)	2 [10]	24 (12)	23 (12)	1 [4]	2 [9]
L4	21 (8)	35 (10)	-14 [-40]	22 (12)	30 (13)	-8 [-27]	1 [5]
L5	39 (12)			32 (20)			-7 [-18]
S1				66 (-)			

A = millimeters (mm)

B = Female minus Male (mm)

C = Shaded cells represent significant difference between females and males ($p \leq 0.05$).

Table 1.39. Left External Obliques mean (s.d.) anterior-posterior moment-arm distance from the center of the vertebral body to the area centroid of the muscle cross-sectional area. Negative values represent right lateral and positive represent left lateral. Data collected (OSU) are compared with literature values for males and females. Differences between literature values and the current data are described in terms of the magnitude (mm) and as a percent of the literature values []. Magnitude and percent difference in lateral moment-arms between male and female subjects are also shown.

Left External Obliques - Corrected Anterior-Posterior Moment Arms

Level	OSU Male mean ^A (s.d.)	McGill et al., (1993) mean ^A (s.d.)	Difference ^A [% Diff.]	OSU Female mean ^A (s.d.)	Chaffin et al., (1990) mean ^A (s.d.)	Difference ^A [% Diff.]	Female vs Male ^{B,C} [% Diff.]
T8							
T9							
T10							
T11							
T12	92 (14)			66 (12)			-26 [-28]
L1	74 (13)			57 (13)			-17 [-23]
L2	50 (14)	28 (11)	22 [79]	37 (12)	20 (11)	17 [85]	-13 [-26]
L3	27 (14)	19 (11)	8 [42]	15 (13)	20 (11)	-5 [-25]	-12 [-44]
L4	20 (11)	32 (18)	-12 [-38]	12 (13)	30 (12)	-18 [-60]	-8 [-40]
L5	35 (12)			25 (9)			-10 [-29]
S1				46 (-)			

A = millimeters (mm)

B = Female minus Male (mm)

C = Shaded cells represent significant difference between females and males ($p \leq 0.05$).

Table 1.40. Right Internal Obliques mean (s.d.) anterior-posterior moment-arm distance from the center of the vertebral body to the area centroid of the muscle cross-sectional area. Negative values represent right lateral and positive represent left lateral. Data collected (OSU) are compared with literature values for males and females. Differences between literature values and the current data are described in terms of the magnitude (mm) and as a percent of the literature values []. Magnitude and percent difference in lateral moment-arms between male and female subjects are also shown.

Right Internal Obliques - Corrected Anterior-Posterior Moment Arms

Level	OSU Male mean ^A (s.d.)	McGill et al., (1993) mean ^A (s.d.)	Difference ^A [% Diff.]	OSU Female mean ^A (s.d.)	Chaffin et al., (1990) mean ^A (s.d.)	Difference ^A [% Diff.]	Female vs Male ^{B,C} [% Diff.]
T8							
T9							
T10							
T11							
T12							
L1				93 (-)			
L2	72 (17)	36 (17)	36 [100]	55 (15)	24 (14)	31 [129]	-17 [-24]
L3	34 (13)	25 (9)	9 [36]	33 (12)	21 (11)	12 [57]	-1 [-3]
L4	25 (11)	41 (12)	-16 [-39]	21 (11)	30 (15)	-9 [-30]	-4 [-16]
L5	45 (10)			36 (15)			-9 [-20]
S1				63 (-)			

A = millimeters (mm)

B = Female minus Male (mm)

C = Shaded cells represent significant difference between females and males ($p \leq 0.05$).

Table 1.41. Left Internal Obliques mean (s.d.) anterior-posterior moment-arm distance from the center of the vertebral body to the area centroid of the muscle cross-sectional area. Negative values represent right lateral and positive represent left lateral. Data collected (OSU) are compared with literature values for males and females. Differences between literature values and the current data are described in terms of the magnitude (mm) and as a percent of the literature values []. Magnitude and percent difference in lateral moment-arms between male and female subjects are also shown.

Left Internal Obliques - Corrected Anterior-Posterior Moment Arms

Level	OSU Male mean ^A (s.d.)	McGill et al., (1993) mean ^A (s.d.)	Difference ^A [% Diff.]	OSU Female mean ^A (s.d.)	Chaffin et al., (1990) mean ^A (s.d.)	Difference ^A [% Diff.]	Female vs Male ^{B,C} [% Diff.]
T8							
T9							
T10							
T11							
T12							
L1				78 (-)			
L2	77 (16)	40 (16)	37 [93]	50 (19)	25 (16)	25 [100]	-27 [-35]
L3	43 (15)	26 (12)	17 [65]	30 (15)	20 (10)	10 [50]	-13 [-30]
L4	27 (10)	41 (17)	-14 [-34]	16 (10)	28 (13)	-12 [-43]	-11 [-41]
L5	45 (13)			30 (15)			-15 [-33]
S1				44 (-)			

A = millimeters (mm)

B = Female minus Male (mm)

C = Shaded cells represent significant difference between females and males ($p \leq 0.05$).

Table 1.42. Right Psoas Major mean (s.d.) anterior-posterior moment-arm distance from the center of the vertebral body to the area centroid of the muscle cross-sectional area. Negative values represent right lateral and positive represent left lateral. Data collected (OSU) are compared with literature values for males and females. Differences between literature values and the current data are described in terms of the magnitude (mm) and as a percent of the literature values []. Magnitude and percent difference in lateral moment-arms between male and female subjects are also shown.

Right Psoas Major - Corrected Anterior-Posterior Moment Arms

Level	OSU Male mean ^A (s.d.)	McGill et al., (1993) mean ^A (s.d.)	Difference ^A [% Diff.]	OSU Female mean ^A (s.d.)	Chaffin et al., (1990) mean ^A (s.d.)	Difference ^A [% Diff.]	Female vs Male ^{B,C} [% Diff.]
T8							
T9							
T10							
T11							
T12		-14 (2)					
L1	-5 (-)	-11 (6)	-6 [-55]	-7 (9)			2 [40]
L2	-7 (5)	-9 (5)	-2 [-22]	-9 (3)	-11 (3)	-2 [-18]	2 [29]
L3	-4 (4)	-7 (5)	-3 [-43]	-8 (4)	-8 (4)	0 [0]	4 [100]
L4	-1 (3)	1 (5)	-2 [-200]	-4 (5)	-2 (5)	2 [100]	3 [300]
L5	8 (5)	18 (9)	-10 [-56]	7 (7)			-1 [-13]
S1	24 (7)			23 (10)			-1 [-4]

A = millimeters (mm)

B = Female minus Male (mm)

C = Shaded cells represent significant difference between females and males ($p \leq 0.05$).

Table 1.43. Left Psoas Major mean (s.d.) anterior-posterior moment-arm distance from the center of the vertebral body to the area centroid of the muscle cross-sectional area. Negative values represent right lateral and positive represent left lateral. Data collected (OSU) are compared with literature values for males and females. Differences between literature values and the current data are described in terms of the magnitude (mm) and as a percent of the literature values []. Magnitude and percent difference in lateral moment-arms between male and female subjects are also shown.

Left Psoas Major - Corrected Anterior-Posterior Moment Arms

Level	OSU Male mean ^A (s.d.)	McGill et al., (1993) mean ^A (s.d.)	Difference ^A [% Diff.]	OSU Female mean ^A (s.d.)	Chaffin et al., (1990) mean ^A (s.d.)	Difference ^A [% Diff.]	Female vs Male ^{B,C} [% Diff.]
T8							
T9							
T10							
T11							
T12		-11 (1)					
L1	-9 (5)	-11 (4)	-2 [-18]	-2 (7)			-7 [-22]
L2	-6 (5)	-8 (2)	-2 [-25]	-10 (4)	-11 (4)	-1 [-9]	4 [67]
L3	-3 (4)	-6 (4)	-3 [-50]	-10 (5)	-8 (5)	2 [25]	7 [233]
L4	-0.2 (5)	2 (4)	-2.2 [-110]	-7 (5)	-2 (4)	5 [250]	7.2 [3600]
L5	8 (6)	19 (8)	-11 [-58]	2 (6)			-6 [-75]
S1	24 (7)			20 (8)			-4 [-17]

A = millimeters (mm)

B = Female minus Male (mm)

C = Shaded cells represent significant difference between females and males ($p \leq 0.05$).

Table 1.44. Right Quadratus Lumborum mean (s.d.) anterior-posterior moment-arm distance from the center of the vertebral body to the area centroid of the muscle cross-sectional area. Negative values represent right lateral and positive represent left lateral. Data collected (OSU) are compared with literature values for males and females. Differences between literature values and the current data are described in terms of the magnitude (mm) and as a percent of the literature values []. Magnitude and percent difference in lateral moment-arms between male and female subjects are also shown.

Right Quadratus Lumborum - Corrected Anterior-Posterior Moment Arms

Level	OSU Male mean ^A (s.d.)	McGill et al., (1993) mean ^A (s.d.)	Difference ^A [% Diff.]	OSU Female mean ^A (s.d.)	Chaffin et al., (1990) mean ^A (s.d.)	Difference ^A [% Diff.]	Female vs Male ^{B,C} [% Diff.]
T8							
T9							
T10							
T11							
T12		-31 (6)					
L1	-27 (-)	-35 (4)	-8 [-23]	-29 (4)			2 [7]
L2	-31 (6)	-37 (6)	-6 [-16]	-30 (4)	-36 (4)	-6 [-17]	-1 [-3]
L3	-31 (7)	-37 (6)	-6 [-16]	-31 (7)	-32 (7)	-1 [-3]	0 [0]
L4	-30 (6)	-36 (9)	-6 [-17]	-26 (8)	-28 (7)	-2 [-7]	-4 [-13]
L5				-18 (-)			
S1							

A = millimeters (mm)

B = Female minus Male (mm)

C = Shaded cells represent significant difference between females and males ($p \leq 0.05$).

Table 1.45. Left Quadratus Lumborum mean (s.d.) anterior-posterior moment-arm distance from the center of the vertebral body to the area centroid of the muscle cross-sectional area. Negative values represent right lateral and positive represent left lateral. Data collected (OSU) are compared with literature values for males and females. Differences between literature values and the current data are described in terms of the magnitude (mm) and as a percent of the literature values []. Magnitude and percent difference in lateral moment-arms between male and female subjects are also shown.

Left Quadratus Lumborum - Corrected Anterior-Posterior Moment Arms

Level	OSU Male mean ^A (s.d.)	McGill et al., (1993) mean ^A (s.d.)	Difference ^A [% Diff.]	OSU Female mean ^A (s.d.)	Chaffin et al., (1990) mean ^A (s.d.)	Difference ^A [% Diff.]	Female vs Male ^{B,C} [% Diff.]
T8							
T9							
T10							
T11							
T12		-31 (6)					
L1	-30 (4)	-35 (4)	-5 [-14]	-26 (3)			-4 [-13]
L2	-31 (6)	-37 (6)	-6 [-16]	-32 (6)	-36 (4)	-4 [-11]	1 [3]
L3	-31 (7)	-37 (6)	-6 [-16]	-36 (10)	-32 (7)	4 [13]	5 [16]
L4	-31 (7)	-36 (9)	-5 [-14]	-32 (10)	-28 (7)	4 [14]	1 [3]
L5				-29 (-)			
S1							

A = millimeters (mm)

B = Female minus Male (mm)

C = Shaded cells represent significant difference between females and males ($p \leq 0.05$).

Table 1.46. Right Latissimus Dorsi mean (s.d.) muscle vector directions (degrees) in the coronal (θ_{Cor}) and sagittal (θ_{Sag}) planes. Negative values represent right lateral or posterior direction, and positive values represent left lateral or anterior direction. Differences between the male and female vector directions are shown, which are the absolute difference in degrees. Significant differences between males and females are indicated when $p \leq 0.05$.

Right Latissimus Dorsi - Muscle Vector Directions (degrees) in the Sagittal and Coronal Planes

Level	Female θ_{Cor} mean ^A (s.d.)	Male θ_{Cor} mean ^A (s.d.)	Difference ^B	Female θ_{Sag} mean ^A (s.d.)	Male θ_{Sag} mean ^A (s.d.)	Difference ^B
T8	-18.4 (5.5)	-19.2 (5.1)	0.8 $p=0.727$	-3.3 (9.5)	-7.0 (8.8)	3.7 $p=0.320$
T9	-20.6 (6.8)	-15.2 (16.0)	5.4 $p=0.328$	-2.2 (10.3)	3.0 (13.5)	5.2 $p=0.245$
T10	-10.9 (7.6)	-13.5 (7.9)	2.6 $p=0.381$	0.1 (8.8)	-1.4 (10.8)	1.5 $p=0.696$
T11	-10.8 (5.6)	-11.8 (4.3)	1.0 $p=0.643$	4.4 (7.9)	1.3 (7.6)	3.1 $p=0.306$
T12	-8.9 (11.6)	-9.7 (4.9)	0.8 $p=0.777$	6.6 (9.2)	-3.4 (12.3)	10.0 $p=0.018$
L1	-11.8 (14.9)	-11.4 (8.2)	0.4 $p=0.928$	10.1 (13.6)	6.4 (8.7)	3.7 $p=0.442$
L2	-3.6 (14.2)	-9.0 (9.2)	5.4 $p=0.297$	16.0 (13.2)	9.7 (9.1)	6.3 $p=0.196$
L3		8.3 (0.4)			2.0 (3.1)	
L4						
L5						

A = Degrees

B = Shaded cells represent significant difference between females and males.

Table 1.47. Left Latissimus Dorsi mean (s.d.) muscle vector directions (degrees) in the coronal (θ_{Cor}) and sagittal (θ_{Sag}) planes. Negative values represent right lateral or posterior direction, and positive values represent left lateral or anterior direction. Differences between the male and female vector directions are shown, which are the absolute difference in degrees. Significant differences between males and females are indicated when $p \leq 0.05$.

Left Latissimus Dorsi - Muscle Vector Directions (degrees) in the Sagittal and Coronal Planes

Level	Female θ_{Cor} mean ^A (s.d.)	Male θ_{Cor} mean ^A (s.d.)	Difference ^B	Female θ_{Sag} mean ^A (s.d.)	Male θ_{Sag} mean ^A (s.d.)	Difference ^B
T8	19.3 (7.6)	23.6 (5.3)	4.3 $p=0.116$	-8.0 (7.7)	2.2 (6.2)	10.2 $p=0.049$
T9	20.9 (6.8)	21.3 (7.1)	0.4 $p=0.900$	-3.6 (8.3)	-0.9 (12.3)	2.7 $p=0.471$
T10	12.4 (7.5)	11.5 (6.1)	0.9 $p=0.769$	-0.5 (10.3)	-1.9 (13.3)	1.4 $p=0.748$
T11	8.6 (6.1)	9.7 (6.8)	1.1 $p=0.636$	-3.3 (9.6)	-4.8 (8.8)	1.5 $p=0.682$
T12	5.3 (12.2)	8.7 (6.5)	3.4 $p=0.412$	3.3 (10.6)	-3.2 (9.3)	6.5 $p=0.113$
L1	9.8 (15.6)	9.1 (7.8)	0.7 $p=0.869$	0.9 (15.4)	-3.7 (10.7)	4.6 $p=0.407$
L2	0.5 (14.4)	9.0 (9.2)	8.5 $p=0.107$	12.0 (12.0)	11.8 (6.9)	0.2 $p=0.969$
L3		-5.5 (3.1)			12.8 (4.5)	
L4						
L5						

A = Degrees

B = Shaded cells represent significant difference between females and males.

Table 1.48. Right Erector Spinae mean (s.d.) muscle vector directions (degrees) in the coronal (θ_{Cor}) and sagittal (θ_{Sag}) planes. Negative values represent right lateral or posterior direction, and positive values represent left lateral or anterior direction. Differences between the male and female vector directions are shown, which are the absolute difference in degrees. Significant differences between males and females are indicated when $p \leq 0.05$.

Right Erector Spinae - Muscle Vector Directions (degrees) in the Sagittal and Coronal Planes

Level	Female θ_{Cor} mean ^A (s.d.)	Male θ_{Cor} mean ^A (s.d.)	Difference ^B	Female θ_{Sag} mean ^A (s.d.)	Male θ_{Sag} mean ^A (s.d.)	Difference ^B
T8	3.1 (5.1)	3.5 (4.9)	0.4 $p=0.847$	1.5 (3.1)	0.0 (4.1)	1.5 $p=0.284$
T9	5.2 (4.5)	7.7 (11.2)	2.5 $p=0.516$	7.4 (3.4)	9.4 (9.3)	2.0 $p=0.520$
T10	4.6 (3.8)	4.3 (4.8)	0.3 $p=0.859$	8.3 (4.4)	5.5 (4.3)	2.8 $p=0.124$
T11	0.8 (5.9)	0.4 (3.5)	0.4 $p=0.874$	9.9 (3.5)	9.0 (3.5)	0.9 $p=0.541$
T12	4.0 (3.6)	7.1 (6.1)	3.1 $p=0.163$	8.8 (4.5)	6.9 (3.5)	1.9 $p=0.247$
L1	0.2 (6.5)	1.0 (4.2)	0.8 $p=0.708$	11.6 (3.6)	9.1 (3.2)	2.5 $p=0.07$
L2	-2.8 (4.9)	-2.7 (3.8)	0.1 $p=0.961$	12.2 (4.4)	7.7 (4.4)	4.5 $p=0.013$
L3	1.8 (4.2)	-3.7 (4.0)	5.5 $p=0.002$	9.2 (4.1)	10.0 (3.1)	0.8 $p=0.602$
L4	-11.0 (10.2)	-7.6 (8.0)	3.4 $p=0.375$	-11.3 (11.5)	-6.9 (6.6)	4.4 $p=0.282$
L5	-10.3 (13.0)	-17.7 (7.0)	7.4 $p=0.106$	-22.3 (7.5)	-17.6 (7.5)	4.7 $p=0.117$

A = Degrees

B = Shaded cells represent significant difference between females and males.

Table 1.49. Left Erector Spinae mean (s.d.) muscle vector directions (degrees) in the coronal (θ_{Cor}) and sagittal (θ_{Sag}) planes. Negative values represent right lateral or posterior direction, and positive values represent left lateral or anterior direction. Differences between the male and female vector directions are shown, which are the absolute difference in degrees. Significant differences between males and females are indicated when $p \leq 0.05$.

Left Erector Spinae - Muscle Vector Directions (degrees) in the Sagittal and Coronal Planes

Level	Female θ_{Cor} mean ^A (s.d.)	Male θ_{Cor} mean ^A (s.d.)	Difference ^B	Female θ_{Sag} mean ^A (s.d.)	Male θ_{Sag} mean ^A (s.d.)	Difference ^B
T8	-5.0 (6.5)	-2.7 (6.5)	2.3 $p=0.350$	0.8 (2.1)	1.2 (4.0)	0.4 $p=0.743$
T9	-4.6 (6.8)	-0.1 (11.4)	4.5 $p=0.186$	8.0 (3.6)	8.1 (9.6)	0.1 $p=0.994$
T10	-2.3 (6.0)	-1.8 (5.3)	0.5 $p=0.831$	9.1 (4.7)	5.9 (5.1)	3.2 $p=0.101$
T11	-3.2 (4.3)	-0.4 (3.2)	2.8 $p=0.084$	7.0 (4.1)	6.5 (3.7)	0.5 $p=0.752$
T12	-4.4 (5.8)	-7.3 (2.9)	2.8 $p=0.085$	5.6 (3.1)	7.0 (5.9)	1.4 $p=0.503$
L1	-1.3 (4.1)	-1.9 (3.2)	0.6 $p=0.731$	8.0 (3.5)	6.1 (3.7)	1.9 $p=0.187$
L2	-0.3 (3.7)	5.7 (4.6)	6.0 $p=0.001$	10.2 (4.2)	8.4 (3.1)	1.8 $p=0.222$
L3	1.4 (3.5)	3.6 (3.6)	2.2 $p=0.121$	9.7 (5.7)	6.9 (2.6)	3.9 $p=0.069$
L4	13.9 (10.4)	10.7 (7.2)	3.2 $p=0.397$	-11.0 (8.8)	-5.4 (9.3)	5.6 $p=0.121$
L5	21.5 (8.7)	20.0 (9.1)	1.5 $p=0.653$	-18.9 (6.2)	-18.8 (8.0)	0.1 $p=0.993$

A = Degrees

B = Shaded cells represent significant difference between females and males.

Table 1.50. Right Rectus Abdominis mean (s.d.) muscle vector directions (degrees) in the coronal (θ_{Cor}) and sagittal (θ_{Sag}) planes. Negative values represent right lateral or posterior direction, and positive values represent left lateral or anterior direction. Differences between the male and female vector directions are shown, which are the absolute difference in degrees. Significant differences between males and females are indicated when $p \leq 0.05$.

Right Rectus Abdominis - Muscle Vector Directions (degrees) in the Sagittal and Coronal Planes

Level	Female θ_{Cor} mean ^A (s.d.)	Male θ_{Cor} mean ^A (s.d.)	Difference ^B	Female θ_{Sag} mean ^A (s.d.)	Male θ_{Sag} mean ^A (s.d.)	Difference ^B
T8						
T9						
T10						
T11						
T12	10.4 (13.0)	10.9 (5.8)	0.4 $p=0.920$	0.1 (7.3)	-6.6 (12.2)	6.7 $p=0.131$
L1	3.9 (11.1)	3.8 (13.4)	0.1 $p=0.982$	-6.2 (8.3)	-14.2 (9.8)	8.0 $p=0.029$
L2	3.5 (7.3)	-2.0 (6.8)	5.5 $p=0.058$	-10.0 (5.6)	-16.7 (5.5)	6.7 $p=0.005$
L3	2.6 (7.6)	0.0 (5.9)	2.6 $p=0.340$	-5.8 (6.7)	-9.2 (7.5)	3.4 $p=0.219$
L4	-0.2 (9.2)	-5.9 (4.2)	5.7 $p=0.028$	2.1 (6.8)	-2.5 (8.1)	4.6 $p=0.113$
L5	-8.0 (8.7)	-3.2 (6.2)	4.8 $p=0.134$	0.4 (8.3)	1.8 (10.7)	1.4 $p=0.683$

A = Degrees

B = Shaded cells represent significant difference between females and males.

Table 1.51. Left Rectus Abdominis mean (s.d.) muscle vector directions (degrees) in the coronal (θ_{Cor}) and sagittal (θ_{Sag}) planes. Negative values represent right lateral or posterior direction, and positive values represent left lateral or anterior direction. Differences between the male and female vector directions are shown, which are the absolute difference in degrees. Significant differences between males and females are indicated when $p \leq 0.05$.

Left Rectus Abdominis - Muscle Vector Directions (degrees) in the Sagittal and Coronal Planes

Level	Female θ_{Cor} mean ^A (s.d.)	Male θ_{Cor} mean ^A (s.d.)	Difference ^B	Female θ_{Sag} mean ^A (s.d.)	Male θ_{Sag} mean ^A (s.d.)	Difference ^B
T8						
T9						
T10						
T11						
T12	1.6 (8.9)	-9.1 (12.5)	10.7 p=0.0343	0.2 (4.8)	-4.4 (9.4)	4.6 p=0.229
L1	3.1 (9.6)	1.4 (11.7)	1.7 p=0.6684	-8.5 (8.2)	-17.9 (7.2)	9.4 p=0.005
L2	0.5 (7.8)	0.6 (4.9)	0.1 p=0.9533	-12.3 (6.4)	-14.1 (4.4)	1.8 p=0.412
L3	-1.9 (5.7)	6.6 (7.0)	8.5 p=0.0013	-6.5 (7.0)	-11.8 (8.0)	5.3 p=0.073
L4	6.4 (6.6)	6.8 (5.8)	0.4 p=0.8571	-1.0 (5.9)	-3.1 (6.6)	2.1 p=0.378
L5	4.1 (8.3)	9.5 (4.2)	5.4 p=0.0269	4.4 (7.1)	-1.6 (11.2)	6.0 p=0.086

A = Degrees

B = Shaded cells represent significant difference between females and males.

Table 1.52. Right External Obliques mean (s.d.) muscle vector directions (degrees) in the coronal (θ_{Cor}) and sagittal (θ_{Sag}) planes. Negative values represent right lateral or posterior direction, and positive values represent left lateral or anterior direction. Differences between the male and female vector directions are shown, which are the absolute difference in degrees. Significant differences between males and females are indicated when $p \leq 0.05$.

Right External Obliques - Muscle Vector Directions (degrees) in the Sagittal and Coronal Planes

Level	Female θ_{Cor} mean ^A (s.d.)	Male θ_{Cor} mean ^A (s.d.)	Difference ^B	Female θ_{Sag} mean ^A (s.d.)	Male θ_{Sag} mean ^A (s.d.)	Difference ^B
T8						
T9						
T10						
T11						
T12	4.1 (9.3)	5.0 (6.2)	0.9 $p=0.798$	0.6 (9.4)	-18.7 (15.2)	19.3 $p=0.005$
L1	-0.4 (10.5)	2.9 (5.4)	3.3 $p=0.257$	-12.5 (11.1)	-21.4 (7.2)	8.9 $p=0.030$
L2	-3.3 (5.7)	-5.0 (5.5)	1.7 $p=0.462$	-13.1 (7.6)	-24.0 (9.0)	10.9 $p=0.002$
L3	6.2 (8.2)	-0.1 (4.4)	6.4 $p=0.030$	4.0 (14.9)	7.7 (7.4)	3.7 $p=0.370$
L4	6.4 (5.8)	-0.7 (8.3)	7.1 $p=0.126$	25.9 (12.5)	23.0 (11.4)	2.9 $p=0.678$
L5	-7.9 (-)			4.1 (-)		

A = Degrees

B = Shaded cells represent significant difference between females and males.

Table 1.53. Left External Obliques mean (s.d.) muscle vector directions (degrees) in the coronal (θ_{Cor}) and sagittal (θ_{Sag}) planes. Negative values represent right lateral or posterior direction, and positive values represent left lateral or anterior direction. Differences between the male and female vector directions are shown, which are the absolute difference in degrees. Significant differences between males and females are indicated when $p \leq 0.05$.

Left External Obliques - Muscle Vector Directions (degrees) in the Sagittal and Coronal Planes

Level	Female θ_{Cor} mean ^A (s.d.)	Male θ_{Cor} mean ^A (s.d.)	Difference ^B	Female θ_{Sag} mean ^A (s.d.)	Male θ_{Sag} mean ^A (s.d.)	Difference ^B
T8						
T9						
T10						
T11						
T12	5.8 (7.9)	-4.8 (10.5)	10.5 $p=0.029$	-5.2 (5.4)	-17.1 (15.2)	11.9 $p=0.052$
L1	2.2 (8.9)	2.2 (4.6)	0.0 $p=0.979$	-19.8 (13.4)	-24.5 (9.6)	4.7 $p=0.332$
L2	2.9 (4.2)	1.8 (2.7)	1.1 $p=0.468$	-20.1 (8.3)	-23.4 (12.7)	3.3 $p=0.396$
L3	-3.7 (4.6)	3.0 (5.1)	6.7 $p=0.001$	2.7 (11.8)	-1.5 (11.5)	4.2 $p=0.359$
L4	-0.3 (6.0)	-0.7 (6.1)	0.4 $p=0.903$	20.6 (8.1)	22.5 (8.2)	1.9 $p=0.699$
L5	16.0 (-)			33.1 (-)		

A = Degrees

B = Shaded cells represent significant difference between females and males.

Table 1.54. Right Internal Obliques mean (s.d.) muscle vector directions (degrees) in the coronal (θ_{Cor}) and sagittal (θ_{Sag}) planes. Negative values represent right lateral or posterior direction, and positive values represent left lateral or anterior direction. Differences between the male and female vector directions are shown, which are the absolute difference in degrees. Significant differences between males and females are indicated when $p \leq 0.05$.

Right Internal Obliques - Muscle Vector Directions (degrees) in the Sagittal and Coronal Planes

Level	Female θ_{Cor} mean ^A (s.d.)	Male θ_{Cor} mean ^A (s.d.)	Difference ^B	Female θ_{Sag} mean ^A (s.d.)	Male θ_{Sag} mean ^A (s.d.)	Difference ^B
T8						
T9						
T10						
T11						
T12						
L1	22.6 (-)					
L2	7.8 (13.9)	5.9 (15.5)	1.9 $p=0.803$	-26.8 (13.6)	-40.1 (15.5)	13.3 $p=0.094$
L3	6.5 (11.7)	-2.0 (8.8)	8.5 $p=0.057$	-11.0 (19.6)	-4.8 (19.9)	6.2 $p=0.431$
L4	6.4 (9.2)	-7.9 (8.5)	14.3 $p=0.024$	27.8 (9.6)	30.0 (4.3)	2.2 $p=0.590$
L5	-17.3 (-)			36.4 (-)		

A = Degrees

B = Shaded cells represent significant difference between females and males.

Table 1.55. Left Internal Obliques mean (s.d.) muscle vector directions (degrees) in the coronal (θ_{Cor}) and sagittal (θ_{Sag}) planes. Negative values represent right lateral or posterior direction, and positive values represent left lateral or anterior direction. Differences between the male and female vector directions are shown, which are the absolute difference in degrees. Significant differences between males and females are indicated when $p \leq 0.05$.

Left Internal Obliques - Muscle Vector Directions (degrees) in the Sagittal and Coronal Planes

Level	Female θ_{Cor} mean ^A (s.d.)	Male θ_{Cor} mean ^A (s.d.)	Difference ^B	Female θ_{Sag} mean ^A (s.d.)	Male θ_{Sag} mean ^A (s.d.)	Difference ^B
T8						
T9						
T10						
T11						
T12						
L1	-12.1 (-)			53.4 (-)		
L2	-2.3 (13.0)	-5.5 (9.3)	3.2 $p=0.577$	-23.2 (8.5)	-31.9 (12.5)	8.7 $p=0.128$
L3	-6.5 (11.0)	4.5 (11.3)	11.0 $p=0.023$	-13.8 (19.1)	-11.9 (18.1)	1.9 $p=0.807$
L4	0.6 (2.2)	6.2 (7.8)	5.6 $p=0.200$	22.0 (8.8)	25.6 (8.9)	3.6 $p=0.516$
L5	25.7 (-)			27.2 (-)		

A = Degrees

B = Shaded cells represent significant difference between females and males.

Table 1.56. Right Psoas Major mean (s.d.) muscle vector directions (degrees) in the coronal (θ_{Cor}) and sagittal (θ_{Sag}) planes. Negative values represent right lateral or posterior direction, and positive values represent left lateral or anterior direction. Differences between the male and female vector directions are shown, which are the absolute difference in degrees. Significant differences between males and females are indicated when $p \leq 0.05$.

Right Psoas Major - Muscle Vector Directions (degrees) in the Sagittal and Coronal Planes

Level	Female θ_{Cor} mean ^A (s.d.)	Male θ_{Cor} mean ^A (s.d.)	Difference ^B	Female θ_{Sag} mean ^A (s.d.)	Male θ_{Sag} mean ^A (s.d.)	Difference ^B
T8						
T9						
T10						
T11						
T12						
L1	8.1 (3.2)	7.5 (-)	0.6	7.1 (4.2)	13.0 (-)	5.9
L2	8.6 (2.0)	10.6 (3.6)	2.0 $p=0.128$	15.6 (6.1)	15.4 (3.4)	0.2 $p=0.928$
L3	12.1 (2.4)	11.3 (2.9)	0.8 $p=0.404$	14.8 (3.6)	13.6 (3.2)	1.2 $p=0.387$
L4	13.9 (3.4)	11.3 (4.0)	2.7 $p=0.070$	14.3 (4.1)	14.3 (2.7)	0.0 $p=0.998$
L5	13.0 (6.2)	9.8 (3.7)	3.2 $p=0.144$	11.0 (6.7)	15.0 (7.4)	4.0 $p=0.157$

A = Degrees

B = Shaded cells represent significant difference between females and males.

Table 1.57. Left Psoas Major mean (s.d.) muscle vector directions (degrees) in the coronal (θ_{Cor}) and sagittal (θ_{Sag}) planes. Negative values represent right lateral or posterior direction, and positive values represent left lateral or anterior direction. Differences between the male and female vector directions are shown, which are the absolute difference in degrees. Significant differences between males and females are indicated when $p \leq 0.05$.

Left Psoas Major - Muscle Vector Directions (degrees) in the Sagittal and Coronal Planes

Level	Female θ_{Cor} mean ^A (s.d.)	Male θ_{Cor} mean ^A (s.d.)	Difference ^B	Female θ_{Sag} mean ^A (s.d.)	Male θ_{Sag} mean ^A (s.d.)	Difference ^B
T8						
T9						
T10						
T11						
T12						
L1	-10.5 (3.9)	-10.9 (3.6)	0.4 $p=0.905$	7.3 (5.0)	17.6 (1.0)	10.3 $p=0.072$
L2	-8.9 (2.5)	-8.0 (2.6)	1.0 $p=0.318$	13.0 (4.0)	16.0 (3.8)	3.0 $p=0.056$
L3	-9.0 (2.7)	-7.9 (2.5)	1.1 $p=0.269$	14.2 (5.2)	12.7 (4.0)	2.5 $p=0.418$
L4	-8.9 (3.0)	-7.5 (2.6)	1.4 $p=0.219$	10.9 (4.8)	12.4 (5.6)	1.5 $p=0.446$
L5	-9.1 (3.9)	-4.0 (3.2)	5.1 $p=0.001$	15.7 (4.7)	14.9 (2.7)	0.8 $p=0.611$

A = Degrees

B = Shaded cells represent significant difference between females and males.

Table 1.58. Right Quadratus Lumborum mean (s.d.) muscle vector directions (degrees) in the coronal (θ_{Cor}) and sagittal (θ_{Sag}) planes. Negative values represent right lateral or posterior direction, and positive values represent left lateral or anterior direction. Differences between the male and female vector directions are shown, which are the absolute difference in degrees. Significant differences between males and females are indicated when $p \leq 0.05$.

Right Quadratus Lumborum - Muscle Vector Directions (degrees) in the Sagittal and Coronal Planes

Level	Female θ_{Cor} mean ^A (s.d.)	Male θ_{Cor} mean ^A (s.d.)	Difference ^B	Female θ_{Sag} mean ^A (s.d.)	Male θ_{Sag} mean ^A (s.d.)	Difference ^B
T8						
T9						
T10						
T11						
T12						
L1	3.3 (9.1)	12.2 (-)	8.9	13.9 (5.8)	5.9 (-)	8.0
L2	21.0 (7.2)	21.9 (4.4)	0.9 $p=0.718$	12.6 (7.6)	10.3 (6.6)	2.3 $p=0.411$
L3	23.4 (4.2)	16.8 (12.3)	6.6 $p=0.129$	14.7 (5.1)	11.2 (4.0)	3.5 $p=0.080$
L4	23.3 (-)			10.6 (-)		
L5						

A = Degrees

B = Shaded cells represent significant difference between females and males.

Table 1.59. Left Quadratus Lumborum mean (s.d.) muscle vector directions (degrees) in the coronal (θ_{Cor}) and sagittal (θ_{Sag}) planes. Negative values represent right lateral or posterior direction, and positive values represent left lateral or anterior direction. Differences between the male and female vector directions are shown, which are the absolute difference in degrees. Significant differences between males and females are indicated when $p \leq 0.05$.

Left Quadratus Lumborum - Muscle Vector Directions (degrees) in the Sagittal and Coronal Planes

Level	Female θ_{Cor} mean ^A (s.d.)	Male θ_{Cor} mean ^A (s.d.)	Difference ^B	Female θ_{Sag} mean ^A (s.d.)	Male θ_{Sag} mean ^A (s.d.)	Difference ^B
T8						
T9						
T10						
T11						
T12						
L1	-11.1 (3.9)	-17.1 (0.2)	6.0 $p=0.078$	8.1 (4.6)	9.8 (8.3)	1.7 $p=0.705$
L2	-23.8 (8.4)	-23.7 (11.3)	0.1 $p=0.970$	8.2 (7.8)	11.3 (5.5)	2.9 $p=0.277$
L3	-17.3 (7.7)	-12.4 (13.7)	4.9 $p=0.315$	14.9 (8.1)	8.4 (5.9)	6.5 $p=0.037$
L4	-20.6 (-)			6.0 (-)		
L5						

A = Degrees

B = Shaded cells represent significant difference between females and males.

Table 1.60. Vertebral body mean (s.d.) muscle vector directions (degrees) in the coronal (θ_{Cor}) and sagittal (θ_{Sag}) planes. Negative values represent right lateral or posterior direction, and positive values represent left lateral or anterior direction. Differences between the male and female vector directions are shown, which are the absolute difference in degrees. Significant differences between males and females are indicated when $p \leq 0.05$.

Vertebral Body - Muscle Vector Directions (degrees) in the Sagittal and Coronal Planes

Level	Female θ_{Cor} mean ^A (s.d.)	Male θ_{Cor} mean ^A (s.d.)	Difference ^B	Female θ_{Sag} mean ^A (s.d.)	Male θ_{Sag} mean ^A (s.d.)	Difference ^B
T8	-0.3 (2.5)	0.8 (2.0)	1.1 $p=0.360$	3.6 (3.0)	1.8 (3.3)	1.8 $p=0.206$
T9	1.5 (2.7)	1.2 (2.6)	0.3 $p=0.401$	6.5 (3.4)	4.3 (3.1)	2.2 $p=0.820$
T10	0.3 (2.4)	0.9 (2.8)	0.6 $p=0.523$	8.3 (5.0)	4.0 (3.8)	4.3 $p=0.021$
T11	-0.2 (3.3)	0.2 (2.5)	0.4 $p=0.779$	9.8 (5.6)	6.6 (3.9)	3.2 $p=0.013$
T12	-0.9 (3.4)	-0.2 (2.9)	0.7 $p=0.570$	12.7 (3.8)	11.2 (5.7)	1.5 $p=0.404$
L1	-1.3 (2.4)	-0.7 (2.3)	0.6 $p=0.527$	14.9 (3.8)	12.0 (5.0)	2.9 $p=0.091$
L2	-0.6 (2.9)	1.2 (2.9)	1.8 $p=0.118$	14.0 (3.9)	11.4 (2.5)	2.6 $p=0.063$
L3	0.6 (2.7)	0.1 (2.8)	0.5 $p=0.673$	8.6 (3.1)	9.1 (1.8)	0.5 $p=0.651$
L4	2.4 (3.8)	1.9 (2.5)	0.5 $p=0.727$	-3.7 (7.2)	0.4 (4.2)	4.1 $p=0.111$
L5	5.4 (5.1)	3.0 (3.3)	2.4 $p=0.203$	-22.0 (10.7)	-15.3 (5.7)	6.7 $p=0.034$

A = Degrees

B = Shaded cells represent significant difference between females and males.

Table 1.61. p-values for regression equations predicting the largest *female* PCSA based on external anthropometric measures. Significant equations are represented by shaded cells ($p \leq 0.05$). Each muscle is the average of the largest right and left side, irrespective of the levels.

Measure Location	Average of Right and Left Largest Muscle						
	Latissimus Dorsi	Erector Spinae	Rectus Abdominis	External Obliques	Internal Obliques	Psoas Major	Quad. Lumborum
XP	0.0053	0.0016	0.0035	0.0333	0.0004	0.5860	0.0102
IC	0.6542	0.5884	0.4361	0.0999	0.7409	0.8613	0.6024
BMI	0.1178	0.0012	0.0223	0.1105	0.0005	0.3756	0.0496

XP = Xyphoid Process;
IC = Iliac Crest;
BMI = Body Mass Index.

Table 1.62. p-values for regression equations predicting the largest *female* PCSA based on external anthropometric measures. Significant equations are represented by shaded cells ($p \leq 0.05$).

Measure Location	Right or Left Muscle													
	RLAT	LLAT	RES	LES	RABD	LABD	REOB	LEOB	RIOB	LIOB	RPSS	LPSS	RQLM	LQLM
XP	0.0043	0.0076	0.0016	0.0019	0.0025	0.0057	0.0371	0.0522	0.0009	0.0006	0.5545	0.6468	0.0155	0.0192
IC	0.7911	0.5276	0.5586	0.6284	0.4386	0.4427	0.1426	0.0998	0.5963	0.9536	0.8134	0.9137	0.6097	0.7729
BMI	0.0855	0.1678	0.0009	0.0019	0.0233	0.0244	0.1580	0.1080	0.0002	0.0039	0.2714	0.5270	0.0485	0.3132

XP = Xyphoid Process;
IC = Iliac Crest;
BMI = Body Mass Index.

Table 1.63. p-values for regression equations predicting the largest *male* PCSA based on external anthropometric measures. Significant equations are represented by shaded cells ($p \leq 0.05$). Each muscle is the average of the largest right and left side, irrespective of the levels.

Measure Location	Average of Right and Left Largest Muscle						
	Latissimus Dorsi	Erector Spinae	Rectus Abdominis	External Obliques	Internal Obliques	Psoas Major	Quad. Lumborum
XP	0.0416	0.0871	0.0742	0.0207	0.0416	0.0404	0.1128
IC	0.2897	0.2219	0.1558	0.3889	0.0609	0.4318	0.0658
BMI	0.0960	0.0332	0.0272	0.2304	0.0596	0.4694	0.5099

XP = Xyphoid Process;
IC = Iliac Crest;
BMI = Body Mass Index.

Table 1.64. p-values for regression equations predicting the largest *male* PCSA based on external anthropometric measures. Significant equations are represented by shaded cells ($p \leq 0.05$).

Measure Location	Right or Left Muscle													
	RLAT	LLAT	RES	LES	RABD	LABD	REOB	LEOB	RIOB	LIQB	RPSS	LPSS	RQLM	LQLM
XP	0.1026	0.0240	0.1036	0.0788	0.0623	0.0904	0.0297	0.0254	0.0884	0.0350	0.0421	0.0478	0.1669	0.0895
IC	0.3533	0.2696	0.2291	0.226	0.1778	0.1376	0.4764	0.3557	0.1093	0.0558	0.3730	0.5369	0.0983	0.0548
BMI	0.0694	0.1503	0.0358	0.0343	0.0276	0.0281	0.2164	0.2707	0.1333	0.0414	0.4707	0.4838	0.4732	0.6170

XP = Xyphoid Process;
IC = Iliac Crest;
BMI = Body Mass Index.

Table 1.65. Regression equations predicting the PCSA (cm²) of the Latissimus Dorsi for Females and Males from various anthropometric measures. Equations were developed for the PCSA of the latissimus dorsi (to represent both the right and left side) using the average of the largest left and right latissimus dorsi, for the right latissimus dorsi, and the left latissimus dorsi. Significant regression equations are indicated by shaded rows when $p \leq 0.05$.

Latissimus Dorsi - Regression Equations Predicting Muscle PCSAs for Females and Males.

Muscle	p-value male vs female regression equation	Females			Males		
		Regression Equation	R ²	p-value	Regression Equation	R ²	p-value
Average of Largest Right and Left Latissimus Dorsi	0.5068 0.0012 0.0020 0.0759	-8.38 + 0.043TDTWXP 16.0 - 0.006TDTWIC 10.05 + 0.004TDTWTR -2.88 + 0.745BMI	0.359 0.011 0.006 0.130	0.0053 0.6542 0.7445 0.1178	-1.67 + 0.031TDTWXP 9.65 + 0.017TDTWIC 5.03 + 0.018TDTWTR -11.0 + 1.26BMI	0.423 0.138 0.189 0.308	0.0416 0.2897 0.2092 0.0960
Right Latissimus Dorsi	0.2826 0.0009 0.0014 0.0645	-8.59 + 0.045TDTWXP 15.5 - 0.003TDTWIC 8.89 + 0.006TDTWTR -4.04 + 0.834BMI	0.372 0.004 0.016 0.155	0.0043 0.7911 0.5961 0.0855	4.55 + 0.024TDTWXP 12.92 + 0.014TDTWIC 12.38 + 0.011TDTWTR -9.79 + 1.26BMI	0.298 0.108 0.084 0.355	0.1026 0.3533 0.4158 0.0694
Left Latissimus Dorsi	0.5379 0.0019 0.0028 0.0989	-8.18 + 0.041TDTWXP 16.48 - 0.008TDTWIC 11.21 + 0.001TDTWTR -1.72 + 0.656BMI	0.335 0.023 0.001 0.103	0.0076 0.5276 0.9123 0.1678	-7.89 + 0.038TDTWXP 6.39 + 0.02TDTWIC -2.33 + 0.025TDTWTR -12.21 + 1.26BMI	0.491 0.150 0.281 0.240	0.0240 0.2696 0.1154 0.1503

TDTWXP = Trunk Depth x Trunk Width (cm²) measured at the Xyphoid Process;

TDTWTR = Trunk Depth x Trunk Width (cm²) measured at the Trochanter ;

TDTWIC = Trunk Depth x Trunk Width (cm²) measured at the Iliac Crest;

BMI = Weight / Height² (kg/m²).

Table 1.66. Regression equations predicting the PCSA (cm²) of the Erector Spinae for Females and Males from various anthropometric measures. Equations were developed for the PCSA of the erector spinae (to represent both the right and left side) using the average of the largest left and right erector spinae, for the right erector spinae, and the left erector spinae. Significant regression equations are indicated by shaded rows when p≤0.05.

Erector Spinae - Regression Equations Predicting Muscle PCSAs for Females and Males.

Muscle	p-value male vs female regression equation	Females			Males		
		Regression Equation	R ²	p-value	Regression Equation	R ²	p-value
Average of Largest Right and Left Erector Spinae	0.0286 0.0000 0.0000 0.0003	1.43 + 0.03TDTWXP	0.432	0.0016	13.3 + 0.021TDTWXP	0.322	0.0871
		15.38 + 0.005TDTWIC	0.017	0.5884	18.6 + 0.015TDTWIC	0.180	0.2291
		8.87 + 0.012TDTWTR	0.123	0.1291	9.68 + 0.022TDTWTR	0.435	0.0381
Right Erector Spinae	0.0236 0.0000 0.0000 0.0005	-2.85 + 0.986BMI	0.452	0.0012	-1.67 + 1.19BMI	0.452	0.0332
		-0.162 + 0.036TDTWXP	0.443	0.0016	14.66 + 0.019TDTWXP	0.297	0.1036
		14.76 + 0.006TDTWIC	0.019	0.5586	19.25 + 0.014TDTWIC	0.175	0.2291
Left Erector Spinae	0.0358 0.0000 0.0000 0.0002	8.86 + 0.012TDTWTR	0.101	0.1715	10.28 + 0.021TDTWTR	0.451	0.0336
		-5.2 + 1.089BMI	0.468	0.0009	-0.111 + 1.125BMI	0.443	0.0358
		3.02 + 0.03TDTWXP	0.423	0.0019	11.93 + 0.023TDTWXP	0.337	0.0788
	0.0000 0.0000	16.0 + 0.004TDTWIC	0.013	0.6284	17.96 + 0.016TDTWIC	0.179	0.2226
		8.89 + 0.012TDTWTR	0.149	0.0928	9.08 + 0.022TDTWTR	0.409	0.0465
		-0.502 + 0.882BMI	0.424	0.0019	-3.458 + 1.264BMI	0.448	0.0343

TDTWXP = Trunk Depth x Trunk Width (cm²) measured at the Xyphoid Process;

TDTWTR = Trunk Depth x Trunk Width (cm²) measured at the Trochanter;

TDTWIC = Trunk Depth x Trunk Width (cm²) measured at the Iliac Crest;

BMI = Weight / Height² (kg/m²).

Table 1.67. Regression equations predicting the PCSA (cm²) of the Rectus Abdominis for Females and Males from various anthropometric measures. Equations were developed for the PCSA of the rectus abdominis (to represent both the right and left side) using the average of the largest left and right rectus abdominis, for the right rectus abdominis, and the left rectus abdominis. Significant regression equations are indicated by shaded rows when p≤0.05.

Rectus Abdominis - Regression Equations Predicting Muscle PCSAs for Females and Males.

Muscle	p-value male vs female regression equation	Females			Males		
		Regression Equation	R ²	p-value	Regression Equation	R ²	p-value
Average of Largest Right and Left Rectus Abdominis	0.1340	-2.82 + 0.018TDTWXP	0.385	0.0035	-0.009 + 0.012TDTWXP	0.345	0.0742
	0.0043	8.51 - 0.004TDTWIC	0.034	0.4361	2.41 + 0.01TDTWIC	0.235	0.1588
	0.0111	5.62 + 0.001TDTWTR	0.002	0.8515	-0.139 + 0.01TDTWTR	0.322	0.0871
	0.3980	-2.88 + 0.433BMI	0.258	0.0223	-8.35 + 0.673BMI	0.476	0.0272
Right Rectus Abdominis	0.2831	-2.785 + 0.018TDTWXP	0.405	0.0025	-0.447 + 0.013TDTWXP	0.370	0.0623
	0.0028	8.28 - 0.004TDTWIC	0.034	0.4386	2.61 + 0.009TDTWIC	0.214	0.1778
	0.0069	5.35 + 0.001TDTWTR	0.003	0.8114	-0.51 + 0.011TDTWTR	0.334	0.0803
	0.2892	-2.56 + 0.412BMI	0.255	0.0233	-8.61 + 0.684BMI	0.474	0.0276
Left Rectus Abdominis	0.2153	-2.85 + 0.019TDTWXP	0.353	0.0057	0.464 + 0.011TDTWXP	0.317	0.0904
	0.0072	8.74 - 0.004TDTWIC	0.033	0.4427	2.21 + 0.01TDTWIC	0.254	0.1376
	0.0189	5.89 + 0.001TDTWTR	0.001	0.8908	-0.377 + 0.01TDTWTR	0.341	0.0762
	0.5183	-3.2 + 0.454BMI	0.251	0.0244	-8.09 + 0.662BMI	0.472	0.0281

TDTWXP = Trunk Depth x Trunk Width (cm²) measured at the Xyphoid Process;

TDTWTR = Trunk Depth x Trunk Width (cm²) measured at the Trochanter;

TDTWIC = Trunk Depth x Trunk Width (cm²) measured at the Iliac Crest;

BMI = Weight / Height² (kg/m²).

Table 1.68. Regression equations predicting the PCSA (cm²) of the External Obliques for Females and Males from various anthropometric measures. Equations were developed for the PCSA of the external obliques (to represent both the right and left side) using the average of the largest left and right external obliques, for the right external obliques, and the left external obliques. Significant regression equations are indicated by shaded rows when $p \leq 0.05$.

External Obliques - Regression Equations Predicting Muscle PCSAs for Females and Males.

Muscle	p-value male vs female regression equation	Females			Males		
		Regression Equation	R ²	p-value	Regression Equation	R ²	p-value
Average of Largest Right and Left External Obliques	0.0318 0.0000 0.0000 0.0002	4.0 + 0.007TDTWXP 5.22 + 0.004TDTWIC 5.2 + 0.003TDTWTR 4.18 + 0.155BMI	0.228 0.143 0.091 0.135	0.0333 0.0999 0.1960 0.1105	1.69 + 0.013TDTWXP 7.7 + 0.005TDTWIC 2.85 + 0.01TDTWTR 2.02 + 0.365BMI	0.508 0.094 0.330 0.174	0.0207 0.3889 0.0823 0.2304
Right External Obliques	0.0534 0.0000 0.0000 0.0003	4.25 + 0.007TDTWXP 5.65 + 0.004TDTWIC 5.05 + 0.003TDTWTR 4.73 + 0.14BMI	0.220 0.116 0.072 0.121	0.0371 0.1426 0.2512 0.1327	3.13 + 0.011TDTWXP 8.56 + 0.004TDTWIC 5.84 + 0.006TDTWTR 2.84 + 0.328BMI	0.466 0.065 0.185 0.184	0.0297 0.4764 0.2151 0.2164
Left External Obliques	0.0036 0.0000 0.0000 0.0005	3.75 + 0.007TDTWXP 4.79 + 0.004TDTWIC 5.35 + 0.002TDTWTR 3.63 + 0.17BMI	0.194 0.143 0.053 0.137	0.0522 0.0998 0.3292 0.1080	0.252 + 0.015TDTWXP 6.83 + 0.007TDTWIC 2.5 + 0.01TDTWTR 1.21 + 0.4BMI	0.484 0.107 0.277 0.149	0.0254 0.3557 0.1885 0.2707

TDTWXP = Trunk Depth x Trunk Width (cm²) measured at the Xyphoid Process;

TDTWTR = Trunk Depth x Trunk Width (cm²) measured at the Trochanter;

TDTWIC = Trunk Depth x Trunk Width (cm²) measured at the Iliac Crest;

BMI = Weight / Height² (kg/m²).

Table 1.69. Regression equations predicting the PCSA (cm²) of the Internal Obliques for Females and Males from various anthropometric measures. Equations were developed for the PCSA of the internal obliques (to represent both the right and left side) using the average of the largest left and right internal obliques, for the right internal obliques, and the left internal obliques. Significant regression equations are indicated by shaded rows when p≤0.05.

Internal Obliques - Regression Equations Predicting Muscle PCSAs for Females and Males.

Muscle	p-value male vs female regression equation	Females			Males		
		Regression Equation	R ²	p-value	Regression Equation	R ²	p-value
Average of Largest Right and Left Internal Obliques	0.3547 0.0000 0.0000 0.0056	-1.83 + 0.016TDTWXP 4.95 + 0.002TDTWIC 4.16 + 0.003TDTWTR -5.27 + 0.543BMI	0.505 0.018 0.042 0.546	0.0009 0.5963 0.4155 0.0005	-0.67 + 0.015TDTWXP 0.233 + 0.015TDTWIC 1.28 + 0.011TDTWTR -6.01 + 0.66BMI	0.470 0.415 0.247 0.419	0.0416 0.0609 0.1731 0.0596
Right Internal Obliques	0.3082 0.0000 0.0000 0.0224	-3.457 + 0.019TDTWXP 4.31 + 0.003TDTWIC 3.9 + 0.003TDTWTR -6.08 + 0.568BMI	0.591 0.026 0.039 0.590	0.0003 0.5228 0.4317 0.0002	0.726 + 0.013TDTWXP 1.41 + 0.014TDTWIC 4.83 + 0.007TDTWTR -3.26 + 0.549BMI	0.359 0.325 0.097 0.292	0.0884 0.1093 0.4150 0.1333
Left Internal Obliques	0.2834 0.0000 0.0000 0.0025	-0.384 + 0.013TDTWXP 6.1 + 0.0001TDTWIC 4.41 + 0.002TDTWTR -1.47 + 0.365BMI	0.535 0.000 0.039 0.415	0.0006 0.9536 0.4332 0.0039	-2.07 + 0.017TDTWXP -0.942 + 0.017TDTWIC -2.27 + 0.015TDTWTR -8.77 + 0.771BMI	0.493 0.428 0.386 0.470	0.0350 0.0558 0.0742 0.0414

TDTWXP = Trunk Depth x Trunk Width (cm²) measured at the Xyphoid Process;
TDTWTR = Trunk Depth x Trunk Width (cm²) measured at the Trochanter;
TDTWIC = Trunk Depth x Trunk Width (cm²) measured at the Iliac Crest;
BMI = Weight / Height² (kg/m²).

Table 1.70. Regression equations predicting the PCSA (cm²) of the Psoas Major for Females and Males from various anthropometric measures. Equations were developed for the PCSA of the psoas major (to represent both the right and left side) using the average of the largest left and right psoas major, for the right psoas major, and the left psoas major. Significant regression equations are indicated by shaded rows when $p \leq 0.05$.

Psoas Major - Regression Equations Predicting Muscle PCSAs for Females and Males.

Muscle	p-value male vs female regression equation	Females				Males			
		Regression Equation	R ²	p-value		Regression Equation	R ²	p-value	
Average of Largest Right and Left Psoas Major	0.0000	90.7 + 0.003TDTWXP	0.017	0.5860		5.77 + 0.018TDTWXP	0.427	0.0404	
	0.0000	10.02 + 0.001TDTWIC	0.002	0.8613		13.94 + 0.007TDTWIC	0.079	0.4318	
	0.0000	8.9 + 0.002TDTWTR	0.020	0.5485		10.62 + 0.009TDTWTR	0.152	0.2655	
	0.0000	7.80 + 0.121BMI	0.044	0.3756		10.32 + 0.366BMI	0.067	0.4694	
Right Psoas Major	0.0000	8.72 + 0.003TDTWXP	0.020	0.5545		3.2 + 0.021TDTWXP	0.422	0.0421	
	0.0000	9.62 + 0.001TDTWIC	0.003	0.8134		11.93 + 0.01TDTWIC	0.100	0.3730	
	0.0000	7.97 + 0.003TDTWTR	0.045	0.3684		8.9 + 0.011TDTWTR	0.149	0.2711	
	0.0000	7.04 + 0.142BMI	0.067	0.2714		8.47 + 0.39BMI	0.067	0.4707	
Left Psoas Major	0.0000	9.42 + 0.002TDTWXP	0.012	0.6468		8.34 + 0.015TDTWXP	0.405	0.0478	
	0.0000	10.43 - 0.0004TDTWIC	0.001	0.9137		15.94 + 0.005TDTWIC	0.049	0.5369	
	0.0000	9.82 + 0.001TDTWTR	0.005	0.7629		12.35 + 0.008TDTWTR	0.146	0.2761	
	0.0000	8.56 + 0.1BMI	0.023	0.5270		12.17 + 0.279BMI	0.063	0.4838	

TDTWXP = Trunk Depth x Trunk Width (cm²) measured at the Xyphoid Process;

TDTWTR = Trunk Depth x Trunk Width (cm²) measured at the Trochanter;

TDTWIC = Trunk Depth x Trunk Width (cm²) measured at the Iliac Crest;

BMI = Weight / Height² (kg/m²).

Table 1.71. Regression equations predicting the PCSA (cm²) of the Quadratus Lumborum for Females and Males from various anthropometric measures. Equations were developed for the PCSA of the quadratus lumborum (to represent both the right and left side) using the average of the largest left and right quadratus lumborum, for the right quadratus lumborum, and the left quadratus lumborum. Significant regression equations are indicated by shaded rows when $p \leq 0.05$.

Quadratus Lumborum - Regression Equations Predicting Muscle PCSAs for Females and Males.

Muscle	p-value male vs female regression equation	Females				Males			
		Regression Equation	R ²	p-value		Regression Equation	R ²	p-value	
Average of Largest Right and Left Quadratus Lumborum	0.0008 0.0000 0.0000 0.0000	1.46 + 0.005TDTWXP	0.329	0.0102		1.78 + 0.008TDTWXP	0.284	0.1128	
		3.36 + 0.001TDTWIC	0.016	0.6024		1.79 + 0.009TDTWIC	0.362	0.0658	
		3.1 + 0.001TDTWTR	0.026	0.5086		-0.87 + 0.01TDTWTR	0.531	0.0168	
		1.48 + 0.108BMI	0.208	0.0496		3.36 + 0.169BMI	0.056	0.5099	
Right Quadratus Lumborum	0.0002 0.0000 0.0000 0.0000	1.156 + 0.005TDTWXP	0.298	0.0155		2.57 + 0.007TDTWXP	0.224	0.1669	
		3.02 + 0.001TDTWIC	0.016	0.6097		2.42 + 0.008TDTWIC	0.304	0.0983	
		2.98 + 0.001TDTWTR	0.012	0.6595		0.066 + 0.008TDTWTR	0.453	0.0329	
		1.054 + 0.113BMI	0.210	0.0485		3.09 + 0.173BMI	0.066	0.4732	
Left Quadratus Lumborum	0.0092 0.0000 0.0000 0.0000	1.46 + 0.005TDTWXP	0.269	0.0192		0.99 + 0.009TDTWXP	0.318	0.0895	
		3.89 + 0.001TDTWIC	0.005	0.7729		1.153 + 0.01TDTWIC	0.387	0.0548	
		3.49 + 0.001TDTWTR	0.017	0.5897		-1.806 + 0.011TDTWTR	0.561	0.0126	
		2.65 + 0.073BMI	0.056	0.3132		3.62 + 0.165BMI	0.044	0.5593	

TDTWXP = Trunk Depth x Trunk Width (cm²) measured at the Xyphoid Process;

TDTWTR = Trunk Depth x Trunk Width (cm²) measured at the Trochanter;

TDTWIC = Trunk Depth x Trunk Width (cm²) measured at the Iliac Crest;

BMI = Weight / Height² (kg/m²).

Table 1.72. p-values for regression equations predicting the *female* coronal plane moment-arms at the origin (L_5) from anthropometric measures. Significant equations are represented by shaded cells ($p \leq 0.05$). The lastissimus dorsi was projected from L_2 through L_5 , the erector spinae and rectus abdominis were present at L_5 , and the external obliques and internal obliques were projected from L_4 through L_5 .

Measure Location	Female Coronal Plane Moment Arm - Origin									
	RLAT	LLAT	RES	LES	RABD	LABD	REOB	LEOB	RIOB	LIQB [#]
XP	0.1591	0.0761	0.9639	0.6501	0.9948	0.6575	0.0237	0.1022	0.6403	0.4988
IC	0.9404	0.6884	0.7683	0.5711	0.8456	0.2227	0.3191	0.4509	0.7317	0.3876
BMI	0.2576	0.1302	0.9681	0.5396	0.5339	0.6294	0.1215	0.1420	0.6566	0.6569

XP = Xyphoid Process;

IC = Iliac Crest;

BMI = Body Mass Index.

Table 1.73. p-values for regression equations predicting the *female* sagittal plane moment-arms at the origin (L_5) from anthropometric measures. Significant equations are represented by shaded cells ($p \leq 0.05$). The lastissimus dorsi was projected from L_2 through L_5 , the erector spinae and rectus abdominis were present at L_5 , and the external obliques and internal obliques were projected from L_4 through L_5 .

Measure Location	Female Sagittal Plane Moment Arm - Origin									
	RLAT	LLAT	RES	LES	RABD	LABD	REOB*	LEOB*	RIOB [#]	LIQB [#]
XP	0.5245	0.6120	0.7970	0.8053	0.2195	0.1314	0.7067	0.4536	0.9447	0.9779
IC	0.0838	0.7810	0.8998	0.6109	0.3749	0.1767	0.2846	0.0902	0.3192	0.4064
BMI	0.2049	0.6559	0.3636	0.3047	0.5038	0.3767	0.7404	0.5514	0.4968	0.3614

XP = Xyphoid Process;

IC = Iliac Crest;

BMI = Body Mass Index.

* The right and left external obliques were projected from L_4 to L_5 at a 45 degree anterior/caudal angle.

The right and left internal obliques were projected from L_4 to L_5 at a 45 degree posterior/caudal angle.

Table 1.74. p-values for regression equations predicting the *female* coronal plane moment-arms at the insertion from anthropometric measures. Significant equations are represented by shaded cells ($p \leq 0.05$). The insertions levels were based on the method of Marras and Granata (1995), with the erector spinae, internal oblique and latissimus dorsi lying between L_3 and L_4 , and the external obliques and rectus abdominis lying between L_1 and L_2 .

Measure Location	Female Coronal Plane Moment Arm - Insertion									
	RLAT	LLAT	RES	LES	RABD	LABD	REOB	LEOB	RIOB	LIOB
XP	0.0274	0.0375	0.1559	0.4041	0.6207	0.0845	0.0012	0.0004	0.0013	0.0111
IC	0.1120	0.1370	0.9598	0.5798	0.6819	0.1147	0.8786	0.9901	0.5317	0.6767
BMI	0.0082	0.0146	0.2822	0.6670	0.4046	0.1249	0.0002	0.0009	0.0001	0.0012

XP = Xyphoid Process;

IC = Iliac Crest;

BMI = Body Mass Index.

Table 1.75. p-values for regression equations predicting the *female* sagittal plane moment-arms at the insertion from anthropometric measures. Significant equations are represented by shaded cells ($p \leq 0.05$). The insertions levels were based on the method of Marras and Granata (1995), with the erector spinae, internal oblique and latissimus dorsi lying between L_3 and L_4 , and the external obliques and rectus abdominis lying between L_1 and L_2 .

Measure Location	Female Sagittal Plane Moment Arm - Insertion									
	RLAT	LLAT	RES	LES	RABD	LABD	REOB	LEOB	RIOB	LIOB
XP	0.5850	0.3973	0.5200	0.9996	0.0086	0.0162	0.8373	0.2577	0.0088	0.1475
IC	0.9560	0.0567	0.0226	0.9475	0.0346	0.0075	0.9341	0.0605	0.3200	0.5417
BMI	0.3774	0.1436	0.1307	0.5720	0.0281	0.0441	0.8706	0.5831	0.0289	0.0436

XP = Xyphoid Process;

IC = Iliac Crest;

BMI = Body Mass Index.

Table 1.76. p-values for regression equations predicting the *male* coronal plane moment-arms at the origin (L_5) from anthropometric measures. Significant equations are represented by shaded cells ($p \leq 0.05$). The lastissimus dorsi was projected from L_2 through L_5 , the erector spinae and rectus abdominis were present at L_5 , and the external obliques and internal obliques were projected from L_4 through L_5 .

Measure Location	Male Coronal Plane Moment Arm - Origin									
	RLAT	LLAT	RES	LES	RABD	LABD	REOB	LEOB	RIOB	LIQB
XP	0.7833	0.6112	0.3283	0.1623	0.9432	0.0772	0.0300	0.0238	0.3817	0.0804
IC	0.7165	0.4304	0.6098	0.4655	0.2891	0.2600	0.0020	0.0001	0.1140	0.2406
BMI	0.0233	0.1266	0.9363	0.7607	0.3099	0.0218	0.0588	0.0067	0.6902	0.1129

XP = Xyphoid Process;

IC = Iliac Crest;

BMI = Body Mass Index.

Table 1.77. p-values for regression equations predicting the *male* sagittal plane moment-arms at the origin (L_5) from anthropometric measures. Significant equations are represented by shaded cells ($p \leq 0.05$). The lastissimus dorsi was projected from L_2 through L_5 , the erector spinae and rectus abdominis were present at L_5 , and the external obliques and internal obliques were projected from L_4 through L_5 .

Measure Location	Male Sagittal Plane Moment Arm - Origin									
	RLAT	LLAT	RES	LES	RABD	LABD	REOB*	LEOB*	RIOB [#]	LIQB [#]
XP	0.4177	0.8218	0.2861	0.7691	0.0578	0.0283	0.2041	0.0280	0.1168	0.0966
IC	0.5400	0.3467	0.4416	0.2508	0.0628	0.1068	0.0403	0.3414	0.0880	0.6164
BMI	0.1476	0.8703	0.3977	0.9381	0.1118	0.0794	0.4619	0.0807	0.5312	0.4493

XP = Xyphoid Process;

IC = Iliac Crest;

BMI = Body Mass Index.

* The right and left external obliques were projected from L_4 to L_5 at a 45 degree anterior/caudal angle.

The right and left internal obliques were projected from L_4 to L_5 at a 45 degree posterior/caudal angle.

Table 1.78. p-values for regression equations predicting the *male* coronal plane moment-arms at the insertion from anthropometric measures. Significant equations are represented by shaded cells ($p \leq 0.05$). The insertions levels were based on the method of Marras and Granata (1995), with the erector spinae, internal oblique and latissimus dorsi lying between L_3 and L_4 , and the external obliques and rectus abdominis lying between L_1 and L_2 .

Measure Location	Male Coronal Plane Moment Arm - Insertion									
	RLAT	LLAT	RES	LES	RABD	LABD	REOB	LEOB	RIOB	LIOB
XP	0.2056	0.0592	0.1232	0.3866	0.3222	0.1669	0.1348	0.0073	0.2736	0.3126
IC	0.2303	0.0316	0.1576	0.1919	0.1344	0.3637	0.0307	0.0346	0.0345	0.1478
BMI	0.2227	0.0196	0.0344	0.0527	0.5509	0.0145	0.2507	0.0014	0.2949	0.0435

XP = Xyphoid Process;

IC = Iliac Crest;

BMI = Body Mass Index.

Table 1.79. p-values for regression equations predicting the *male* sagittal plane moment-arms at the insertion from anthropometric measures. Significant equations are represented by shaded cells ($p \leq 0.05$). The insertions levels were based on the method of Marras and Granata (1995), with the erector spinae, internal oblique and latissimus dorsi lying between L_3 and L_4 , and the external obliques and rectus abdominis lying between L_1 and L_2 .

Measure Location	Male Sagittal Plane Moment Arm - Insertion									
	RLAT	LLAT	RES	LES	RABD	LABD	REOB	LEOB	RIOB	LIOB
XP	0.7655	0.3841	0.1876	0.6351	0.0028	0.0006	0.3819	0.2742	0.3907	0.1404
IC	0.7255	0.7275	0.4896	0.2042	0.0194	0.0892	0.2467	0.7771	0.7803	0.7938
BMI	0.3930	0.5523	0.1923	0.7417	0.0023	0.0004	0.5299	0.1305	0.8619	0.2036

XP = Xyphoid Process;

IC = Iliac Crest;

BMI = Body Mass Index.

Table 1.80. Regression equations predicting the coronal and sagittal plane moment arm (cm) of the muscle centroid of the right Latissimus Dorsi to the centroid of the vertebral body for Females and Males from various anthropometric measures. Significant regression equations are indicated by shaded rows when $p \leq 0.05$.

Right Latissimus Dorsi - Regression Equations Predicting Muscle Moment-Arms for Females and Males.

Plane/Location	Females			Males		
	Regression Equation	R ²	p-value	Regression Equation	R ²	p-value
Coronal/Origin (L ₃)	0.008 - 0.252TWXP	0.107	0.1591	-6.56 - 0.054TWXP	0.010	0.7833
	-7.1 + 0.011TWIC	0.000	0.9404	-6.35 - 0.064TWIC	0.017	0.7165
	-3.54 - 0.154BMI	0.071	0.2576	-0.272 - 0.334BMI	0.494	0.0233
Sagittal/Origin (L ₃)	-2.53 - 0.083TDXP	0.023	0.5245	-0.666 - 0.153TDXP	0.084	0.4177
	-0.51 - 0.179TDIC	0.157	0.0838	-1.63 - 0.114TDIC	0.049	0.5400
	-1.64 - 0.114BMI	0.088	0.2049	2.23 - 0.25BMI	0.243	0.1476
Coronal/Insertion (L ₃ /L ₄)	-0.393 - 0.324TWXP	0.285	0.0274	-4.11 - 0.188TWXP	0.192	0.2056
	-3.94 - 0.181TWIC	0.160	0.1120	-5.27 - 0.163TWIC	0.174	0.2303
	-3.4 - 0.27BMI	0.382	0.0082	-6.07 - 0.16BMI	0.179	0.2227
Sagittal/Insertion (L ₃ /L ₄)	-4.81 + 0.095TDXP	0.020	0.5850	-3.22 - 0.042TDXP	0.012	0.7655
	-3.23 + 0.008TDIC	0.000	0.9560	-5.27 - 0.049TDIC	0.016	0.7255
	-5.35 + 0.11BMI	0.052	0.3774	-1.28 - 0.113BMI	0.093	0.3930

TDXP = Trunk Depth measured at the Xyphoid Process (cm);

TDIC = Trunk Depth measured at the Iliac Crest (cm);

TWXP = Trunk Depth measured at the Xyphoid Process (cm);

TWIC = Trunk Width measured at the Iliac Crest (cm);

BMI = Body Mass Index (kg/m²).

Table 1.81. Regression equations predicting the coronal and sagittal plane moment arm (cm) of the muscle centroid of the left Latissimus Dorsi to the centroid of the vertebral body for Females and Males from various anthropometric measures. Significant regression equations are indicated by shaded rows when $p \leq 0.05$.

Left Latissimus Dorsi - Regression Equations Predicting Muscle Moment-Arms for Females and Males.

Plane/Location	Females			Males		
	Regression Equation	R ²	p-value	Regression Equation	R ²	p-value
Lateral Origin (L ₅)	-1.56 + 0.32TWXP 8.75 - 0.06TWIC 2.68 + 0.21BMI	0.164 0.009 0.123	0.0761 0.6884 0.1302	5.87 + 0.075TWXP 5.12+ 0.105TWIC 3.49 + 0.188BMI	0.034 0.080 0.267	0.6112 0.4304 0.1266
Sagittal Origin (L ₅)	-4.85 - 0.067TDXP -3.0 - 0.03TDIC -2.72 - 0.04BMI	0.015 0.004 0.011	0.6120 0.7810 0.6559	-4.06 + 0.03TDXP -0.754 - 0.118TDIC -2.86 - 0.021BMI	0.007 0.111 0.004	0.8218 0.3467 0.8703
Lateral Insertion (L ₃ /L ₄)	0.874 + 0.314TWXP 4.34 + 0.176TWIC 3.83 + 0.26BMI	0.243 0.133 0.319	0.0375 0.1370 0.0146	2.058 + 0.258TWXP 2.57 + 0.26TWIC 3.56 + 0.268BMI	0.376 0.458 0.514	0.0592 0.0316 0.0196
Sagittal Insertion (L ₃ /L ₄)	-6.74 + 0.151TDXP -9.25 + 0.27TDIC -7.8 + 0.184BMI	0.045 0.209 0.129	0.3973 0.0567 0.1436	-7.65 + 0.164TDXP -2.54 - 0.061TDIC -6.49 + 0.1BMI	0.110 0.016 0.046	0.3841 0.7275 0.5523

TDXP = Trunk Depth measured at the Xyphoid Process (cm);

TDIC = Trunk Depth measured at the Iliac Crest (cm);

TWXP = Trunk Depth measured at the Xyphoid Process (cm);

TWIC = Trunk Width measured at the Iliac Crest (cm);

BMI = Body Mass Index (kg/m²).

Table 1.82. Regression equations predicting the coronal and sagittal plane moment arm (cm) of the muscle centroid of the right Erector Spinae to the centroid of the vertebral body for Females and Males from various anthropometric measures. Significant regression equations are indicated by shaded rows when $p \leq 0.05$.

Right Erector Spinae - Regression Equations Predicting Muscle Moment-Arms for Females and Males.

Plane/Location	Females			Males		
	Regression Equation	R ²	p-value	Regression Equation	R ²	p-value
Coronal/Origin (L ₅)	-2.69 - 0.003TWXP	0.000	0.9639	-6.58 + 0.112TWXP	0.119	0.3283
	-2.14 - 0.016TWIC	0.005	0.7683	-4.6 + 0.054TWIC	0.034	0.6098
	-2.65 + 0.002BMI	0.000	0.9681	-2.74 - 0.008BMI	0.001	0.9363
Sagittal/Origin (L ₅)	-5.11 - 0.017TDXP	0.004	0.7970	-3.43 - 0.116TDXP	0.140	0.2861
	-5.28 - 0.007TDIC	0.001	0.8998	-4.23 - 0.083TDIC	0.076	0.4416
	-6.29 + 0.041BMI	0.046	0.3636	-3.80 - 0.089BMI	0.091	0.3977
Coronal/Insertion (L ₃ /L ₄)	-1.8 - 0.059TWXP	0.109	0.1559	-1.68 - 0.065TWXP	0.271	0.1232
	-3.42 + 0.002TWIC	0.000	0.9598	-2.12 - 0.055TWIC	0.233	0.1576
	-2.66 - 0.033BMI	0.064	0.2822	-1.88 - 0.074BMI	0.448	0.0344
Sagittal/Insertion (L ₃ /L ₄)	-4.16 - 0.043TDXP	0.023	0.5200	-2.6 - 0.134TDXP	0.206	0.1876
	-2.646 - 0.116TDIC	0.257	0.0226	-4.06 - 0.071TDIC	0.062	0.4896
	-3.49 - 0.068BMI	0.122	0.1307	-2.41 - 0.126BMI	0.202	0.1923

TDXP = Trunk Depth measured at the Xyphoid Process (cm);

TDIC = Trunk Depth measured at the Iliac Crest (cm);

TWXP = Trunk Depth measured at the Xyphoid Process (cm);

TWIC = Trunk Width measured at the Iliac Crest (cm);

BMI = Body Mass Index (kg/m²).

Table 1.83. Regression equations predicting the coronal and sagittal plane moment arm (cm) of the muscle centroid of the left Erector Spinae to the centroid of the vertebral body for Females and Males from various anthropometric measures. Significant regression equations are indicated by shaded rows when $p \leq 0.05$.

Left Erector Spinae - Regression Equations Predicting Muscle Moment-Arms for Females and Males.

Plane/Location	Females			Males		
	Regression Equation	R ²	p-value	Regression Equation	R ²	p-value
Coronal/Origin (L ₅)	1.91 + 0.031TWXP	0.012	0.6501	6.85 - 0.114TWXP	0.229	0.1623
	1.89 + 0.03TWIC	0.018	0.5711	4.87 - 0.057TWIC	0.068	0.4655
	2.08 + 0.031BMI	0.021	0.5396	3.75 - 0.023BMI	0.012	0.7607
Sagittal/Origin (L ₅)	-5.34 - 0.02TDXP	0.004	0.8053	-5.29 - 0.035TDXP	0.011	0.7691
	-6.36 + 0.033TDIC	0.015	0.6109	-3.21 - 0.129TDIC	0.161	0.2508
	-6.9 + 0.057BMI	0.058	0.3047	-5.87 - 0.009BMI	0.001	0.9381
Coronal/Insertion (L ₃ /L ₄)	2.711 + 0.03TWXP	0.039	0.4041	2.73 + 0.038TWXP	0.115	0.3386
	3.08 + 0.016TWIC	0.017	0.5798	2.57 + 0.046TWIC	0.203	0.1919
	3.29 + 0.011BMI	0.010	0.6670	2.36 + 0.062BMI	0.392	0.0527
Sagittal/Insertion (L ₃ /L ₄)	-5.3 - 0.0TDXP	0.000	0.9996	-4.6 - 0.043TDXP	0.030	0.6351
	-5.52 - 0.004TDIC	0.000	0.9475	-3.19 - 0.107TDIC	0.193	0.2042
	-4.665 - 0.03BMI	0.018	0.5720	-4.85 - 0.029BMI	0.014	0.7417

TDXP = Trunk Depth measured at the Xyphoid Process (cm);

TDIC = Trunk Depth measured at the Iliac Crest (cm);

TWXP = Trunk Depth measured at the Xyphoid Process (cm);

TWIC = Trunk Width measured at the Iliac Crest (cm);

BMI = Body Mass Index (kg/m²).

Table 1.84. Regression equations predicting the coronal and sagittal plane moment arm (cm) of the muscle centroid of the right Rectus Abdominis to the centroid of the vertebral body for Females and Males from various anthropometric measures. Significant regression equations are indicated by shaded rows when $p \leq 0.05$.

Right Rectus Abdominis - Regression Equations Predicting Muscle Moment-Arms for Females and Males.

Plane/Location	Females			Males		
	Regression Equation	R ²	p-value	Regression Equation	R ²	p-value
Coronal/Origin (L ₅)	-3.86 + 0.001TWXP -4.33 + 0.018TWIC -4.97 + 0.053BMI	0.000 0.002 0.022	0.9948 0.8456 0.5339	-4.34 + 0.007TWXP -6.72 + 0.086TWIC -6.18 + 0.08BMI	0.001 0.139 0.128	0.9432 0.2891 0.3099
Sagittal/Origin (L ₅)	3.36 + 0.17TDXP 4.47 + 0.102TDIC 5.1 + 0.066BMI	0.083 0.044 0.025	0.2195 0.3749 0.5038	-1.53 + 0.398TDXP -0.959 + 0.383TDIC -0.871 + 0.329BMI	0.380 0.368 0.285	0.0578 0.0628 0.1118
Coronal/Insertion (L ₁ /L ₂)	-2.2 - 0.047TWXP -4.33 - 0.03TWIC -2.07 - 0.066BMI	0.015 0.010 0.041	0.6207 0.6819 0.4046	0.392 - 0.159TWXP 1.6 - 0.21TWIC -2.53 - 0.087BMI	0.122 0.258 0.046	0.3222 0.1344 0.5509
Sagittal/Insertion (L ₁ /L ₂)	3.378 + 0.312TDXP 4.744 + 0.22TDIC 4.48 + 0.216BMI	0.342 0.237 0.253	0.0086 0.0346 0.0281	1.93 + 0.423TDXP 3.67 + 0.356TDIC 1.145 + 0.408BMI	0.694 0.515 0.708	0.0028 0.0194 0.0023

TDXP = Trunk Depth measured at the Xyphoid Process (cm);
 TDIC = Trunk Depth measured at the Iliac Crest (cm);
 TWXP = Trunk Depth measured at the Xyphoid Process (cm);
 TWIC = Trunk Width measured at the Iliac Crest (cm);
 BMI = Body Mass Index (kg/m²).

Table 1.85. Regression equations predicting the coronal and sagittal plane moment arm (cm) of the muscle centroid of the left Rectus Abdominis to the centroid of the vertebral body for Females and Males from various anthropometric measures. Significant regression equations are indicated by shaded rows when $p \leq 0.05$.

Left Rectus Abdominis - Regression Equations Predicting Muscle Moment-Arms for Females and Males.

Plane/Location	Females			Males		
	Regression Equation	R ²	p-value	Regression Equation	R ²	p-value
Coronal/Origin (L ₅)	2.076 + 0.043TWXP	0.011	0.6575	-4.16 + 0.229TWXP	0.339	0.0772
	5.85 - 0.093TWIC	0.081	0.2227	-1.01 + 0.141TWIC	0.155	0.2600
	2.5 + 0.036BMI	0.013	0.6294	-3.08 + 0.247BMI	0.502	0.0218
Sagittal/Origin (L ₅)	2.35 + 0.205TDXP	0.122	0.1314	-3.03 + 0.464TDXP	0.472	0.0283
	3.12 + 0.151TDIC	0.099	0.1767	-0.359 + 0.356TDIC	0.292	0.1068
	4.3 + 0.086BMI	0.044	0.3767	-1.99 + 0.373BMI	0.335	0.0794
Coronal/Insertion (L ₁ /L ₂)	-0.446 + 0.149TWXP	0.165	0.0845	-1.32 + 0.164TWXP	0.224	0.1669
	6.6 - 0.107TWIC	0.140	0.1147	0.913 + 0.102TWIC	0.104	0.3637
	1.21 + 0.111BMI	0.133	0.1249	-1.83 + 0.227BMI	0.547	0.0145
Sagittal/Insertion (L ₁ /L ₂)	2.99 + 0.335TDXP	0.295	0.0162	0.807 + 0.479TDXP	0.785	0.0006
	3.0 + 0.31TDIC	0.351	0.0075	5.13 + 0.298TDIC	0.319	0.0892
	4.19 + 0.232BMI	0.218	0.0441	-0.179 + 0.466BMI	0.814	0.0004

TDXP = Trunk Depth measured at the Xyphoid Process (cm);
 TDIC = Trunk Depth measured at the Iliac Crest (cm);
 TWXP = Trunk Depth measured at the Xyphoid Process (cm);
 TWIC = Trunk Width measured at the Iliac Crest (cm);
 BMI = Body Mass Index (kg/m²).

Table 1.86. Regression equations predicting the coronal and sagittal plane moment arm (cm) of the muscle centroid of the right External Obliques to the centroid of the vertebral body for Females and Males from various anthropometric measures. Significant regression equations are indicated by shaded rows when $p \leq 0.05$.

Right External Obliques - Regression Equations Predicting Muscle Moment-Arms for Females and Males.

Plane/Location	Females			Males		
	Regression Equation	R ²	p-value	Regression Equation	R ²	p-value
Coronal/Origin (L ₅)	-4.077 - 0.264TWXP -8.477 - 0.098TWIC -8.22 - 0.141BMI	0.253 0.055 0.128	0.0237 0.3191 0.1215	-5.5 - 0.222TWXP -5.1 - 0.252TWIC -8.14 - 0.178BMI	0.465 0.716 0.378	0.0300 0.0020 0.0588
Sagittal/Origin (L ₅ at a 45 degree anterior caudal angle from L ₄)	4.47 + 0.06TWXP 8.38 - 0.141TWIC 4.79 + 0.038BMI	0.008 0.063 0.006	0.7067 0.2846 0.7404	2.04 + 0.167TWXP 0.446 + 0.243TWIC 3.41 + 0.096BMI	0.193 0.428 0.069	0.2041 0.0403 0.4619
Coronal/Insertion (L ₁ /L ₂)	-3.38 - 0.278TWXP -10.53 - 0.013TWIC -5.67 - 0.246BMI	0.452 0.001 0.555	0.0012 0.8786 0.0002	-4.78 - 0.256TWXP -3.62 - 0.313TWIC -8.47 - 0.18BMI	0.257 0.461 0.161	0.1348 0.0307 0.2507
Sagittal/Insertion (L ₁ /L ₂)	4.88 + 0.038TDXP 6.44 - 0.044TDIC 5.76 - 0.009BMI	0.002 0.000 0.002	0.8373 0.9341 0.8706	3.17 + 0.11TDXP 2.577 + 0.14TDIC 3.73 + 0.076BMI	0.097 0.163 0.051	0.3819 0.2467 0.5299

TDXP = Trunk Depth measured at the Xyphoid Process (cm);
 TDIC = Trunk Depth measured at the Iliac Crest (cm);
 TWXP = Trunk Depth measured at the Xyphoid Process (cm);
 TWIC = Trunk Width measured at the Iliac Crest (cm);
 BMI = Body Mass Index (kg/m²).

Table 1.87. Regression equations predicting the coronal and sagittal plane moment arm (cm) of the muscle centroid of the left External Oblique to the centroid of the vertebral body for Females and Males from various anthropometric measures. Significant regression equations are indicated by shaded rows when $p \leq 0.05$.

Left External Obliques - Regression Equations Predicting Muscle Moment-Arms for Females and Males.

Plane/Location	Females			Males		
	Regression Equation	R ²	p-value	Regression Equation	R ²	p-value
Coronal/Origin (L ₅)	5.457 + 0.2TWXP 8.71 + 0.074TWIC 7.946 + 0.134BMI	0.141 0.032 0.116	0.1022 0.4509 0.1420	1.55 + 0.323TWXP 0.283 + 0.388TWIC 3.75 + 0.322BMI	0.492 0.855 0.622	0.0238 0.0001 0.0067
Sagittal/Origin (L ₅ at a 45 degree anterior caudal angle from L ₄)	2.179 + 0.133TWXP -0.106 + 0.239TWIC 3.056 + 0.074BMI	0.032 0.151 0.020	0.4536 0.0902 0.5514	-1.817 + 0.329TWXP 2.21 + 0.158TWIC -1.05 + 0.264BMI	0.473 0.113 0.333	0.0280 0.3414 0.0807
Coronal/Insertion (L ₁ /L ₂)	2.11 + 0.325TWXP 10.92 - 0.001TWIC 5.98 + 0.232BMI	0.516 0.000 0.465	0.0004 0.9901 0.0009	0.109 + 0.382TWXP 3.5 + 0.297TWIC 2.94 + 0.372BMI	0.614 0.447 0.740	0.0073 0.0346 0.0014
Sagittal/Insertion (L ₁ /L ₂)	1.33 + 0.189TDXP -0.128 + 0.25TDIC 3.44 + 0.065BMI	0.071 0.182 0.017	0.2577 0.0605 0.5831	1.06 + 0.229TDXP 7.65 - 0.06TDIC -1.19 + 0.292BMI	0.147 0.011 0.262	0.2742 0.7771 0.1305

TDXP = Trunk Depth measured at the Xyphoid Process (cm);

TDIC = Trunk Depth measured at the Iliac Crest (cm);

TWXP = Trunk Depth measured at the Xyphoid Process (cm);

TWIC = Trunk Width measured at the Iliac Crest (cm);

BMI = Body Mass Index (kg/m²).

Table 1.88. Regression equations predicting the coronal and sagittal plane moment arm (cm) of the muscle centroid of the right internal oblique to the centroid of the vertebral body for Females and Males from various anthropometric measures. Significant regression equations are indicated by shaded rows when $p \leq 0.05$.

Right Internal Obliques - Regression Equations Predicting Muscle Moment-Arms for Females and Males.

Plane/Location	Females			Males		
	Regression Equation	R ²	p-value	Regression Equation	R ²	p-value
Coronal/Origin (L ₅)	-8.61 - 0.072TWXP -9.41 - 0.041TWIC -11.73 + 0.056BMI	0.014 0.008 0.013	0.6403 0.7317 0.6566	-6.38 - 0.151TWXP -4.167 - 0.235TWIC -9.677 - 0.062BMI	0.097 0.282 0.021	0.3817 0.1140 0.6902
Sagittal/Origin (L ₅ at a 45 degree posterior caudal angle from L ₄)	-1.505 + 0.011TWXP 1.28 - 0.13TWIC 0.468 - 0.084BMI	0.000 0.062 0.029	0.9447 0.3192 0.4968	-6.83 + 0.243TWXP -6.94 + 0.255TWIC -3.81 + 0.099BMI	0.279 0.321 0.051	0.1168 0.0880 0.5312
Coronal/Insertion (L ₃ /L ₄)	1.88 - 0.431TWXP -7.619 - 0.075TWIC -0.811 - 0.424BMI	0.487 0.025 0.695	0.0013 0.5317 0.0001	-6.775 - 0.146TWXP -4.49 - 0.232TWIC -8.32 - 0.124BMI	0.147 0.447 0.136	0.2736 0.0345 0.2949
Sagittal/Insertion (L ₃ /L ₄)	10.7 - 0.404TDXP 6.02 - 0.139TDIC 8.94 - 0.27BMI	0.358 0.062 0.265	0.0088 0.3200 0.0289	-0.55 + 0.167TDXP 2.07 + 0.054TDIC 2.43 + 0.033BMI	0.093 0.010 0.004	0.3907 0.7803 0.8619

TDXP = Trunk Depth measured at the Xyphoid Process (cm);

TDIC = Trunk Depth measured at the Iliac Crest (cm);

TWXP = Trunk Depth measured at the Xyphoid Process (cm);

TWIC = Trunk Width measured at the Iliac Crest (cm);

BMI = Body Mass Index (kg/m²).

Table 1.89. Regression equations predicting the coronal and sagittal plane moment arm (cm) of the muscle centroid of the left Internal Oblique to the centroid of the vertebral body for Females and Males from various anthropometric measures. Significant regression equations are indicated by shaded rows when $p \leq 0.05$.

Left Internal Obliques - Regression Equations Predicting Muscle Moment-Arms for Females and Males.

Plane/Location	Females			Males		
	Regression Equation	R ²	p-value	Regression Equation	R ²	p-value
Coronal/Origin (L ₅)	8.47 + 0.066TWXP 8.44 + 0.065TWIC 9.5 + 0.036BMI	0.029 0.047 0.013	0.4988 0.3876 0.6569	4.04 + 0.199TWXP 5.05 + 0.178TWIC 6.33 + 0.162BMI	0.374 0.190 0.319	0.0804 0.2406 0.1129
Sagittal/Origin (L ₅ at a 45 degree posterior caudal angle from L ₄)	-1.91 + 0.004TWXP -3.86 + 0.102TWIC 0.374 - 0.105BMI	0.000 0.044 0.052	0.9779 0.4064 0.3614	-8.06 + 0.308TWXP -3.147 + 0.098TWIC -4.36 + 0.133BMI	0.345 0.038 0.084	0.0966 0.6164 0.4493
Coronal/Insertion (L ₃ /L ₄)	-2.146 + 0.43TWXP 7.74 + 0.06TWIC 0.473 + 0.425BMI	0.340 0.011 0.492	0.0111 0.6767 0.0012	3.54 + 0.231TWXP -1.195 + 0.4TWIC 1.647 + 0.364BMI	0.145 0.274 0.464	0.3126 0.1478 0.0435
Sagittal/Insertion (L ₃ /L ₄)	8.306 - 0.291TDXP 0.889 + 0.104TDIC 9.37 - 0.305BMI	0.127 0.024 0.231	0.1475 0.5417 0.0436	-3.906 + 0.346TDXP 5.57 - 0.064TDIC -2.76 + 0.267BMI	0.283 0.010 0.219	0.1404 0.7938 0.2036

TDXP = Trunk Depth measured at the Xyphoid Process (cm);
 TDIC = Trunk Depth measured at the Iliac Crest (cm);
 TWXP = Trunk Depth measured at the Xyphoid Process (cm);
 TWIC = Trunk Width measured at the Iliac Crest (cm);
 BMI = Body Mass Index (kg/m²).

Table 1.90. Mean (s.d.) differences between the largest right and left PCSAs (mm²), for both male and females, irrespective of vertebral level location. Shaded cells represent significant differences between the right and left sides, at $p \leq 0.05$.

Muscle Group	Females				Males			
	Mean Diff* (s.d.)	Sample Size	% Diff [#]	p-value	Mean Diff* (s.d.)	Sample Size	% Diff [#]	p-value
Latissimus Dorsi	146.9 (132.5)	20	12.1	0.0001	245.6 (282.0)	10	12.3	0.0223
Erector Spinae	-31.9 (94.3)	20	-1.8	0.1465	2.3 (107.9)	10	0.0	0.9486
Rectus Abdominis	-24.5 (64.2)	20	-3.8	0.1043	5.3 (35.6)	10	0.6	0.6524
External Obliques	47.2 (68.8)	20	6.5	0.0063	-27.8 (120.6)	10	-2.4	0.4850
Internal Obliques	-6.1 (81.5)	18	-1.0	0.7566	-21.7 (156.7)	9	-2.0	0.6887
Psoas Major	-61.2 (96.3)	20	-5.7	0.0104	-78.0 (139.1)	10	-4.0	0.1100
Quadratus Lumborum	-65.2 (50.0)	19	-15.6	0.0001	-31.6 (70.9)	10	-4.0	0.1924

* Mean difference is calculated as the largest PCSA from the right side minus the left side (mm²).

Percent difference is calculated as right PCSA minus left PCSA, divided by the right PCSA.

Table 1.91. p-values for Analysis of Variance results for the right versus left side PCSA, on a level-by-level basis. Shaded cells represent significant differences of the vertebral level \times side interaction at the $p \leq 0.05$ level.

Muscle	Females	Males
Latissimus Dorsi	0.0001	0.0068
Erector Spinae	0.4365	0.6416
Rectus Abdominis	0.9949	0.2849
External Obliques	0.8278	0.5154
Internal Obliques	0.3097	0.6228
Psoas Major	0.1657	0.5651
Quadratus Lumborum	0.0007	0.7886

Table 1.92. Post-hoc results of Analysis of Variance of right versus left side PCSA (R=right, L=left).

Muscle	Gender	T8	T9	T10	T11	T12	L1	L2	L3	L4	L5	S1
Latissimus Dorsi	Male	R>L	R>L	R>L								
	Female	R>L	R>L	R>L								
Quad Lumb.	Female								L>R	L>R		

Table 1.93. Difference (mm²) between *female* right and left side PCSA for each muscle group. Percent difference shown in [], calculated as right minus left, divided by the left. Statistically significant differences (p≤0.05) between right and left side PCSAs are indicated by shaded cells.

Muscle	Vertebral Level										
	T ₈	T ₉	T ₁₀	T ₁₁	T ₁₂	L ₁	L ₂	L ₃	L ₄	L ₅	S ₁
Latissimus Dorsi	140.0 [11.6]	101.1 [9.4]	80.8 [8.6]	39.7 [4.6]	43.1 [5.9]	-26.5 [4.6]	-20.1 [5.5]	-21.8 [13.2]			
Erector Spinae	-20.3 [-2.6]	-2.5 [-0.3]	-12.8 [-1.3]	-5.9 [-0.6]	-33.0 [-2.8]	30.0 [-2.1]	-13.1 [-0.8]	-18.6 [-1.1]	-44.8 [-2.6]	18.0 [1.9]	-25.5 [-4.9]
Rectus Abdominis					-41.0 [-9.1]	-5.9 [-1.2]	-16.4 [-3.8]	-7.0 [-1.6]	-15.6 [-3.1]	-6.8 [-1.3]	-17.7 [2.9]
External Obliques					38.6 [8.6]	40.4 [8.1]	22.7 [3.8]	26.8 [4.0]	18.4 [2.7]	-8.4 [-1.4]	-25.1 [-6.8]
Internal Obliques						43.7 [33.2]	11.0 [3.7]	17.2 [4.3]	-13.1 [-2.1]	-59.6 [-12.1]	-89.7 [-20.5]
Quadratus Lumborum						-1.3 [-0.7]	0.8 [0.4]	-34.7 [-12.9]	-72.2 [-17.0]	-58.9 [-12.6]	
Psoas Major						-4.5 [-2.0]	-25.7 [-7.3]	-16.8 [-2.6]	-46.0 [-4.8]	-74.0 [-7.1]	-8.3 [-0.9]

Table 1.94. Difference (mm²) between *male* right and left side PCSAs for each muscle group. Percent difference shown in [], calculated as right minus left, divided by the left. Statistically significant differences (p≤0.05) between right and left side PCSA are indicated by shaded cells.

Muscle	Vertebral Level											
	T ₈	T ₉	T ₁₀	T ₁₁	T ₁₂	L ₁	L ₂	L ₃	L ₄	L ₅	S ₁	
Latissimus Dorsi	217.1 [10.9]	196.2 [10.9]	157.1 [10.2]	53.6 [3.7]	94.4 [8.0]	21.6 [2.4]	25.4 [4.1]	-1.9 [0.7]				
Erector Spinae	-9.8 [-0.8]	-12.0 [-0.9]	-67.6 [-4.3]	-69.9 [-3.9]	-28.4 [-1.5]	-8.0 [-0.4]	17.6 [0.7]	-26.0 [-0.9]	-1.7 [-0.1]	-52.7 [-2.9]	-29.2 [-3.6]	
Rectus Abdominis					-36.3 [-6.1]	-26.9 [-4.2]	-19.4 [-3.3]	-49.3 [-6.5]	21.6 [3.2]	-18.2 [-2.1]	10.3 [1.2]	
External Obliques					38.2 [6.5]	46.1 [6.1]	7.7 [0.9]	-0.2 [0.0]	-27.4 [-2.5]	-65.6 [-7.9]		
Internal Obliques							-76.9 [-21.6]	-18.0 [-2.4]	-43.9 [-4.2]	-43.0 [-7.0]		
Quadratus Lumborum						-11.4 [-4.1]	16.4 [5.4]	-26.4 [-4.3]	-24.5 [-3.5]			
Psoas Major						-54.0 [-17.5]	-91.2 [-11.9]	-45.7 [-3.5]	-60.9 [-3.4]	-41.2 [-2.2]	-35.9 [-2.2]	

Table 1.95. Muscle vector locations for the *muscle origins*, in the coronal and sagittal plane for males and females, as a function of anthropometric measurements at the xyphoid process and the iliac crest. Negative values in the coronal plane represent right lateral and positive represent left lateral. Negative values for the sagittal plane represent posterior, and positive values represent anterior to the centroid of the vertebral body.

Muscle	Coronal Plane				Sagittal Plane			
	Female		Male		Female		Male	
	Xyphoid Process	Iliac Crest	Xyphoid Process	Iliac Crest	Xyphoid Process	Iliac Crest	Xyphoid Process	Iliac Crest
RLAT	-0.25	-0.24	-0.26	-0.28	-0.22	-0.21	-0.18	-0.19
LLAT	0.26	0.25	0.26	0.28	-0.20	-0.18	-0.15	-0.15
RES	-0.10	-0.09	-0.09	-0.10	-0.30	-0.28	-0.27	-0.27
LES	0.10	0.10	0.10	0.10	-0.31	-0.29	-0.27	-0.27
RABD	-0.14	-0.14	-0.13	-0.14	0.35	0.33	0.33	0.34
LABD	0.12	0.12	0.10	0.11	0.33	0.31	0.33	0.34
REOB	-0.42	-0.40	-0.39	-0.42	0.14	0.13	0.13	0.14
LEOB	0.40	0.39	0.37	0.40	0.11	0.10	0.14	0.15
RIOB	-0.39	-0.38	-0.35	-0.37	0.16	0.15	0.13	0.13
LI OB	0.38	0.37	0.32	0.34	0.15	0.14	0.17	0.18

Latissimus Dorsi: Projected From T₈ through L₂ to L₅;

Erector Spinae: L₅;

Rectus Abdominis: L₅;

External Obliques: Projected from L₁ through L₄ to L₅;

Internal Obliques: Projected from L₃ through L₄ to L₅.

Table 1.96. Muscle vector locations for the *muscle origins*, in the coronal and sagittal plane for males and females, as a function of anthropometric measurements at the xyphoid process and the iliac crest. Negative values in the coronal plane represent right lateral and positive represent left lateral. Negative values for the sagittal plane represent posterior, and positive values represent anterior to the centroid of the vertebral body.

Muscle	Coronal Plane				Sagittal Plane			
	Female		Male		Female		Male	
	Xyphoid Process	Iliac Crest	Xyphoid Process	Iliac Crest	Xyphoid Process	Iliac Crest	Xyphoid Process	Iliac Crest
RLAT	-0.25	-0.24	-0.26	-0.28	-0.22	-0.21	-0.18	-0.19
LLAT	0.26	0.25	0.26	0.28	-0.20	-0.18	-0.15	-0.15
RES	-0.10	-0.09	-0.09	-0.10	-0.30	-0.28	-0.27	-0.27
LES	0.10	0.10	0.10	0.10	-0.31	-0.29	-0.27	-0.27
RABD	-0.14	-0.14	-0.13	-0.14	0.35	0.33	0.33	0.34
LABD	0.12	0.12	0.10	0.11	0.33	0.31	0.33	0.34
REOB	-0.42	-0.40	-0.39	-0.42	0.31	0.29	0.26	0.26
LEOB	0.40	0.39	0.37	0.40	0.25	0.23	0.25	0.26
RIOB	-0.39	-0.38	-0.35	-0.37	0.16	0.15	0.13	0.13
LI OB	0.38	0.37	0.32	0.34	0.15	0.14	0.17	0.18

Latissimus Dorsi: Projected From T₈ through L₂ to L₅;

Erector Spinae: L₅;

Rectus Abdominis: L₅;

External Obliques: L₄ to L₅ at a 45 degree angle;

Internal Obliques: Projected from L₃ through L₄ to L₅.

Table 1.97. Muscle vector locations for the *muscle origins*, in the coronal and sagittal plane for males and females, as a function of anthropometric measurements at the xyphoid process and the iliac crest. Negative values in the coronal plane represent right lateral and positive represent left lateral. Negative values for the sagittal plane represent posterior, and positive values represent anterior to the centroid of the vertebral body.

Muscle	Coronal Plane				Sagittal Plane			
	Female		Male		Female		Male	
	Xyphoid Process	Iliac Crest	Xyphoid Process	Iliac Crest	Xyphoid Process	Iliac Crest	Xyphoid Process	Iliac Crest
RLAT	-0.25	-0.24	-0.26	-0.28	-0.22	-0.21	-0.18	-0.19
LLAT	0.26	0.25	0.26	0.28	-0.20	-0.18	-0.15	-0.15
RES	-0.10	-0.09	-0.09	-0.10	-0.30	-0.28	-0.27	-0.27
LES	0.10	0.10	0.10	0.10	-0.31	-0.29	-0.27	-0.27
RABD	-0.14	-0.14	-0.13	-0.14	0.35	0.33	0.33	0.34
LABD	0.12	0.12	0.10	0.11	0.33	0.31	0.33	0.34
REOB	-0.42	-0.40	-0.39	-0.42	0.31	0.29	0.26	0.26
LEOB	0.40	0.39	0.37	0.40	0.25	0.23	0.25	0.26
RIOB	-0.39	-0.38	-0.35	-0.37	-0.07	-0.07	-0.06	-0.06
LI OB	0.38	0.37	0.32	0.34	-0.10	-0.09	-0.05	-0.05

Latissimus Dorsi: Projected From T₈ through L₂ to L₅;

Erector Spinae: L₅;

Rectus Abdominis: L₅;

External Obliques: L₄ to L₅ at a 45 degree angle;

Internal Obliques: Projected from L₄ to L₅ at a -45 degree angle.

Table 1.98. Muscle vector locations for the **muscle insertions**, in the coronal and sagittal plane for males and females, as a function of anthropometric measurements at the xyphoid process and the iliac crest. Negative values in the coronal plane represent right lateral and positive represent left lateral. Negative values for the sagittal plane represent posterior, and positive values represent anterior to the centroid of the vertebral body.

Muscle	Coronal Plane				Sagittal Plane			
	Female		Male		Female		Male	
	Xyphoid Process	Iliac Crest	Xyphoid Process	Iliac Crest	Xyphoid Process	Iliac Crest	Xyphoid Process	Iliac Crest
RLAT	-0.49	-0.47	-0.47	-0.51	-0.09	-0.08	-0.08	-0.08
LLAT	0.49	0.47	0.46	0.50	-0.04	-0.04	-0.03	-0.03
RES	-0.10	-0.09	-0.10	-0.10	-0.24	-0.22	-0.23	-0.24
LES	0.10	0.10	0.10	0.11	-0.23	-0.21	-0.21	-0.22
RABD	-0.13	-0.12	-0.14	-0.15	0.52	0.48	0.54	0.56
LABD	0.14	0.13	0.13	0.13	0.53	0.49	0.55	0.57
REOB	-0.40	-0.39	-0.40	-0.43	0.30	0.29	0.29	0.30
LEOB	0.41	0.39	0.39	0.42	0.31	0.29	0.32	0.33
RIOB	-0.36	-0.35	-0.36	-0.38	0.19	0.17	0.15	0.15
LIOB	0.35	0.34	0.34	0.36	0.17	0.15	0.18	0.19

Latissimus Dorsi: T₈;

Erector Spinae: T₈;

Rectus Abdominis: L₁;

External Obliques: L₁;

Internal Obliques: L₃.

Table 1.99. Linear regression equations predicting vertical distance (cm) from the L₅ vertebral level to different muscle vertebral levels in the coronal direction, as a function of standing height.

Vertebral Levels	Females			Males		
	Regression Equation*	R ²	p-value	Regression Equation*	R ²	p-value
T ₈ - L ₅ (cm)	8.834 + 0.106Height	0.392	0.0032	5.703 + 0.129Height	0.639	0.0055
L ₁ - L ₅ (cm)	4.734 + 0.053Height	0.261	0.0214	1.759 + 0.072Height	0.580	0.0105
L ₃ - L ₅ (cm)	3.678 + 0.019Height	0.144	0.0989	0.377 + 0.040Height	0.527	0.0028

Table 1.100. Muscle vector locations for the *muscle insertions*, in the coronal and sagittal plane for males and females, as a function of anthropometric measurements at the xyphoid process and the iliac crest. Negative values in the coronal plane represent right lateral and positive represent left lateral. Negative values for the sagittal plane represent posterior, and positive values represent anterior to the centroid of the vertebral body.

Muscle	Coronal Plane				Sagittal Plane			
	Female		Male		Female		Male	
	Xyphoid Process	Iliac Crest	Xyphoid Process	Iliac Crest	Xyphoid Process	Iliac Crest	Xyphoid Process	Iliac Crest
RLAT	-0.34	-0.32	-0.32	-0.34	-0.17	-0.16	-0.18	-0.19
LLAT	0.35	0.33	0.32	0.35	-0.22	-0.21	-0.17	-0.18
RES	-0.13	-0.12	-0.12	-0.13	-0.27	-0.25	-0.25	-0.26
LES	0.13	0.13	0.12	0.13	-0.29	-0.27	-0.25	-0.25
RABD	-0.13	-0.12	-0.15	-0.16	0.50	0.46	0.51	0.52
LABD	0.13	0.13	0.12	0.13	0.50	0.46	0.52	0.53
REOB	-0.40	-0.39	-0.40	-0.43	0.27	0.25	0.25	0.26
LEOB	0.40	0.39	0.39	0.41	0.26	0.24	0.28	0.29
RIOB	-0.36	-0.35	-0.36	-0.38	0.18	0.17	0.15	0.16
LI OB	0.35	0.34	0.34	0.36	0.16	0.15	0.18	0.18

Latissimus Dorsi: L₃/L₄;

Erector Spinae: L₃/L₄;

Rectus Abdominis: L₁/L₂;

External Obliques: L₁/L₂;

Internal Obliques: L₃/L₄;

Table 1.101. Distribution (percentage of total sample, and frequency of occurrence in parenthesis) of the largest muscle area by vertebral level, for the right and left latissimus dorsi.

Vertebral Level	Right Latissimus Dorsi		Left Latissimus Dorsi	
	Female	Male	Female	Male
T ₈	95% (19)	80% (8)	90% (18)	80% (8)
T ₉	5% (1)	20% (2)	10% (2)	20% (2)

Table 1.102. Distribution (percentage of total sample, and frequency of occurrence in parenthesis) of the largest muscle area by vertebral level, for the right and left erector spinae.

Vertebral Level	Right Erector Spinae		Left Erector Spinae	
	Female	Male	Female	Male
L ₂	15% (3)	10% (1)	15% (3)	10% (1)
L ₃	40% (8)	50% (5)	45% (9)	60% (6)
L ₄	45% (9)	40% (4)	40% (8)	30% (3)
L ₅	5% (1)	--	--	--

Table 1.103. Distribution (percentage of total sample, and frequency of occurrence in parenthesis) of the largest muscle area by vertebral level, for the right and left rectus abdominis.

Vertebral Level	Right Rectus Abdominis		Left Rectus Abdominis	
	Female	Male	Female	Male
T ₁₂	--	--	5% (1)	--
L ₁	--	--	15% (3)	--
L ₂	5% (1)	--	5% (1)	--
L ₃	--	--	--	30% (3)
L ₄	10% (2)	--	5% (1)	--
L ₅	15% (3)	40% (4)	25% (5)	30% (3)
S ₁	70% (14)	60% (6)	45% (9)	40% (4)

Table 1.104. Distribution (percentage of total sample, and frequency of occurrence in parenthesis) of the largest muscle area by vertebral level, for the right and left external obliques.

Vertebral Level	Right External Oblique		Left External Oblique	
	Female	Male	Female	Male
L1	--	10% (1)	--	--
L ₂	15% (3)	--	10% (2)	--
L ₃	40% (8)	30% (3)	40% (8)	20% (2)
L ₄	45% (9)	40% (4)	45% (9)	70% (7)
L ₅	--	20% (2)	5% (1)	10% (1)

Table 1.105. Distribution (percentage of total sample, and frequency of occurrence in parenthesis) of the largest muscle area by vertebral level, for the right and left internal obliques.

Vertebral Level	Right Internal Oblique		Left Internal Oblique	
	Female	Male	Female	Male
L ₂	--	--	5.6% (1)	--
L ₃	16.7% (3)	20% (2)	5.6% (1)	11.1% (1)
L ₄	83.3% (15)	80% (8)	88.8% (16)	88.9% (8)

Table 1.106. Distribution (percentage of total sample, and frequency of occurrence in parenthesis) of the largest muscle area by vertebral level, for the right and left quadratus lumborum.

Vertebral Level	Right Quadratus Lumborum		Left Quadratus Lumborum	
	Female	Male	Female	Male
L ₂	5.3% (1)	--	--	--
L ₃	15.8% (3)	10% (1)	10% (2)	10% (1)
L ₄	73.7% (14)	90% (9)	85% (17)	90% (9)
L ₅	5.3% (1)	--	5% (1)	--

Table 1.107. Distribution (percentage of total sample, and frequency of occurrence in parenthesis) of the largest muscle area by vertebral level, for the right and left psoas major.

Vertebral Level	Right Psoas Major		Left Psoas Major	
	Female	Male	Female	Male
L ₄	35% (7)	40% (4)	20% (4)	40% (4)
L ₅	40% (8)	60% (6)	65% (13)	40% (4)
S ₁	25% (5)	--	15% (3)	20% (2)

Part 2: Physiological measurement of the in-vivo muscular length-strength and force-velocity relationships in the female trunk torso.

Introduction

The estimation of moments and forces about the lower back using the EMG-assisted biomechanical model consists of adding the predicted muscle forces in three dimensions, and then using muscle moment-arm relationships, adding and partitioning the resulting moment in three dimensions. The determination of muscle force, however, is a function of muscle dynamics, which affect the EMG signal and the force output, and the force producing capability of the muscle, which includes the gain and the size of the muscle. The muscle physiological cross-sectional areas and geometry (e.g., location of the vector coordinates for insertion and origins) relationships for females were determined in Part 1. The muscle gains should remain constant in an individual. The force output of a muscle however, depends on the length of the muscle and the velocity of contraction at any point in time during the exertion. These factors also affect the EMG activity elicited from the muscle. Thus, in order to develop a valid dynamic biomechanical EMG-assisted model to estimate spinal loading, the muscle length-strength and force-velocity relationships must be determined.

Background and Objectives

The objective of Part 2 was to develop the empirical muscle length-strength and muscle force-velocity relationships that describe the dynamic muscle behavior of military age females, which then will be incorporated into a female specific dynamic EMG-assisted biomechanical model. Past research has found that the length of the muscle and the velocity of the muscle contraction have an affect on the maximum muscle force capabilities, as well as the electromyographic activity elicited from the muscles (Wilkie, 1950; Bigland and Lippold, 1954; Hill, 1938; Komi, 1973; Granata and Marras, 1993; Raschke and Chaffin, 1996; Davis et al., 1998). Additionally, these relationships have been developed on muscle activities from males. Thus, in order to permit accurate assessments of spinal loading and associated LBD risk of

females performing *dynamic* material handling tasks, it is necessary to generate the physiologic description of muscle dynamics that accurately describes military age women.

Administrative Note

In the accepted research proposal, the experimental design and methods for Part 2 called for collecting the electromyographic, kinetic and kinematic data from 35 females in a free-dynamic mode. After the 35 subjects had been collected, quality control checks indicated that nine subjects had to be excluded from the dataset of 35 females due to unacceptable data. Efforts continue to collect the agreed upon 35 subjects for this part of the research.

The free-dynamic mode of lifting allows the subjects to lift the weights at different controlled isokinetic trunk velocities while their body remained unconstrained, except for their feet. Preliminary analyses from these free-dynamic lifting trials did not result in acceptable model performances, with low r^2 's and high muscle gain values. Thus, it was hypothesized that the subjects were allowing their hips and pelvis's to rotate during the lifting motions, resulting in highly variable length-strength and force-velocity results. Therefore, to remove the potential confounding effect of the rotation of the pelvis and hips, additional subjects were collected in a device called a pelvic support structure (PSS), which restricts movement to the trunk only, and not the pelvis. Thirty-six subjects have been collected in the PSS, and the modulation factors determined from this new dataset are very promising as the performance of the biomechanical model using these modulations have enhanced the performance parameters far above those solely on the free-dynamic data. Similarly, when the modulation factors determined from the PSS were applied to the data from the free-dynamic exertions, the biomechanical model performance parameters were again more acceptable than those when the modulation factors were determined solely from the free-dynamic exertions. Thus, the approach used was to determine the muscle length-strength and force-velocity relationships that we know are valid (from the PSS lifting trials), and apply these relationships to the free-dynamic lifting exertions.

The results reported as of October 24, 1998, for Part 2 include 1) the derivation of the female length-strength and force-velocity modulation factors from 36 female subjects performing lifting exertions while constrained at the hips (i.e., in the PSS), and 2) the application of these modulation factors to the kinematic, kinetic, and electromyographic data collected from the 26

subjects in the free-dynamic mode to assess the model performance during controlled sagittally symmetric free-dynamic lifting. The results presented are promising, and it is expected that the additional subjects to be collected to finish out this phase will solidify the current relationships.

Methods

Subjects

The subjects consisted of 36 females for the lifting performed while constrained at the hips (in a pelvic support structure, described later), and 26 females for the free-dynamic lifts, all recruited from the local community. The anthropometric measurements for subjects in both lifting modes are shown in Table 2.1. None of the subjects were experiencing any low back pain at the time of the testing.

Table 2.1 Anthropometric data (mean and s.d.) from the female subjects for the lifting in the PSS and from the free-dynamic lifts.

Anthropometric Variable	Pelvic Support Structure (N=36)	Free-Dynamic (N=26)
Age (yrs)	23.6 (4.9)	23.0 (3.2)
Standing Height (cm)	166.3 (6.3)	167.8 (5.0)
Weight (kg)	60.9 (8.9)	61.3 (7.8)
Trunk Width at Iliac Crest (cm)	27.1 (2.1)	26.7 (2.2)
Trunk Depth at Iliac Crest (cm)	18.8 (2.2)	18.5 (2.1)
Trunk Width at Xyphoid Process (cm)	26.7 (1.4)	27.4 (1.4)
Trunk Depth at Xyphoid Process (cm)	19.4 (1.7)	19.4 (1.7)
Body Mass Index (kg/m ²)	21.9 (2.3)	21.7 (2.0)

Experimental Design

The experimental design described below applies to the data collected from the free-dynamic mode as well as the lifting with the hips constrained in the PSS. The dependent variable consisted of the normalized electromyographic (EMG) activity from each of ten trunk muscles. The independent variables consisted of the weight of lift (15 lbs or 30 lbs), speed of the lifting motion (15, 30, 45, and 60 degrees per second) through a range of 50 degrees forward flexion to an upright standing position, as well as a static holding position (0 deg/sec) at forward trunk flexion angles of 5, 20, 35, and 50 degrees. The various weight and velocity lifting conditions were presented to each subject in a random order.

Equipment

A lumbar motion monitor (LMM), which is essentially an exoskeleton of the spine, was used to collect the kinematic trunk variables (Marras et al., 1992). The LMM was placed on the subjects back, and provided feedback via a computer screen as to when the subject reached the starting trunk angle. The LMM also measured and provided feedback on the trunk extension velocity, as the subject viewed the trunk velocity trace and their performance on a computer screen.

Electromyographic (EMG) activity was collected through the use of bipolar silver-silver chloride surface electrodes, spaced approximately 3 cm apart over ten trunk muscles (Mirka and Marras, 1993). The ten trunk muscles included the right and left pairs of the latissimus dorsi, erector spinae, rectus abdominis, external obliques, and the internal obliques. The subjects performed the lifting exertions while standing on a force plate (Bertec 4060A, Worthington, OH), which measured the three dimensional ground reaction moments and forces generated during the lifting exertions.

While the LMM, electromyography, and a force plate were used for both segments of this study (i.e., the lifting performed with the hips constrained and also for the free-dynamic mode), the external structures were different between the two modes. For the free-dynamic conditions, the subjects were not constrained in any way except for the requirement that they keep their feet on the force plate during the lifting exertion. To translate the moments and forces measured from the force plate to the estimated location of the L₅/S₁ intervertebral disc, the location and

orientation of the subjects' lumbosacral joint was monitored by use of a *sacral location orientation monitor* (SLOM) and a *pelvic orientation monitor* (POM, see Figure 2.1), (Fathallah et al., 1997). For lifting trials performed with the hips constrained, the subjects were positioned into a *pelvic support structure* (PSS) that was attached to the force plate. The PSS restrained the subject's pelvis and hips in a fixed position (see Figure 2.2). The position of the L₅/S₁ relative to the center of the force plate remained constant for all lifting trials, which allowed the forces and moments measured by the force plate to be rotated and translated to the position of the L₅/S₁ (Granata et al., 1995).

All data signals from the above equipment were collected simultaneously through customized Windows™ based software developed in-house. The signals were collected at 100 Hz and recorded on a 486 computer via an analog-to-digital conversion board and stored for later analysis.

To allow the subjects to control their lifting velocity in an isokinetic manner, an additional computer was used to display the instantaneous velocity recorded by the LMM in real time. The signal was transferred from the LMM to the computer through an analog-to-digital board and converted into velocity by customized software. The subjects were then to control their isokinetic lifting velocity by keeping the trace of the velocity within tolerance lines displayed on the computer.

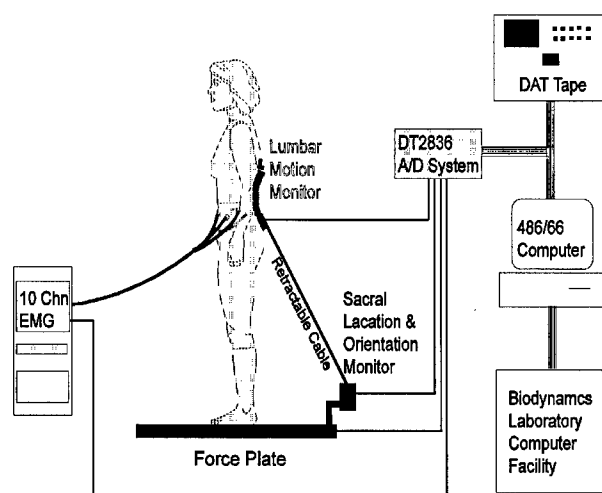


Figure 2.1. Experimental equipment for the Free Dynamic lifting conditions.

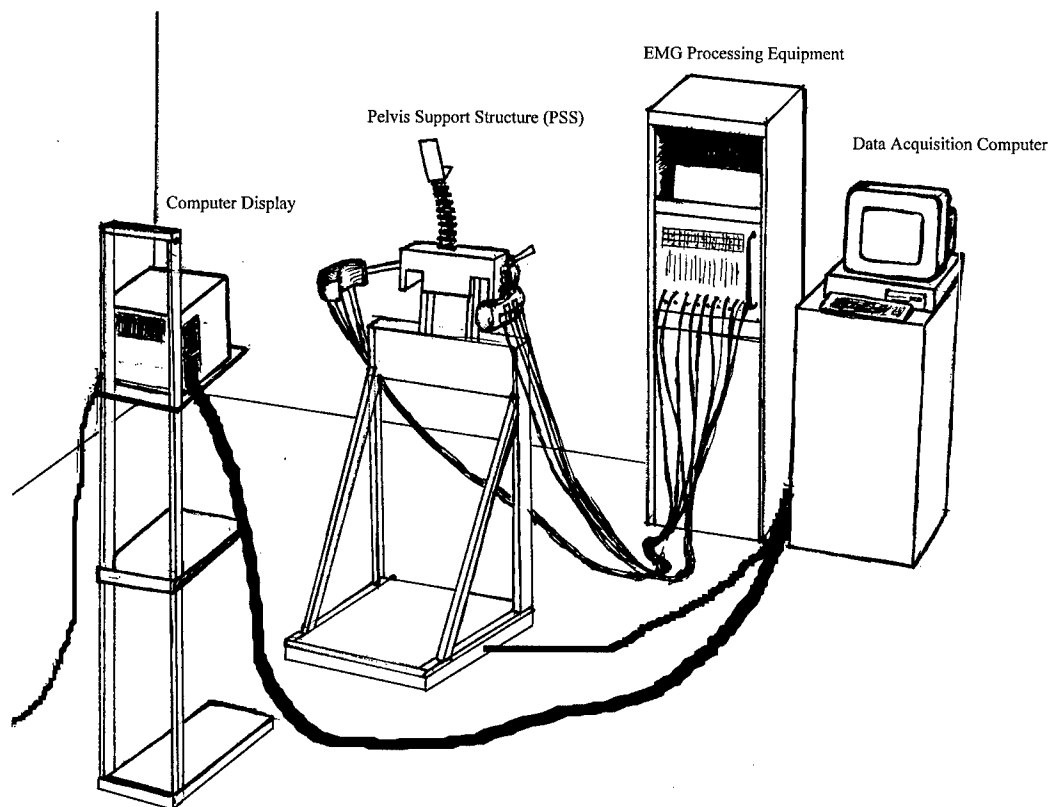


Figure 2.2. Experimental equipment for the lifting trials using the Pelvic Support Structure.

Experimental Procedures

Upon the subjects arrival to the testing laboratory, the subjects read and signed a consent form, and took a pregnancy test so as to determine their pregnancy status. Once they were determined not to be pregnant, anthropometric data and demographic information were obtained. The surface electrodes for the EMG were then applied over each of ten trunk muscles, while skin impedance's were kept below 500 k Ω . Maximum voluntary contractions (MVCs) for each of the trunk muscles were obtained, with the subjects performing MVCs for trunk extension and flexion static exertions, as well as right and left twisting and right and left lateral bending, all against a constant resistance. All resulting trunk muscle EMG data obtained from the experimental trials were then normalized to the maximum EMG activity obtained during these six directional MVCs. Thus, the normalized EMG activity represents the fraction of maximum muscle activity that is applied at any point in time, and also allows relative muscle activity comparisons across subjects as well as within subjects. Following the MVCs, an LMM was placed on the subject's back, and the subject was then allowed to practice the lifting motion to become proficient with

the different controlled trunk velocities. The experimental task required the subjects to control and maintain their trunk lifting velocity between tolerance limits (displayed on a computer screen) for each of the different velocity conditions. If the subject failed to maintain the trunk motion within the tolerance limits, the trial was rerun. A three percent tolerance was used by displaying two lines that were 1.5 percent above and below the target velocity.

Modulation Factor Determination

The determination of the muscle length-strength and force-velocity modulation factors consisted of a biomechanical analysis of the normalized EMG data collected from the subjects in the PSS. This was accomplished by comparing the measured sagittal trunk moment from the force plate with the un-modulated (i.e., without the muscle length-strength and muscle force-velocity relationships) predicted sagittal trunk moment (Granata and Marras, 1995; Granata, 1993). Specifically, this included a systematic analysis procedure incorporating different inputs into an EMG-assisted biomechanical model using the general form of equations 2.1 and 2.2 (Marras and Sommerich, 1991a, 1991b; Granata and Marras, 1993; Marras and Granata, 1995; Granata and Marras, 1995; Marras and Granata, 1997). This method then minimized the average variation of the ratio of external to internal sagittal moment as a function of muscle length and velocity. Additionally, a simplifying assumption was made that the erector spinae group are the sole muscles that counteract the external moment during the sagittally symmetric lifting exertions. This assumption seemed reasonable as antagonistic muscle activity was shown to be minimal during similar motions of other studies (Granata and Marras, 1995; Davis et al., 1998).

$$\text{Force}_j = \text{Gain} \times (\text{EMG}_t / \text{EMG}_{\max}) \times \text{Area}_j \times f(\text{Vel}) \times f(\text{Length}) \quad (\text{Eq } 2.1)$$

$$M_{x\text{-pred}} = \sum r_j \times \text{Force}_j \quad (\text{Eq } 2.2)$$

where:

- Force_j = tensile force for muscle j ;
- Gain = physiological muscle stress (N/cm^2);
- EMG_t = integrated EMG from the lifting exertion;
- EMG_{\max} = integrated EMG from MVCs;
- Area_j = maximum physiological cross-sectional area of muscle j ;
- $f(\text{Vel})$ = the muscle force-velocity modulation factor;
- $f(\text{Length})$ = the muscle length-strength modulation factor;
- $M_{x\text{-pred}}$ = predicted sagittal trunk moment during the lifting exertion;
- r_j = moment-arm for muscle j .

Initially, the data for the dynamic lifting exertions were restricted to the range of 0 degrees to 45 degrees sagittal flexion, as the passive structures of the lower back are estimated to begin sharing the loading at increasing rates at sagittal flexion angles greater than 45 degrees (McGill et al., 1986; Kirking, 1997). Thus, restricting the range of dynamic exertion data to less than 45 degrees sagittal flexion ensures that the active structures (e.g., muscles) are fully contributing to the spinal loading. The exertions from each subject were run through the EMG-assisted model without any modulation factors (i.e., without Gain, $f[\text{Vel}]$ and $f[\text{Length}]$) to determine the subject specific average gain value. Next, the average gain per subject was input into the biomechanical model, and all the exertions were modeled again using the unmodulated versions of equations 2.1 and 2.2 (i.e., $f[\text{Vel}]$ and $f[\text{Length}]$ factors equal to 1.0). The measured sagittal moment from the force plate ($M_{x\text{-meas}}$) was then compared with the predicted sagittal moment ($M_{x\text{-pred}}$) at each point in time, to obtain a vector of the ratio of $M_{x\text{-meas}}$ divided by $M_{x\text{-pred}}$. This vector of the moment ratio was then used as the dependent variable in a multiple linear regression model to predict the moment ratio as a function of the muscle length for the erector spinae. Specifically, the form of the multiple linear regression model was:

$$Y = \beta_0 + \beta_1(\text{Length}) + \beta_2(\text{Length}^2) + \beta_3(\text{Length}^3) \quad (\text{Eq. 2.3})$$

where:

Y = ratio of measured sagittal moment ($M_{x\text{-meas}}$) and predicted sagittal moment ($M_{x\text{-pred}}$);
 Length = Muscle length expressed as a ratio of estimated muscle length divided by the resting muscle length.

The resulting regression equation consisting of the β_0 , β_1 , β_2 and β_3 coefficients for the muscle length factor was then used as the muscle length-strength modulation factor. The length-strength modulation factor was then input into equations 2.1 and 2.2, and the EMG-assisted biomechanical model was then run again with the muscle force-velocity modulation factor [$f(\text{Vel})$] set equal to 1.0 to identify the force-velocity effects. The measured sagittal moment from the force plate was again compared with the predicted sagittal moment at each point in time to obtain a vector of the ratio of $M_{x\text{-meas}}$ divided by $M_{x\text{-pred}}$. This vector of the moment ratio was then used as the dependent variable in a multiple linear regression model, to predict this moment

ratio as a function of the erector spinae muscle velocity. Specifically, the form of the multiple regression model was:

$$Y = \beta_0 + \beta_1(\text{Vel}) \quad (\text{Eq. 2.4})$$

where:

Y = ratio of measured sagittal moment ($M_{x\text{-meas}}$) and predicted sagittal moment ($M_{x\text{-pred}}$);
Vel = Muscle velocity expressed as a ratio ≤ 1.0 , where a static condition results in a ratio of 1.0, with increasing velocities having smaller ratios.

The resulting beta coefficients (β_0 and β_1) for the muscle velocity factor was then used as the muscle force-velocity modulation factor in Equation 2.1, which is used to determine the instantaneous muscle force.

Development of Female Specific Biomechanical Model

Since the EMG-assisted biomechanical model is an interactive system, a systematic procedure was necessary to determine which combinations of muscle vector locations and physiological cross-sectional areas (PCSAs) result in the best estimates of the modulation factors for the muscle length-strength and muscle force-velocity relationships. A step-by-step approach was used to assess any improvements or decrements in model performance indices as the PCSAs, muscle vector orientations, and length-strength and force-velocity parameters were varied. As shown in Table 2.2, a ten-step model building procedure was performed, varying only one variable at a time.

In order to establish a benchmark against which model performance could be judged, Model 1 was built using the male EMG-assisted biomechanical model, with the regression equations predicting the maximum PCSAs from the body mass index (BMI) (Tables 1.65 to 1.69 from Part 1) as well as the muscle vector locations at the origin and insertion points and the length-strength and force-velocity modulation factors, all based on male data (Granata and Marras, 1993; Marras and Granata, 1995, 1997). Model 2 used the length-strength and force-velocity modulation factors determined from the female lifting exertions performed in the PSS, with all other model parameters based on male data as in Model 1 (i.e., PCSAs and muscle vector locations). Model 3 was developed using the regression equations for the largest PCSAs based

on the BMI for the females from Part 1 (Tables 1.65 to 1.69) along with the female length-strength and force-velocity modulations, with the muscle vector locations based on the male biomechanical model. Model 4 was developed using the regression equations predicting the PCSA using trunk depth and trunk width measures about the xyphoid process (Tables 1.65 to 1.69), along with the female length-strength and force-velocity modulations, and the vector locations determined from the male biomechanical model. Model 5 consisted of the PCSAs predicted from either the xyphoid process or BMI (dependent upon which variable had the larger predictability for each muscle), the female length-strength and force-velocity modulation factors, and the female vector locations determined directly from the MRI scans (Table 1.95 for the origin and Table 1.99 for the insertion). Model 6 was the same as Model 5 except for the location of the origin and insertion. The vector locations at the origin were determined from Table 1.97, which included the external obliques projected at a 45 degree caudal and anterior angle (from L₃ through L₅), and the internal obliques projected at a 45 degree caudal and posterior angle (from L₃ through L₅). The vector location for the insertion were allowed to occur at the most superior level where the muscle was observed (Table 1.98). Model 7a included the PCSAs determined from either the BMI or trunk measures about the xyphoid process, the female length-strength and force-velocity modulation factors, and the female origin vector locations from Table 1.95 and insertion vector locations from Table 1.99. Finally, Model 8a was the same as Model 7a, except the vector locations at the origin included the internal and external obliques projected at 45 degree angles from L₃ through the origin (Table 1.97), as in Model 6. Except for Model 1 where the female EMG, kinetic and kinematic data were applied to an existing male biomechanical model with already determined male length-strength and force-velocity modulation factors, the length-strength and force-velocity modulation determination procedures were developed specifically for each of the models based on the varied PCSA and vector orientations locations at the origin and insertion. Thus, in theory, the modulation factors will vary between the different models depending upon the differences in the prediction of the other factors (e.g., gain, PCSA).

To determine the validity of the new length-strength and force-velocity modulation factors, the performance of each of the ten models was examined by comparing the predicted and measured moment profiles quantitatively by means of a statistical squared correlation (r^2), the

average absolute error (AAE) of the comparison, along with the existence of a physiologically valid muscle gain. The value of the r^2 indicates how well the measured and predicted sagittal moment variability coincide. The AAE indicates the average magnitude of the difference between the predicted and measured sagittal moments. For gain values to be physiologically valid, the predicted gain values must lie between 30 and 90 N-cm⁻² (McGill et al, 1988; Reid and Costigan, 1987; Weis-Fogh and Alexander, 1977). Thus, a high r^2 value, combined with low AAEs and physiologically valid gain values implies that the inputs into the model accounts for the variability of the lifting moment.

Table 2.2. Data sources for maximum cross-sectional muscle areas and muscle vector locations for different biomechanical models used to assess the muscle length-strength (L-S) and force-velocity (F-V) modulation factors.

Model	Cross-Sectional Areas		Muscle Vector Locations		L-S and F-V Factors	
	Male	Female	Male	Female	Male	Female
1	X		X		X	
2	X		X			X
3		X	X			X
4		X	X			X
5		X		X		X
6		X		X		X
7a		X		X		X
7b		X		X		Individual
8a		X		X		X
8b		X		X		Individual

Statistical Analysis

The objectives of the research of Part 2 were to 1) investigate how the muscles responsible for spinal loading respond to different conditions such as velocity and weight of lift, and 2) document how the biomechanical models with different parameters behave under these different conditions. Therefore, the normalized muscle activity as a function of the different conditions were documented, as well as the magnitudes and changes of the biomechanical performance parameters (i.e., gain, r^2 , and AAE) as a function of the different inputs.

First, descriptive statistics on all the dependent variables, consisting of the mean and standard deviation were first determined, for both the PSS and free-dynamic portions of this

study. Next, the normalized EMG data were analyzed to assess the effects of different task parameters on the resulting normalized EMG values, again for both the PSS and free-dynamic portions of the study. Multivariate Analysis of Variance (MANOVA) and ANOVA techniques were used to assess the effects of the task parameters, using a repeated measures approach since multiple observations were taken from the same subjects. The dependent variable consisted of the normalized EMG value from each of the ten trunk muscles at the time of the maximum sagittal moment during each of the lifting exertions. Analysis of Variance was performed for each of the 10 muscles for the independent variables which were significant in the MANOVA. Post-hoc test included Tukey pair-wise comparisons. Significance was judged relative to an α value of 0.05.

Results

Mean Normalized Muscle Activity

The descriptive statistics for the mean (s.d.) measured sagittal moment and normalized muscle activity for lifting trials performed in the PSS are shown in Table 2.3. Generally, the greatest muscle activity across all velocities and weights occurred in the trunk extensor muscles, with the erector spinae muscles resulting in the largest normalized muscle activity, with smaller levels of activity present in the internal obliques. The sagittal moment remained relatively constant across all velocity and weight conditions.

The results of the MANOVA on the normalized muscle activity as a function of the task parameters is shown in Table 2.4. There was a significant effect on the collective muscle activity from the weight and velocity effects, but no significant effect of the weight by velocity interaction. Thus, ANOVA was run independently for each muscle while reporting only the main effects of velocity and weight.

Table 2.3. Descriptive results for the mean (s.d.) normalized muscle activity (percent of maximum muscle activity) occurring at the maximum moment, and maximum sagittal moment (Nm) as a function of velocity and weight, for lifting trials performed in the Pelvic Support Structure.

Variable	Velocity (deg/s)				Weight (lbs)	
	15	30	45	60	15	30
Sagittal Moment	68.2 (14.2)	70.8 (14.7)	71.6 (14.6)	71.9 (15.0)	66.7 (13.3)	74.8 (15.0)
RLAT	0.09 (0.07)	0.09 (0.09)	0.09 (0.07)	0.11 (0.09)	0.08 (0.06)	0.11 (0.09)
LLAT	0.10 (0.10)	0.10 (0.12)	0.09 (0.07)	0.11 (0.10)	0.08 (0.07)	0.12 (0.12)
RES	0.42 (0.14)	0.49 (0.17)	0.54 (0.20)	0.59 (0.20)	0.44 (0.16)	0.59 (0.19)
LES	0.43 (0.18)	0.49 (0.18)	0.53 (0.22)	0.58 (0.22)	0.44 (0.19)	0.57 (0.20)
RABD	0.07 (0.06)	0.08 (0.05)	0.07 (0.05)	0.07 (0.04)	0.07 (0.04)	0.08 (0.04)
LABD	0.08 (0.06)	0.07 (0.05)	0.08 (0.05)	0.08 (0.06)	0.07 (0.05)	0.08 (0.05)
REOB	0.06 (0.04)	0.07 (0.04)	0.07 (0.04)	0.07 (0.04)	0.07 (0.04)	0.07 (0.04)
LEOB	0.06 (0.03)	0.06 (0.03)	0.06 (0.03)	0.07 (0.10)	0.06 (0.08)	0.06 (0.03)
RIOB	0.21 (0.13)	0.25 (0.17)	0.25 (0.15)	0.29 (0.19)	0.22 (0.21)	0.29 (0.18)
LI OB	0.20 (0.12)	0.24 (0.15)	0.25 (0.14)	0.29 (0.18)	0.21 (0.13)	0.28 (0.17)

Table 2.4. MANOVA and ANOVA results for the normalized muscle activity for the effects of velocity, weight, and the velocity by weight interaction, for lifting trials performed in the Pelvic Support Structure. Shaded cells represent significant effects ($p \leq 0.05$).

MANOVA	Velocity	Weight	Velocity \times Weight
	p=0.0001	p=0.0001	p=0.2351
Muscle			
R. Latissimus Dorsi	p=0.0432	p=0.0001	
L. Latissimus Dorsi	p=0.1892	p=0.0001	
R. Erector Spinae	p=0.0001	p=0.0001	
L. Erector Spinae	p=0.0001	p=0.0001	
R. Rectus Abdominis	p=0.1080	p=0.4092	
L. Rectus Abdominis	p=0.4579	p=0.0176	
R. External Oblique	p=0.0101	p=0.0002	
L. External Oblique	p=0.3107	p=0.6916	
R. Internal Oblique	p=0.0001	p=0.0001	
L. Internal Oblique	p=0.0001	p=0.0001	

The ANOVA results for the PSS lifting trials generally found that there were significant effects of weight for all but the right rectus abdominis, and the left external oblique. The velocity of lifting had significant effects on all but the left latissimus dorsi, right and left rectus abdominis, and the left external oblique. Consistent trends existed when examining the results of the post-hoc tests on the significant effects across all the muscles. Where there were significant differences in muscle activity due to the weight effect (see Table 2.5), post-hoc tests found that that the 30 lb. condition always resulted in significantly greater muscle activity than the 15 lb. condition. Inspection of the magnitude of the differences, however, reveals that except for the erector spinae muscles, the difference of the muscle activities between the 15 and 30 lb. conditions was very small (Table 2.3). For the muscles that resulted in significant different muscle activity as a function of lifting velocity, in every case, the 60 degree/sec velocity condition resulted in higher normalized muscle activity than the 15 degree/sec velocity condition for the lifting trials, with the 60 degree/sec velocity condition also resulting in greater muscle activity than the 30 degree/sec condition for the extensors (erector spinae and internal obliques). The magnitudes of the difference, however, were very small for all muscles except for the erector spinae (Table 2.3).

Model Parameters

The model performance results from systematic analysis of the inputs into the force and moment equations (Eq. 2.1 and 2.2) for the prediction of the sagittal moment for each of the ten models are shown in Table 2.5. The use of only the dynamic lifting trials resulted in better model parameters (lower gains and higher r^2 s) than when using both the static and dynamic trials. This is expected since the static exertions do not induce a *change* in the moment, which is what is tracked by the r^2 statistic. Generally, five of the ten models resulted in good model performance parameters, as indicated by the shaded cells in Table 2.5. Using the male EMG-assisted biomechanical model and applying the female kinematic, kinetic, and EMG data (Model 1), the mean and median r^2 s were very acceptable (0.91 and 0.95, respectively), however, the mean and median muscle gains (25.7 and 21.9 N-cm⁻²) were below the valid range of muscle gain (between 30 and 90 N-cm⁻²). When the female PCSAs, female length-strength and force-velocity modulation factors and female vector locations were used (Model 7a), the r^2 s and AAEs remained virtually unchanged from Model 1, and the muscle gains increased to a mean and median of 35.0 and 33.4 N-cm⁻², respectively, which represent values that are physiologically reasonable. Model 8a (same inputs as Model 7a except the obliques were projected at 45 degree angles from L₃ through the origin) resulted in physiological valid muscle gains (mean and median of 32.9 and 30.5 N-cm⁻², respectively), and r^2 s similar to Model 7a. Thus, the combination of PCSAs predicted by female anthropometry, vector locations observed from the female MRI scans, and the female derived modulation factors resulted in very good model performance (i.e., Model 7a and 8a).

Model 7a and Model 8a resulted in very acceptable model performance parameters. However, the length-strength and force-velocity modulation factors for these models were developed by collapsing the data from all subjects into one data set for the development of the regression equations. Although the model performance parameters were very acceptable, it was hypothesized that further increases in model performance might be obtained by reducing the variability due to individual differences. Thus, the inputs used for Model 7a and Model 8a were used to develop subject specific, or individual length-strength and force-velocity modulation factors for each subject (Models 7b and 8b). As shown in Table 2.5, the model performance based upon the individually determined length-strength and force-velocity modulation factors

(Model 7b and Model 8b) increased the mean r^2 s by 5% over both Model 7a and Model 8a, slightly reduced the AAE measure, and the muscle gain still remained in the physiologically valid range. Thus, accounting for individual differences between subjects improved the predictability of the already acceptable models.

Model Selection

Model 7a and Model 8a were developed based upon female data for inputs. For example, both models included PCSAs predicted from female anthropometry, included modulation factors for muscle force-velocity and muscle length-strength relationships from female lifting trials, and the muscle vector locations were based upon female MRI data. However, Model 7a used vector locations at the origin based strictly upon observations from the MRI scans, whereas Model 8a used vector locations determined from the 45 degree angle of force direction assumed by Schultz and Anderson (1981). Thus, Model 7a was completely data-driven, whereas Model 8a was data-driven with an adjustment in vector location at the origin (L_5) based upon an assumption of force direction for the oblique muscles. Therefore, given that both models performed similarly, it was our decision to select the model which was most data-driven as the “Female Model.” Thus, Model 7a was selected for further study.

As shown in Figure 2.3, the distribution of the r^2 s shows both a high mean and median for Model 7a. The Model 7a length-strength and force-velocity modulation factors determined from the PSS lifting trials were applied to the data from the Free Dynamic lifting trials (Table 2.6). This resulted in higher but still valid gains (mean=67.7 N-cm⁻²), and still respectable mean and median r^2 values (0.87 and 0.90, respectively), where its distribution can be found in Figure 2.4.

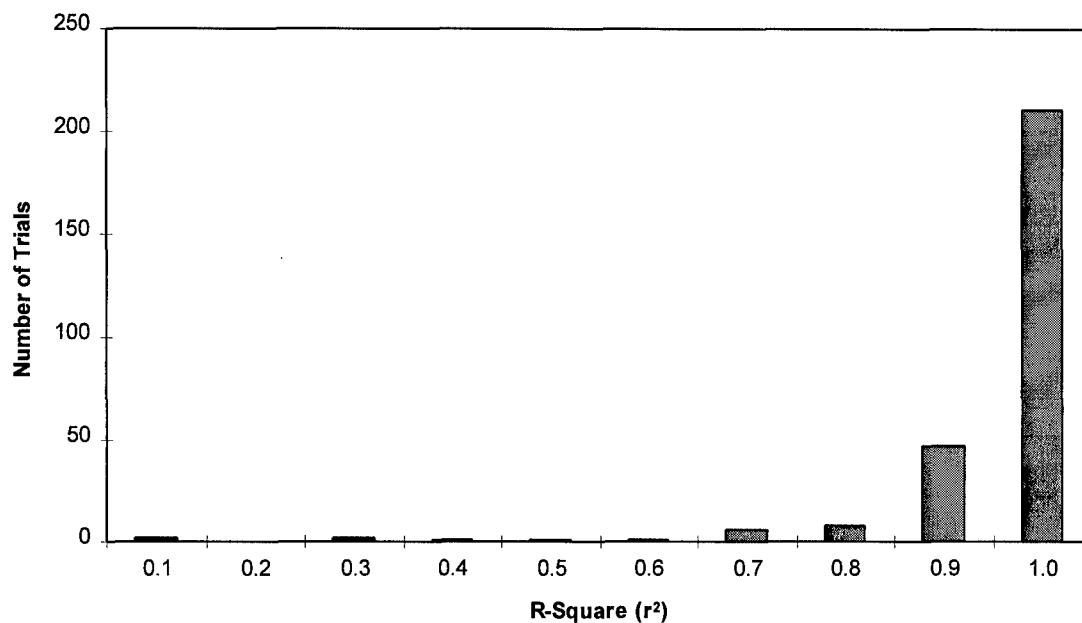


Figure 2.3. Distribution of the r^2 's for the performance of Model 7a, applied to female subjects (N=35) in the Pelvic Support Structure.

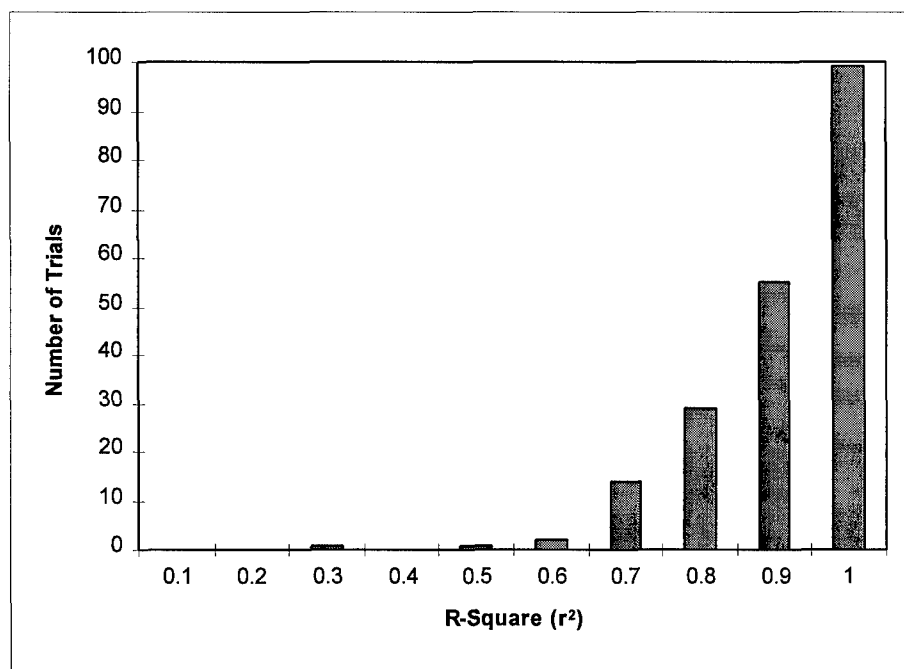


Figure 2.4. Distribution of the r^2 's for the performance of Model 7a, when the length-strength and force-velocity modulation factors derived from trials in the PSS were applied to the lifting trials performed in the free-dynamic conditions (N=26).

Modulation Factors

The final female muscle length-strength and force-velocity modulation factors from Model 7a are shown below, where equation 2.5 is the female length-strength modulation factor, and equation 2.6 is the female force-velocity modulation factor:

$$f(\text{Length}_j) = 10.79 - 31.99 \times \text{Length}_j + 31.39 \times \text{Length}_j^2 - 9.15 \times \text{Length}_j^3 \quad (\text{Eq. 2.5})$$

$$f(\text{Vel}_j) = 1.029 - 0.05 \times \text{Velocity}_j \quad (\text{Eq. 2.6}).$$

For comparison purposes, the male muscle length-strength and force-velocity modulation factors determined by Granata and Marras (1993) are shown below in Equations 2.7 and 2.8, respectively:

$$f(\text{Length}_j) = -3.25 + 10.2 \times \text{Length}_j - 10.4 \times \text{Length}_j^2 + 4.59 \times \text{Length}_j^3 \quad (\text{Eq. 2.7})$$

$$f(\text{Vel}_j) = 0.4e^{(V/-0.38)} + 0.76 \quad (\text{Eq. 2.8}).$$

Additionally, the male muscle length-strength and force-velocity modulation factors developed in this Part 2 using the trunk muscle geometry from Part 1 (i.e., PCSA, muscle vector locations) are shown below in Equations 2.9 and 2.10:

$$f(\text{Length}_j) = 28.83 - 79.21 \times \text{Length}_j + 79.55 \times \text{Length}_j^2 - 25.12 \times \text{Length}_j^3 \quad (\text{Eq. 2.9})$$

$$f(\text{Vel}_j) = 1.037 - 0.036 \times \text{Velocity}_j \quad (\text{Eq. 2.10})$$

As shown in Figure 2.5, the regression line of the female length-strength modulation factor (equation 2.5) is plotted against the male length-strength modulation factor from equation 2.7 (Granata and Marras, 1993), and also against the male length-strength modulation factor determined from the male MRI data from Part 1 (equation 2.9). The general shape of the three curves are very similar. As shown in Figure 2.6, the female force-velocity modulation factor regression equation (equation 2.6) is plotted against the male force-velocity modulation factor from equation 2.8 (Granata and Marras, 1993) and also against the force-velocity modulation factor for males developed using trunk geometry inputs determined in Part 1 (equation 2.10). The male and female force-velocity modulation factors developed using trunk geometry inputs determined in Part 1 of this study are similar in shape and slope, with the females exhibiting slightly lower moment ratios at every muscle velocity. These two curves developed in this study are different in slope and shape, however, from the male force-velocity modulation factor

developed by previous researchers (Granata and Marras, 1993), where the males from the prior study exhibited a greater moment ratio near the slower velocities, and smaller moment ratios as the velocity of contraction increases.

Table 2.5. Model results as a function of each of the ten models, with different combinations of inputs for the cross-sectional areas, length-strength (L-S) and force-velocity (F-V) modulation factors, and vector locations. See Table 2.2 for specific inputs for each of the ten models.

Model	Muscle Areas	L-S and F-V Factors	Vector Locations	Subjects	Statistic	Pelvic Support Structure (N=35)		
						Gain	r^2	AAE
1	Male	Male	Male	All	Mean	25.7	0.91	4.8
					s.d.	12.7	0.14	2.8
					Median	21.9	0.95	4.1
2	Male	Female	Male	All	Mean	42.5	0.72	8.9
					s.d.	21.1	0.28	4.9
					Median	36.7	0.81	8.1
3	Female	Female	Male	All	Mean	30.8	0.89	2.8
					s.d.	14.9	0.16	5.6
					Median	27.7	0.94	4.1
4	Female	Female	Male	All	Mean	33.6	0.85	5.6
					s.d.	14.6	0.18	3.1
					Median	30.2	0.91	4.9
5	Female	Female	Female	All	Mean	0.0	0.41	15.4
					s.d.	0.0	0.29	4.9
					Median	0.0	0.39	14.9
6	Female	Female	Female	All	Mean	21.8	0.73	7.5
					s.d.	8.9	0.26	3.4
					Median	20.2	0.83	7.1
7a	Female	Female	Female	All	Mean	35.0	0.91	4.9
					s.d.	13.5	0.12	2.6
					Median	33.4	0.95	4.3
7b	Female	Female	Female	Individual	Mean	35.2	0.96	3.4
					s.d.	13.3	0.06	1.9
					Median	32.6	0.97	3.0
8a	Female	Female	Female	All	Mean	32.9	0.90	5.0
					s.d.	13.1	0.14	2.7
					Median	30.5	0.94	4.3
8b	Female	Female	Female	Individual	Mean	39.5	0.95	3.3
					s.d.	16.2	0.08	1.8
					Median	36.3	0.97	2.8

Table 2.6. Model performance results from Model 7a (see Table 2.2), compared to the model performance results when applied to trials from the free-dynamic lifting exertions.

Model	Statistic	Pelvic Support Structure			Free Dynamic		
		Gain	r^2	AAE	Gain	r^2	AAE
7a	Mean	35.0	0.91	4.9	67.7	0.87	16.2
	s.d.	13.5	0.12	2.6	30.3	0.11	9.5
	Median	33.4	0.95	4.3	61.5	0.90	14.2

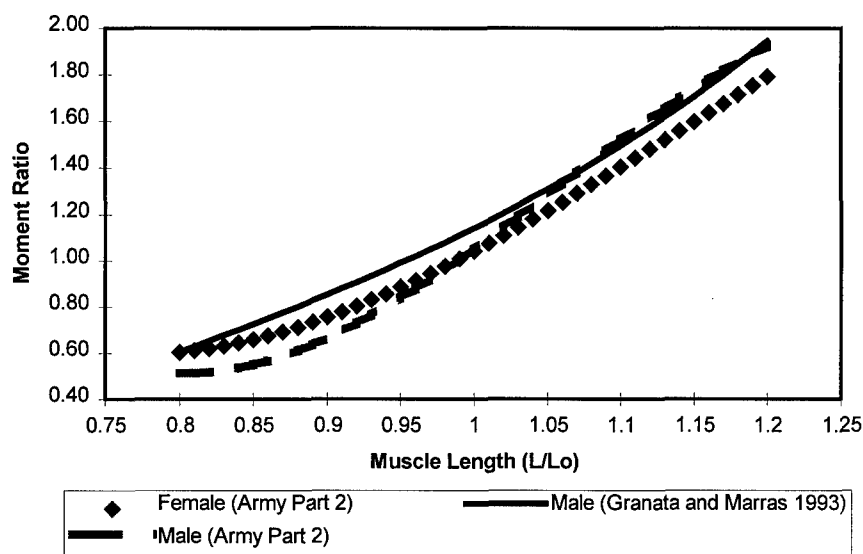


Figure 2.5 Female length-strength versus male length-strength modulation factor comparison.

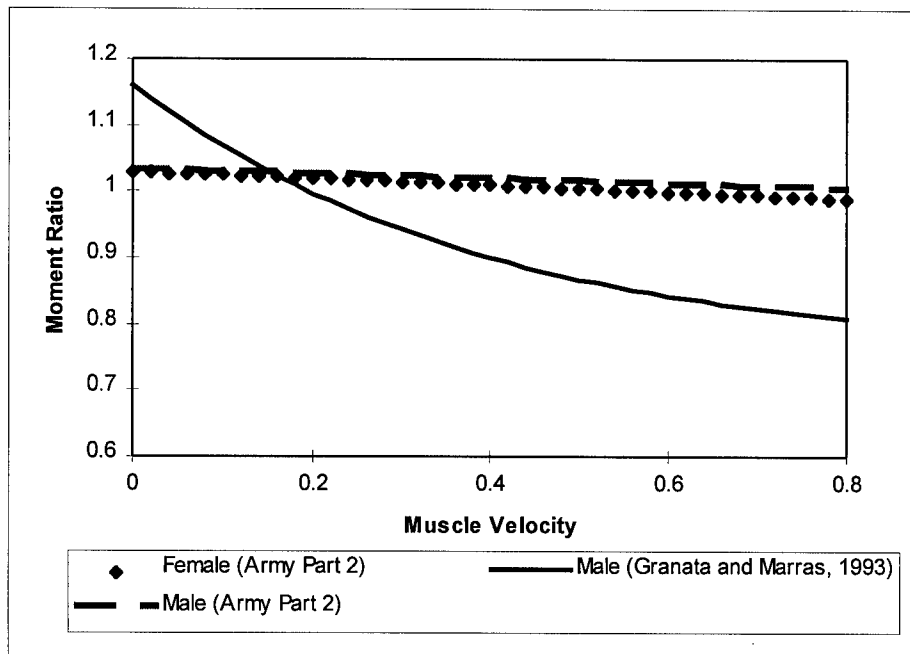


Figure 2.6 Female force-velocity versus male force-velocity modulation factor comparison.

Discussion

The results described in this research on female muscle length-strength and force-velocity relationships have not previously been reported by other researchers. Thus, there are no other female datasets available for comparison purposes. The length-strength modulation factor for the females (Figure 2.5) appears to follow very closely the shape of the length-strength relationship found by other researchers (Marras and Sommerich, 1991b; Granata and Marras 1993; Davis et al. 1993), as well as the male biomechanical model (Granata and Marras, 1993) modified to include the PCSAs and vector locations determined from Part 1. However, this study did result in different shapes for the force-velocity modulation factors from previously published research, especially at the extremes of the velocities. As shown in Figure 2.6, the female force-velocity modulation curve is similar in slope to the male force-velocity modulation curve developed from the male data from Part 1, with the females having a slightly lower moment ratio at every muscle velocity. However, these curves are different from that determined on males from previous literature (Granata and Marras, 1993). These differences may be indicative of more realistic and more accurate trunk muscle geometry used as inputs into the models, including the PCSAs and

the muscle vector locations and directions between the origin and insertion. The development of these modulation factors for the females followed previously used methods, including restricting the data to a sagittal flexion range to ensure that the active loading structures as well as limiting the lifting trials to sagittally symmetric exertions, and modeling the erector spinae muscle only. The decision to model only the erector spinae muscle appears valid, as the descriptive results for the normalized muscle activity revealed that this muscle group was by far the most active at all velocities and weights examined.

The systematic approach to developing the length-strength and force-velocity modulation factors allowed a systematic evaluation of the contribution of different inputs into the biomechanical model, through examination of the model performance parameters of r^2 s, muscle gains, and the average absolute error between the predicted and measured moments. The improvement of the biomechanical model performance of the female model (Model 7a) over the male model (Model 1) was accentuated when utilizing the female specific physiological cross-sectional area equations as well as the female length-strength and force-velocity modulation factors. The mean and median muscle gain increased into the physiologically valid range (35.0 N-cm⁻² and 33.4 N-cm⁻², respectively), predictability of the sagittal moment remained acceptable with high r^2 s (mean and median r^2 of 0.91 and 0.95, respectively), and the average absolute error between the predicted and measured sagittal moment remained low.

Accounting for individual differences due to factors such as different lifting mechanics and different muscle recruitment strategies by the development of individual length-strength and force-velocity modulation factors appears promising. Utilizing Model 7a inputs for PCSAs and muscle vector locations, development of the modulation factors for individuals resulted in increases of model performance parameters. The muscle gains remained virtually unchanged. However, the association between the measured and predicted sagittal moments increased to even higher values (mean and median r^2 of 0.95 and 0.97, respectively) than those high values found from Model 7a (mean and median r^2 of 0.91 and 0.95, respectively), with corresponding moderate decreases in the AAE. Although the calibration of the female EMG-assisted biomechanical model for individual differences appears very promising, further research is needed to determine the minimum number of calibration lifts needed to provide these modulation factors. Thus, Model 7a which combines the data from all subjects appears to provide inputs

which hold promise for a valid biomechanical model predicting dynamic loads on the L₅/S₁ joint of females.

Although the original research proposal called for the development of the length-strength and force-velocity modulation factors solely from free-dynamic lifting exertions, these trials resulted in unacceptable model performance parameters. Thus, it was decided to develop these modulation factors from trials where the hips were secured, and apply the resulting model to the free-dynamic data. The model performance parameters from the free-dynamic trials changed when the model based on data from the PSS trials were applied. The mean gain increased from 35.0 N/cm² to 67.7 N/cm², and the mean and median r^2 decreased to still respectable values of 0.87 and 0.90, respectively. The gain values are still within the physiologically valid range, and the distribution of the r^2 's is still respectable. Similar model performance parameters were found for free-dynamic exertions by males modeled by Granata and Marras (1995), with a mean muscle gain of 64.9 N/cm², mean r^2 of 0.81, and an AAE of 17.5 N-m for sagittally symmetric exertions. Thus, although slight decreases in model performance were observed for free-dynamic trials when compared to the PSS trials, the parameters are still acceptable, and similar to previously modeled male free-dynamic exertions. The differences between the gain values between the two experimental modes may be attributed to changes in the muscle length associated with allowing the hips and pelvis to rotate during free-dynamic exertions, unlike the exertions in the PSS which stabilize the hips and pelvis. Differences in muscle length which may affect the length-strength modulation and ultimately the gain may also occur due to how the LMM is situated on the subject, as in the PSS, the LMM is attached directly to the PSS, whereas in the free-dynamic mode, the LMM is attached and secured directly around the waist of the subject.

Limitations

A few limitations do exist at this point in the research. First, the lifting exertions which were modeled consisted of only sagittally symmetric exertions, and the relationship between spinal loading and muscle activity may be different in asymmetric conditions. These relationships, however, will be investigated in Part 3 of this, during a validation phase.

Decreases in the model performance parameters occurred when applying the length-strength and force-velocity modulation factors to the lifting trials performed in the free-dynamic mode. Specifically, the mean r^2 decreased from 0.91 to 0.87, and the mean muscle gains increased from 35.0 to 67.7 N-cm⁻², although they were still within the physiologically valid range. This may be a function of allowing the pelvis and hips to rotate and further changing the length-strength and force-velocity relationships in the free-dynamic mode, and thus changing the mechanics of the lifting and resulting EMG values. This very subject is currently being investigated in our lab, to determine the influence of allowing the hips and pelvis to rotate during lifting activities.

Conclusions

The derived female muscle length-strength and force-velocity relationships, when applied to the EMG-assisted biomechanical models resulted in very good model performance parameters, including high r^2 's between the predicted and measured moment, physiologically valid muscle gain values, and small magnitudes of error between the predicted and measured moment. The original procedure used to collect the data, however, had to be adjusted to reduce the variability in the length-strength and force-velocity modulations resulting from allowing the hips and pelvis to rotate during the lifting exertions. Thus, the lifting trials performed with the pelvis constrained resulted in very good model performance, and when applied to the trials collected during the free dynamic conditions resulted in somewhat lower, but still acceptable model performance parameters.

The use of the female physiological cross-sectional muscle areas derived in Part 1 resulted in increases in performance over the male-only biomechanical model. This data, combined with the length-strength and force-velocity modulation factors for the females and vector locations determined from Part 1 results in a promising dynamic EMG-assisted biomechanical model, which positions us well for the analysis of asymmetric lifting exertions in Part 3 of this research.

Part 3: Implementation and Validation of the EMG-assisted Model for Female Subjects.

Introduction

Much of the manual material handling activities (e.g., lifting) are not performed in a sagittally symmetric posture, but must be performed with trunk asymmetry involved. Thus, motions such as twisting or lateral side bending most likely are involved to some degree in most lifting activities. The biomechanical model parameters determined in Part 2 were developed under sagittally symmetric lifting exertions. The goal of Part 3 was to use the parameters developed for the females and apply to asymmetric lifting exertions, and adjust the model such that the model performs well under sagittally symmetric exertions as well as asymmetric exertions.

Background and Objectives

The Biodynamics Laboratory EMG-assisted model, which predicts the three-dimensional spinal loading experienced by subjects during manual handling tasks currently has only been validated for males. The results of Part 1 and Part 2 as reported in this progress report indicate that females differ from males with respect to muscle anthropometry (e.g., muscle physiological cross-sectional areas as a function of external anthropometry, and muscle lines of action), as well as muscle length-strength and force-velocity relationships. These differences undoubtedly will have an affect on the accuracy of the spinal loads predicted by the EMG-assisted biomechanical model. Thus, the objectives of Part 3 include 1) utilizing the model parameters derived from Part 1 and Part 2 and implementing these into the current form of the EMG-assisted biomechanical model, and 2) validation of the female-specific EMG-assisted biomechanical model for sagittally-symmetric and asymmetric lifting exertions.

Administrative Note

Data collection for Part 3 is nearing completion. The accepted research proposal calls for 40 military age female subjects and 20 male subjects to be used for comparison purposes, whereas at this time, data from 17 males and 35 females have been collected. It is expected that an additional five female subjects and three male subjects will not drastically alter the current

findings. In the accepted research proposal, weight conditions of 15, 50 and 80 lbs were to be used for female as well as male subjects. However, we were unable to find a female capable of lifting 80 lbs up to a height of 102 cm above the floor. Thus, the experimental design has been modified to still allow three weight levels, including 15, 30, and 50 lbs. It is felt that this weight range is more realistic for the capabilities of the female population, especially for the number of repetitions required by our experimental design for this study.

Methods

Experimental Design

The subjects performed free-standing lifts representative of select military material handling tasks, using different weights, different starting and destination heights, as well as asymmetric exertions.

The independent variables are intended to simulate a range of realistic military material handling conditions as specified in the MOS Physical Task list (U.S. Army Infantry School), and to assess model sensitivity and applicability for female subjects. The independent variables include gender, weight of lift (15, 30, and 50 lbs), degree of asymmetry for the starting position of the lift (0 and 60 degrees), and lift condition (floor to waist, floor to 102 cm, knee to waist, and knee to 102 cm above the floor). Each combination of the task independent variable was performed twice by each subject. This repeated measures design resulted in 48 experimental trials per subject, thus permitting sensitivity analysis of those material handling factors that might influence model performance, as well as identifying gender differences in model performance as a function of the other independent variables. The presentation order of the experimental conditions were randomized and subjects were allowed at least two minute rest (Caldwell et al. 1974) or as much time as needed between trials to minimize the risk of fatigue and carryover effects on the results.

The dependent variables consisted of several model measures of performance. For a model to be considered robust and accurate it must, 1) accurately represent the changes in trunk and spine loading over time and, 2) accurately estimate the magnitude of the trunk loading during the lift. The squared correlation (r^2) between the measured and predicted trunk moments will

serve as an indicator of the model ability to accurately assess the changes in trunk loading. Measured versus predicted magnitudes of the load imposed upon the trunk were assessed by examining the average absolute error (AAE) between the two measures. In addition, predicted muscle gains were used as a measure of the physiologic validity.

Subjects

The subjects to date for this part of the study included 35 females and 17 males, all of generally observed military age. Male subjects were recruited to permit comparison and calibration of model performance and results with female subjects. Subject anthropometric measures are shown in Table 3.1.

Table 3.1 Anthropometric measurements (mean and s.d.) from female and male subjects.

Anthropometric Variable	Females (N=35)	Males (N=17)
Age (yrs)	23.8 (5.9)	23.8 (3.8)
Standing Height (cm)	165.8 (6.8)	174.7 (6.3)
Weight (kg)	61.2 (9.0)	72.2 (10.9)
Trunk Width at Iliac Crest (cm)	26.7 (2.8)	28.2 (3.7)
Trunk Depth at Iliac Crest (cm)	18.6 (2.7)	20.6 (2.5)
Trunk Width at Xyphoid Process (cm)	26.7 (1.6)	29.7 (3.3)
Trunk Depth at Xyphoid Process (cm)	19.1 (1.8)	21.3 (3.5)
Body Mass Index (kg/m ²)	22.2 (2.3)	23.7 (3.7)

Equipment

The equipment used in this part has been previously described in Part 2. Specifically, subjects stood on a force plate (not moving their feet), and performed the lifts from ankle and knee heights to destinations of waist height and 102 cm above the floor. The forces and moments measured by the force plate were rotated and translated to the estimated position of the

L₅/S₁ through the use of a sacral location orientation monitor (SLOM) and a pelvic orientation monitor (Fathallah et al., 1997). The subjects trunk three-dimensional position, velocity, and acceleration were measured by an LMM (Marras et al, 1992), and trunk muscle activity was measured through electromyography, placed over right and left sides of five trunk muscle groups (Mirka and Marras, 1993).

All data signals were collected simultaneously through customized Windows™ based software developed in-house. The signals were collected at 100 Hz and recorded on a 486 computer and stored for later analysis.

Experimental Procedure

Upon the subjects arrival to the testing laboratory, the subjects read and signed a consent form. Female subjects took a pregnancy test to determine their pregnancy status. None of the female subjects tested positive on the pregnancy test, and were permitted to continue with the study. Anthropometric data and demographic information were recorded next. Surface electrodes for the EMG were then applied over each of ten trunk muscles, while skin impedance's were kept below 500 kΩ. Maximum voluntary contractions (MVCs) for each of the trunk muscles were obtained, with the subjects performing MVCs for trunk extension and flexion static exertions, as well as right and left twisting and right and left lateral bending, all against a constant resistance. All resulting trunk muscle EMG data obtained from the experimental trials were then normalized to the maximum EMG activity obtained during these six directional MVCs. Following the MVCs, an LMM was placed on the subject's back, and the subject was attached to the SLOM as they stood upon the force plate. Each of the 48 experimental trials were then presented to the subject in a randomized order. The subjects were allowed to lift the load from the starting position to the destination using a free-style lift, however, they were instructed to keep their feet stationary on the force plate during the lifting exertion.

Data Analyses

Female biomechanical Model 7a developed in Part 2 was used in this part of the study. The normalized EMG signals, trunk position and velocity data from the LMM, and the predicted physiological cross-sectional muscle areas and vector locations from Part 1 were input into the

biomechanical model to predict the forces and moments imposed upon the L₅/S₁ joint. Experimental data collected from the male subjects was input into the EMG-assisted biomechanical model validated for males (Granata and Marras, 1993) which was updated to include the predictions of the physiological cross-sectional areas and vector locations determined from the males in Part 1. The model performance parameters from the male biomechanical model were used for comparison purposes to those from the female model.

Model performance was assessed by examining the predictability, accuracy, and validity of model performance parameters. Time dependent predicted trunk moments were compared with the measured trunk moment via an r^2 statistic. An r^2 value of 0.80 or above across all trials indicates the model is working well. The accuracy of the model prediction was assessed by examining the absolute error between the measured and predicted moment, as a function of the measured moment, averaged continuously over the duration of the exertion. Thus, the average absolute error was expressed as a percent of the maximum measured moment in the sagittal plane. The model was considered acceptable in accuracy if the average absolute error was no greater than 20% of the measured moment in the sagittal plane. Predicted muscle gains were also examined to assure physiological feasibility. To be considered valid, the predicted muscle gains must fall between 30 N-cm⁻² and 90 N-cm⁻² (McGill et al, 1988; Reid and Costigan, 1987; Weis-Fogh and Alexander, 1977).

Statistical Analysis

Descriptive statistics describing the central tendency (mean and median) and the variability of the model performance parameters were first performed. The data was further described by determining the percent of trials where the r^2 was above 0.80, collapsed over all conditions, as well as a function of the experimental conditions. The muscle gain was also described by determining the percent of trials with gains in the physiological range (30 N-cm⁻² to 90 N-cm⁻²), collapsed across all experimental conditions, as well as a function of the experimental conditions.

Analysis of Variance (ANOVA) procedures were used to test the significance of the model performance parameters (i.e., r^2 , gain, and AAE) as a function of the independent variables. The statistical analysis consisted of a mixed four-way repeated measures ANOVA,

with one between factor (gender) and three repeated factors (weight, asymmetry and lift condition). Significant gender effects in model performance parameters were examined by testing the two-way interactions between gender and the other independent variables (i.e., weight, asymmetry and lift condition). Significant differences will indicate different levels of model performance between the conditions and can be used as a model sensitivity measure. Tukey post-hoc procedures were used to understand the nature of these differences. Significance was indicated for the ANOVA and post-hoc procedures using a Type I error rate of $\alpha=0.05$.

Results

The Analysis of Variance on the biomechanical model performance parameters indicated that model performance varied significantly as a function of the experimental conditions (Table 3.2). The muscle gain varied as a function of gender for the lifting condition and weight of the lift, and also as a function of asymmetry. Post-hoc tests revealed that the females had a significantly higher gain for the 15 lb condition (3.4 N-cm^{-2} higher), whereas males exhibited greater gains for the 30 lb (2.6 N-cm^{-2} higher) and 50 lb condition (8.3 N-cm^{-2} higher). Males exhibited greater gains for lifts originating at the knee, whereas females had higher gains for the floor to waist lift condition (Table 3.4 and Table 3.5). Asymmetric lifts resulted in increased gains over sagittally symmetric lifts (50.9 N-cm^{-2} to 58.5 N-cm^{-2}), independent of gender.

The squared correlation coefficient (r^2) was less influenced statistically by differences in the experimental conditions than the predicted muscle gain. As shown in Table 3.2, gender differences existed as a function of the lift condition, and weight had a significant effect on r^2 independent of gender. Tukey post-hoc test revealed that males had significantly higher r^2 for the knee to chest lift condition, and females had significantly higher r^2 for the floor to waist condition. The magnitude of these differences were rather small, however, ranging from 4% to 5% (Table 3.4 and Table 3.5). Post-hoc tests also indicated that the r^2 at the 15 lb condition ($r^2=0.88$) was significantly higher than that for the 50 lb condition ($r^2=0.85$), although again, the difference was rather small.

The ANOVA results indicated that differences also existed for the average absolute error of the predicted sagittal moment, expressed as a percent of the measured moment in the sagittal plane as a function of the experimental conditions (Table 3.2). The average percent error varied

as a function of gender for the lift condition, however, the significant differences ranged between 1.0% and 1.6%, which are very small in magnitude. Weight of the load also exhibited a significant effect on the average percent error, with post-hoc tests revealing that the 15 lb condition had higher percent error than the 30 lb and 50 lb conditions, however, these differences were less than 1%, and deemed very small in magnitude.

Table 3.2 Analysis of Variance p-values on the EMG biomechanical model performance parameters as a function of the independent variables for both males and females. Shaded cells represent significant effects at $p \leq 0.05$.

Independent Variable	Model Performance Parameter		
	Gain	r^2	AAE/Moment
Gender (G)	0.5893	0.4790	0.7840
Weight (W)	0.0024	0.0191	0.0086
Asymmetry (A)	0.0001	0.1735	0.2930
Lift Condition (L)	0.0001	0.1520	0.0020
G \times W	0.0001	0.2780	0.8485
G \times A	0.0771	0.9943	0.1494
G \times L	0.0003	0.0049	0.0010

The distribution of r^2 for both genders can be examined as a function of the different experimental conditions, as shown in Table 3.6. Both females and males exhibited mean r^2 s above 0.80, with females ranging generally between 0.84 and 0.88 across all levels of the experimental conditions. The r^2 s for males spanned a similar range (between 0.83 and 0.90) across all levels of the experimental conditions. The median r^2 across the different levels of the experimental conditions were generally between 0.90 and 0.93, indicating a slightly skewed distribution of the r^2 s. Overall, 78.4% of the female trials resulted in r^2 s greater than 0.80 with between 76% and 81% of the female trials resulted in r^2 s greater than 0.80 across the different experimental conditions (Table 3.6). For males, 81.8% of all trials resulted in r^2 s greater than 0.80, with between 74.4% to 90.7% of the trials across the different experimental conditions resulting in r^2 s greater than 0.80. Thus, across all experimental conditions, more than three-fourths of the trials resulted in r^2 s greater than 0.80. Collectively, the distribution of the r^2 values indicates acceptable response to changes of the sagittal moment for both male and female biomechanical models.

The distribution parameters for the gain for both genders as a function of the experimental conditions are shown in Table 3.7. Overall, the gains between male and female were similar in magnitude (mean gains of 54.0 and 56.1 N-cm⁻² for females and males, respectively). The percent of trials with gains within the physiologic range (30 to 90 N-cm⁻²) was slightly higher for females (82.9%) than males (75.0%). The mean and median gains for both genders were similar, indicating a symmetric distribution, with the magnitudes falling within the estimated physiologic range. The percent of trials falling within the physiological range as a function of experimental condition ranged between 79.5% and 87.2% for females, and between 72.4% and 77.9% for males. Thus, the majority of the trials resulted in valid predicted muscle gains.

Finally, the error in prediction of the lifting moment as compared to the measured sagittal moment was within an acceptable range for both males and females. The overall AAE as a percent of the measured moment in the sagittal plane for females was 9.0% for both females and males. Thus, the AAE was well within the 20% boundary of an acceptable model prediction error.

Table 3.3 Overall biomechanical model performance parameters for males and females, collapsed across all experimental conditions.

Statistical Measure	Females			Males		
	Gain (N-cm ⁻²)	r^2	AAE/Moment	Gain (N-cm ⁻²)	r^2	AAE/Moment
mean	54.0	0.86	0.09	56.1	0.87	0.09
s.d.	21.1	0.16	0.05	23.8	0.16	0.06
median	50.1	0.91	0.08	53.3	0.92	0.08

Table 3.4 Descriptive statistics (mean and standard deviation) for the muscle gain, r^2 and AAE (as a percent of measured moment) model performance parameters for the female biomechanical model.

Variable	Weight (lbs)			Asymmetry (deg)		Lift Condition*		
	15	30	50	0	60	F - W	F - C	K - C
Gain (N/cm ²)	57.4 (23.2)	53.3 (20.5)	50.0 (17.7)	49.7 (18.5)	58.3 (22.6)	52.3 (18.7)	50.2 (19.0)	55.4 (22.1)
r^2	0.88 (0.13)	0.85 (0.17)	0.84 (0.17)	0.87 (0.15)	0.85 (0.16)	0.87 (0.16)	0.85 (0.17)	0.85 (0.16)
AAE/Moment	0.10 (0.05)	0.09 (0.05)	0.09 (0.05)	0.09 (0.05)	0.10 (0.05)	0.09 (0.05)	0.09 (0.05)	0.10 (0.05)

* F-W = Floor to Waist;

F-C = Floor to Chest (102 cm above the floor);

K-W = Knee to Waist;

K-C = Knee to Chest (102 cm above the floor);

Table 3.5 Descriptive statistics (mean and standard deviation) for the muscle gain, r^2 and AAE (as a percent of measured moment) model performance parameters for the male biomechanical model.

Variable	Weight (lbs)			Asymmetry (deg)		Lift Condition*		
	15	30	50	0	60	F - W	F - C	K - C
Gain (N/cm ²)	54.0 (24.2)	55.9 (23.8)	58.3 (23.4)	53.3 (22.9)	58.8 (24.4)	49.8 (22.2)	52.4 (22.5)	61.6 (24.6)
r^2	0.87 (0.14)	0.88 (0.14)	0.85 (0.19)	0.88 (0.16)	0.86 (0.16)	0.83 (0.20)	0.87 (0.16)	0.90 (0.12)
AAE/Moment	0.10 (0.06)	0.09 (0.05)	0.09 (0.06)	0.09 (0.05)	0.09 (0.06)	0.09 (0.06)	0.10 (0.06)	0.09 (0.06)

* F-W = Floor to Waist;

F-C = Floor to Chest (102 cm above the floor);

K-W = Knee to Waist;

K-C = Knee to Chest (102 cm above the floor);

Table 3.6 Model r^2 descriptive statistics for male and female biomechanical models as a function of the independent variables.

Independent Variable		Female			Male		
		Mean	Median	% $r^2 \geq 0.80$	Mean	Median	% $r^2 \geq 0.80$
Weight (lbs)	15	0.88	0.92	78.4	0.87	0.92	81.6
	30	0.85	0.91	80.9	0.88	0.93	85.7
	50	0.84	0.91	76.2	0.85	0.91	78.2
Asymmetry (deg)	0	0.87	0.92	79.4	0.87	0.93	82.6
	60	0.85	0.91	77.4	0.86	0.91	81.1
Lifting Condition*	F - W	0.87	0.91	80.5	0.83	0.90	74.4
	F - C	0.85	0.90	76.3	0.87	0.92	81.4
	K - W	0.87	0.92	80.2	0.88	0.93	80.9
	K - C	0.85	0.91	76.5	0.90	0.93	90.7
Overall Results		0.86	0.91	78.4	0.87	0.92	81.8

* F-W = Floor to Waist;

F-C = Floor to Chest (102 cm above the floor);

K-W = Knee to Waist;

K-C = Knee to Chest (102 cm above the floor);

Table 3.7 Model muscle gain descriptive statistics for male and female biomechanical models as a function of the independent variables.

Independent Variable	Female			Male		
	Mean	Median	Percent 30≤Gain≤90	Mean	Median	Percent 30≤Gain≤90
Weight (lbs)	15	57.4	55.0	79.5	54.0	50.6
	30	53.3	49.7	83.1	55.9	53.7
	50	50.0	47.8	87.2	58.3	56.1
Asymmetry (deg)	0	49.7	47.4	83.4	53.3	50.3
	60	58.3	55.3	82.2	58.8	55.4
Lifting Condition*	F - W	52.3	49.7	82.7	49.8	45.9
	F - C	50.2	47.9	86.1	52.4	48.8
	K - W	58.0	54.5	81.3	60.4	58.1
	K - C	55.4	52.9	81.1	61.6	57.2
Overall Results		54.0	50.1	82.8	56.1	53.3
						75.0

* F-W = Floor to Waist;

F-C = Floor to Chest (102 cm above the floor);

K-W = Knee to Waist;

K-C = Knee to Chest (102 cm above the floor);

Discussion

Collectively, these findings indicate that the female model (Model 7a from Part 2) utilizing inputs from the MRI results from Part 1 and the length-strength and force-velocity modulation factors developed in Part 2 resulted in an acceptable model based on the magnitudes and distribution of the biomechanical model performance parameters. The majority of the trials resulted in acceptable r^2 s (78.4% greater than $r^2=0.80$ with a mean of 0.86 and median of 0.91), with physiologically valid gains (mean gain of 54.0 N-cm⁻²) and a low error magnitude of prediction of the sagittal moment (9.0% error).

The model performance parameters from the female biomechanical model compare favorably with the model performance parameters from a male biomechanical model (Granata and Marras, 1993), which was updated using the results of male PCSA and vector locations from Part 1 of this study. Although the lift condition showed a significant gender effect for r^2 and AAE, the differences between genders were between 0.04 and 0.05 for r^2 , and between 1.0% and 1.7% error for the AAE. Thus, these significant gender differences represent a very small biological effect. Muscle gain also showed a significant gender effect with the weight of the lift, where the largest difference was 8.3 N-cm⁻² at the 50 lb condition. This represents a 16.6% larger gain for males over females at this weight. This increase may be reflective of a multitude of differences between males and females, including differences in muscle size, fiber type composition of the extensor muscles, differences attributed to the length-strength and force-velocity modulation factors, as well as real differences in the force producing capability of the muscles. Thus, while a significant difference exists for muscle gain between genders as a function of weight, there may be many factors contributing to this difference, and more research is needed to identify the true effect.

Results of this validation effort compare favorably with the results of the biomechanical model performance parameters resulting from Part 2 of this study. The overall model performance parameters during this validation phase were consistent with those observed in Part 2, determined during the development of the length-strength and force-velocity modulation factors. The model, developed from sagittally symmetric controlled velocity lifts in Part 2 resulted in mean r^2 s of 0.95, with the mean gain of 35.0 N-cm⁻² for the data derived with the hips

secured, and mean r^2 of 0.87, and a gain and AAE of 44.8 N-cm⁻² and 13.8 Nm, respectively, when applied to the data from sagittally symmetric controlled velocity lifts performed under free dynamic conditions. The mean r^2 and gain from Part 3 were 0.86 and 54.0 N-cm⁻², and an AAE of 13.6 Nm. Partitioning the trials in Part 3 as a function of asymmetry, the trials with sagittally symmetric lifts resulted in similar r^2 s, gains, and AAE's as observed in Part 2. The asymmetric lifting trials, however, resulted in a minor decrease in mean r^2 (0.87 to 0.85), a slight increase in AAE, and a larger increase in the gain. Thus, going from free-dynamic sagittally symmetric controlled velocity lifting trials to free-dynamic uncontrolled velocity with asymmetric lifts resulted in similar r^2 s and AAEs, with increases in the gain although the gain still remains in the physiologically valid range.

The model performance parameters for both female and male models also compare favorably with other EMG-assisted biomechanical models validated under similar experimental conditions. Granata and Marras (1995) found an average gain for free-dynamic exertions of 64.9 N-cm⁻² for sagittally symmetric lifts, with mean r^2 s of 0.82, and percent error prediction less than 15%. Thus, the results for both male and female biomechanical models developed in Part 2 and Part 3, which utilizes trunk geometry data determined from MRI scans from Part 1, as compared to previously validated models, resulted in predictions which were better able to predict changes in the measured moment (e.g., higher r^2 s), had lower but still valid gain values, and resulted in less prediction error.

Limitations

Although the biomechanical models which have been developed up to this point have resulted in very acceptable model performance, the model is only capable of assessing active trunk forces and is not sensitive to passive loading of the spine. While it is possible that some MMH activities do involve extreme trunk flexion (greater than 45 degrees sagittal flexion) which then rely increasingly on passive structures of the low back, surveillance studies have demonstrated that trunk flexion in excess of 45 degrees account for less than 5% of industrial MMH lifts (Marras et al. 1993, 1995). Thus, neglecting passive spine loading does not present a large problem.

Conclusions

The resulting female EMG-assisted biomechanical model, which used trunk geometry inputs developed in Part 1, and the length-strength and force-velocity modulation factors derived in Part 2 has resulted in very acceptable model performance parameters. The high mean and median r^2 s, low error of prediction for the measured moment, combined with physiologically valid muscle gains indicates that the biomechanical model is a valid model for the prediction of female spinal loading during free-dynamic three-dimensional lifting exertions.

The validation of the female biomechanical model positions us well to assess the prediction of spinal loading characteristics on the female spine during free-dynamic three-dimensional lifting exertions in Part 4.

Part 4: Assess Biomechanical Loads on the Female Spine During Military MMH

Introduction

Biomechanical risk of injury to the low back can be assessed using estimates of spinal loading derived from validated biomechanical models and comparing these estimates to tolerance limits of the soft tissues of interest. Thus, assessing risk of low back injury to female army personnel during military MMH would be assessed by predicting the shear forces and compression forces on the L₅/S₁ intervertebral joint, and comparing these resulting values with intervertebral disc tolerance data as a function of age and gender.

Background and Objectives

Damage to the soft tissues of the lower back can occur when the magnitude of loading on the soft tissues increases to levels above the threshold level of the tissue (McGill 1997; NIOSH 1981). According to NIOSH (1981), microfractures of the vertebral endplates would be expected in 50% of the working population at compression values of 6400 N. Increases in the magnitudes of biomechanical variables such as awkward postures of the trunk (asymmetry) and increases in the weight of the load lifted have been shown to result in increases of spinal loading as predicted by dynamic male biomechanical models (Marras and Sommerich 1991a,b; Granata and Marras 1993; Mirka and Marras 1993; Marras and Granata 1995, 1997; Granata and Marras 1995). These studies are further supported by cadaveric research (Adams and Hutton 1983; Adams et al. 1993; Adams et al. 1994) that shown the initiation of failures to the intervertebral disc segments occurred under increases in magnitude and repetitive exposure to similar types of loading (e.g., increases in bending moments, compression forces).

Past research has indicated that females possess lower tolerance levels to compression force for the intervertebral discs than males (Jager et al. 1991). Thus, when males and females are exposed to the same material handling conditions, females may be closer to the spinal tolerance levels than males, which may indicate an increased risk of injury. However, spinal loading for females has not been investigated to date as up to this point, as female specific

biomechanical models have not been developed. Thus, it is currently unknown what levels of spinal loading occur during MMH tasks, and how the loading compares to spinal loading experienced by males performing the same MMH tasks.

The objectives of Part 4, therefore, are threefold: 1) examine the spinal loads experienced by females as a function of specific MMH tasks by using the female biomechanical model developed and validated in the previous parts of this study; 2) compare the female loads to those experienced by males performing the same MMH tasks; and 3) compare the spinal loading to tolerance data as a function of gender and the experimental MMH lifting task conditions.

Administrative Note

The accepted proposal calls for Part 4 to have begun during the most recent two quarters, and continuing on into the final year of the study period. The data collection for the agreed upon 40 female subjects and 20 male subjects necessary to complete Part 3 and Part 4 is almost complete. Thus, the results presented here in Part 4 reflect preliminary analysis from 35 female subjects and 17 male subjects. It is anticipated that the last few subjects will be collected in a timely manner, with the completion of Part 4 to occur within the agreed upon time frame.

Methods

Subjects

The subjects for this part consisted of the same subjects which participated in Part 3. Thus, all anthropometric characteristics for the 35 female and 17 male subjects can be found in Table 3.1 in Part 3 of this report.

Experimental Design

Since the data for this part were collected to complete Part 3, the experimental design is identical to that described in Part, except for the dependent variables.

The independent variables include gender, weight of lift (15, 30, and 50 lbs), degree of asymmetry for the starting position of the lift (0 and 60 degrees), and lift condition (floor to waist, floor to 102 cm, knee to waist, and knee to 102 cm above the floor). Each combination of the task independent variable was performed twice by each subject. This repeated measures

design resulted in 48 experimental trials per subject, thus permitting sensitivity analysis of those material handling factors that influence spinal loading, as well as any gender differences in spinal loading as a function of the experimental conditions. The presentation order of the experimental conditions were randomized and subjects were allowed at least two minute rest (Caldwell et al. 1974) or as much time as needed between trials to minimize the risk of fatigue and carryover effects on the results.

The dependent variables included the maximum externally measured moments in the sagittal, coronal, and transverse plane, as well as the resultant moment. Spinal loading included the mean and average shear forces in the sagittal and coronal plane and the compression force.

Equipment

Inputs into the EMG-assisted biomechanical model for evaluation of material handling activities includes estimates of trunk position and motion, external measures of the sagittal plane lifting moment, and monitoring of muscle activity via EMG. All equipment used to collect the data, including the LMM, EMG electrodes, force plate, pelvic orientation monitor, and sacral location orientation monitor, as well as signal processing and conditioning have been previously described in Part 2, and also apply to this Part 4 of this study.

Data Analyses

The female data from the normalized EMG, trunk velocity from the LMM, sagittal moment measured by the force plate were input into female Model 7a from Part 3 to determine the gain for each of the female subjects. Male lifting trial data were input into Model 1 from Part 3. Spinal loading forces in each of the three planes (i.e., lateral shear, anterior/posterior shear, and compression force) for each gender was estimated by summing the directional muscle forces determined from each of the muscles by using *Eq 2.1*, and the predicted sagittal moment was determined using *Eq 2.2*.

$$\text{Force}_j = \text{Gain} \times (\text{EMG}_t / \text{EMG}_{\max}) \times \text{Area}_j \times f(\text{Vel}) \times f(\text{Length}) \quad (\text{Eq } 2.1)$$

$$M_{x\text{-pred}} = \sum r_j \times \text{Force}_j \quad (\text{Eq } 2.2)$$

where:

Force_j = tensile force for muscle j ;

Gain = physiological muscle stress (N/cm^2);

EMG_t = integrated EMG from the lifting exertion;
 EMG_{max} = integrated EMG from MVCs;
 $Area_j$ = maximum cross-sectional area of muscle j;
 $f(Vel)$ = the muscle force-velocity modulation factor;
 $f(Length)$ = the muscle length-strength modulation factor;
 M_{x-pred} = predicted sagittal trunk moment during the lifting exertion;
 r_j = moment-arm for muscle j.

Mean and maximum lifting moments about each of the three planes were determined from measurements from the force plate.

Spinal compression tolerance limits were calculated as a function of age and gender using the following regression equations from Jager et al. (1991):

Male:

$$\text{Tolerance (kN)} = 10.53 - 0.974(\text{age/decade}) \quad \text{Eq. 4.1}$$

Female:

$$\text{Tolerance (kN)} = 7.03 - 0.591(\text{age/decade}) \quad \text{Eq. 4.2}$$

where:

Tolerance = compressive strength of the intervertebral disc in kN;
 age/decade = age of the individual in decades of life.

The predicted compression force for each trial was divided by the predicted tolerance to obtain a spinal compression tolerance ratio for each trial for each subject.

Statistical Analyses

Initially, descriptive statistics (mean and standard deviation) were generated, describing the maximum lifting moments, spinal forces, and compression tolerance ratio as a function of each of gender and the other experimental conditions. Analysis of Variance (ANOVA) procedures were used to test the significance of the spinal loading variables as a function of the experimental conditions. The statistical analysis consisted of a mixed four-way repeated measures ANOVA, with one between factor (gender) and three repeated factors (weight, asymmetry and lift condition). Trials with r^2 greater than 0.8 were included in the analyses in this section. Significant gender effects for spinal loading were examined by testing the two-way interactions between gender and the other independent variables (i.e., weight, asymmetry and lift condition). Significant differences will indicate different levels of spinal loading due to gender,

when both genders were exposed to the same external loading conditions. Tukey post-hoc procedures were used to understand the nature of these differences. Significance was indicated for the ANOVA and post-hoc procedures using a Type I error rate of $\alpha=0.05$.

Results

Descriptive results for the measured lifting moments and predicted spinal loading as a function of gender and the experimental conditions are shown in Table 4.1. The results of the ANOVA for measured moments and spinal loading are shown in Table 4.2. The weight of the load had the largest impact on spinal loading, as there were significant effects on the moment in the sagittal and coronal plane as well as the resultant moment, in addition to significant effects on shear forces in the coronal plane (lateral shear) and sagittal plane (A/P shear). Post-hoc Tukey multiple comparisons indicated that for every significant main effect, each of the three weights were significantly different from each other, with the 15 lb condition resulting in the lowest spinal loading magnitude and the 50 lb condition resulting in the highest spinal loading magnitude. The asymmetry condition for the starting lift position had a significant on the lifting moment in the sagittal and transverse plane, as well as differences in lateral shear force as a function of asymmetry. Post-hoc comparisons indicated that for each of the significant effects, the 60 degree asymmetric starting position resulted in higher lifting moment (sagittal and transverse plane) and lateral shear force than when the starting position was sagittally symmetric.

Table 4.2 Analysis of Variance results on female spinal loading as a function of the experimental conditions.

Independent Variable	Moment (Nm)				Spinal Load (N)		
	Sagittal Plane	Coronal Plane	Transverse Plane	Resultant	Lateral Shear	A/P Shear	Compression
Gender (G)	0.1013	0.2124	0.2919	0.1012	0.2717	0.6638	0.5011
Weight (W)	0.0001	0.0001	0.0005	0.0001	0.0001	0.0001	0.0001
Asymmetry (A)	0.0001	0.0001	0.0001	0.0001	0.0001	0.0001	0.0001
Lift Condition (L)	0.0001	0.0001	0.0001	0.0001	0.0049	0.0001	0.0001
G \times W	0.0814	0.3488	0.0025	0.3612	0.6446	0.7851	0.0357
G \times A	0.2482	0.0039	0.0837	0.8149	0.0766	0.0282	0.0424
G \times L	0.0002	0.0655	0.0582	0.0002	0.1724	0.1433	0.0100

The ANOVA also indicated that spinal loading differed between genders as a function of the experimental conditions (Table 4.2). Significant differences in the twisting moment resulted as a function of gender and weight of the load, where post-hoc comparisons indicated that females exhibited greater moments than males for the 30 and 50 lb condition. Gender differences in A/P shear forces were also present as a function of the asymmetry of the starting position. Post-hoc analysis found that no significant gender difference in shear force at the 60 degree starting position, however, males had significantly higher shear forces during the sagittally symmetric lifts (Figure 4.1).

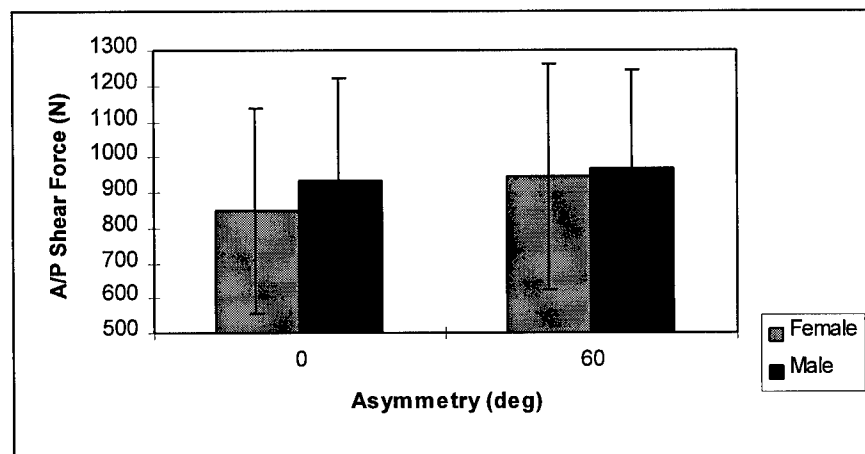


Figure 4.1 Anterior/Posterior shear force (N) on the L₅/S₁ intervertebral disc as a function of gender and asymmetry of the starting lift position.

Table 4.1 Descriptive statistics from biomechanical model results for both male and female.

Independent Variables		Moment (Nm)						Spinal Loading (N)							
		Sagittal Plane		Coronal Plane		Transverse Plane		Resultant		Lateral Shear		A/P Shear		Compression	
		Female	Male	Female	Male	Female	Male	Female	Male	Female	Male	Female	Male	Female	Male
Weight (lbs)	15	120.2 (34.8)	138.3 (37.9)	54.8 (27.8)	63.4 (26.4)	29.4 (17.6)	27.9 (17.3)	138.3 (38.5)	157.4 (39.6)	287.6 (262.6)	226.9 (206.4)	778.1 (208.1)	825.1 (185.4)	3949.2 (1210.5)	4121.9 (930.8)
	30	146.6 (39.8)	165.0 (42.1)	60.8 (26.9)	69.8 (32.1)	32.4 (18.5)	28.8 (17.2)	164.6 (42.2)	184.6 (43.9)	354.8 (313.2)	276.0 (241.0)	908.7 (283.3)	951.4 (261.3)	4838.8 (1355.2)	4995.0 (1142.2)
	50	180.0 (50.1)	198.6 (51.7)	70.7 (29.7)	75.0 (34.3)	37.9 (22.4)	28.5 (16.5)	200.1 (51.9)	217.2 (53.3)	411.3 (390.0)	344.6 (308.2)	1055.8 (388.5)	1078.0 (333.2)	5940.3 (1694.7)	6157.3 (1272.6)
Asymmetry (deg)	0	136.8 (43.3)	162.5 (50.8)	55.8 (26.5)	55.5 (24.7)	28.6 (18.4)	21.3 (13.9)	153.2 (45.6)	176.0 (48.7)	192.6 (147.9)	197.8 (139.8)	848.1 (290.8)	933.0 (286.5)	4401.7 (1320.9)	4929.4 (1300.3)
	60	153.0 (49.3)	171.1 (49.5)	66.3 (29.7)	83.3 (31.3)	36.8 (19.7)	35.6 (16.9)	173.8 (51.6)	196.0 (52.7)	498.1 (372.0)	366.4 (317.0)	943.5 (319.1)	966.5 (281.4)	5151.0 (1761.1)	5220.5 (1463.5)
Lift Condition*	F-W	138.9 (46.4)	150.5 (46.3)	59.0 (27.6)	64.1 (28.5)	34.8 (20.1)	32.5 (19.6)	157.7 (49.1)	169.9 (47.6)	337.9 (321.1)	250.4 (223.6)	794.5 (243.0)	832.9 (261.9)	4644.1 (1586.1)	4529.4 (1225.9)
	F-C	141.5 (51.4)	154.8 (49.6)	56.5 (27.4)	62.7 (27.6)	32.5 (20.0)	30.7 (19.4)	159.0 (52.7)	172.9 (50.4)	353.1 (331.5)	267.9 (226.5)	910.9 (318.4)	935.7 (272.4)	4645.8 (1667.6)	4849.7 (1341.2)
	K-W	148.6 (44.7)	177.8 (48.5)	65.0 (30.0)	74.9 (31.7)	31.9 (19.0)	25.2 (13.3)	168.1 (48.4)	197.3 (49.4)	348.6 (322.8)	288.8 (289.9)	868.7 (270.3)	956.1 (261.0)	4932.4 (1575.2)	5323.4 (1389.2)
	K-C	150.2 (44.7)	181.0 (49.6)	63.2 (28.8)	74.5 (34.8)	31.1 (18.8)	25.9 (14.3)	168.6 (47.7)	200.4 (51.8)	332.3 (306.0)	312.4 (279.2)	1012.7 (355.0)	1051.6 (295.6)	4858.3 (1546.4)	5496.7 (1383.4)

* F - W = Floor to Waist;

F - C = Floor to Chest;

K - W = Knee to Waist;

K - C = Knee to Chest.

Gender differences were also indicated for predicted compression force on the L₅/S₁ as a function of the weight of the load as well as the asymmetry of the starting lift position. Post-hoc tests revealed that males and females did not differ in compression force when lifting 15 and 30 lbs, however, lifting 50 lbs resulted in higher compression forces for males than females (Figure 4.2). Loading on the L₅/S₁ did not differ between genders when lifting from asymmetric starting positions, however, males exhibited higher compression forces when lifting from sagittally symmetric starting positions (Figure 4.3).

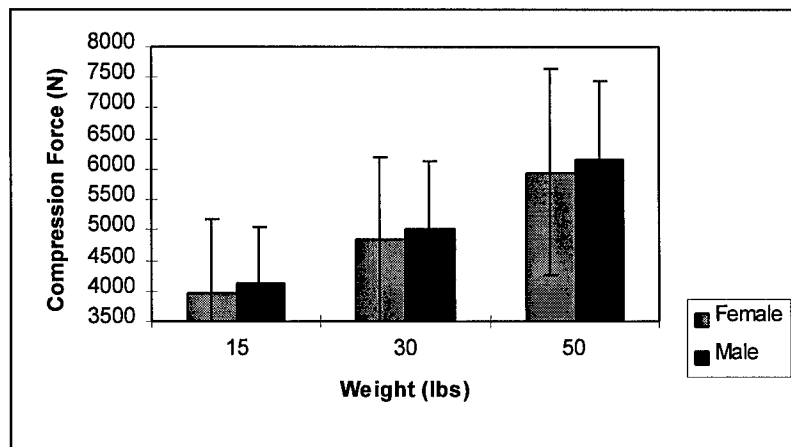


Figure 4.2 Compression force (N) on the L₅/S₁ intervertebral disc as a function of gender and weight of the load.

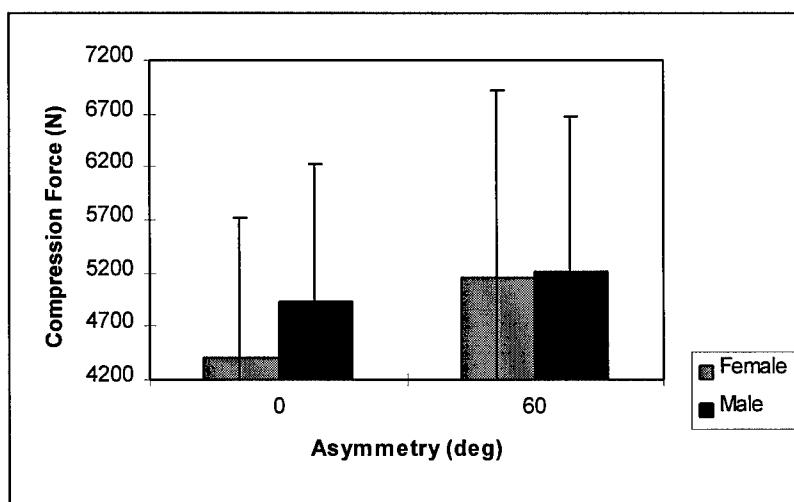


Figure 4.3 Compression force (N) on the L₅/S₁ intervertebral disc as a function of gender and asymmetry of the starting lift position.

Descriptive statistics on the spinal compression tolerance ratio as a function of gender and the experimental conditions are shown in Table 4.3. Descriptively, for every level of every experimental condition, females exhibited higher compression tolerance ratios than males.

Analysis of Variance on the spinal compression tolerance ratio (Table 4.4) indicated that gender differences were present as a function of the asymmetry of the starting lift position, and that the compression tolerance ratio differed as a function of the weight of the load, independent of gender. Tukey post-hoc pairwise comparisons indicated that the tolerance ratios were all significantly different at all three weights, with the tolerance ratio at 50 lbs greater than the tolerance ratio at 30 lbs, and the tolerance at 30 lbs greater than that at 15 lbs. Females exhibited a greater tolerance ratio than males at both levels of asymmetry (0 deg and 60 deg starting position), however, the difference was greater at the 60 degree position than the 0 degree asymmetry position (Figure 4.4).

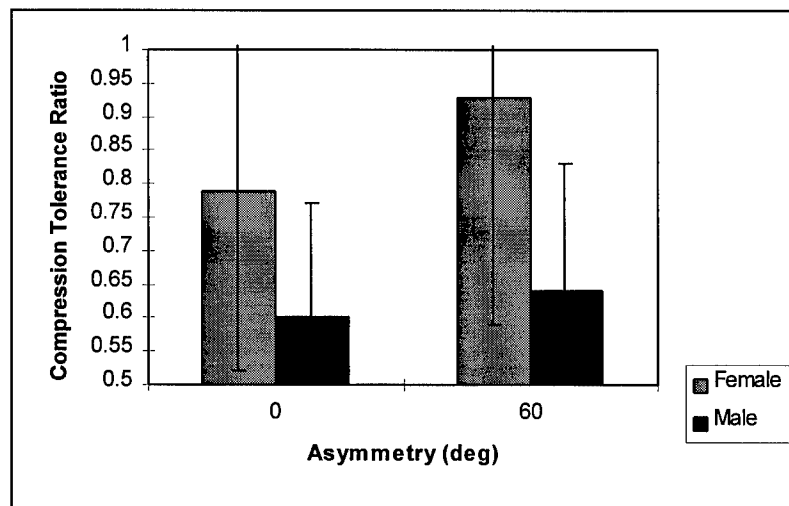


Figure 4.4 Compression tolerance ratio for the L_5/S_1 intervertebral disc as a function of gender and asymmetry of the starting lift position.

Table 4.3 Compression tolerance ratio for females and males. Ratio's were determined by dividing the predicted compression force by the predicted disc tolerance using equations from Jager et al. (1991).

Independent Variables		Compression Tolerance Ratio	
		Female	Male
Weight (lbs)	15	0.71 (0.25)	0.50 (0.13)
	30	0.87 (0.28)	0.61 (0.15)
	50	1.07 (0.34)	0.75 (0.17)
Asymmetry (deg)	0	0.79 (0.27)	0.60 (0.17)
	60	0.93 (0.34)	0.64 (0.19)
Lift Condition	F-W	0.84 (0.32)	0.55 (0.16)
	F-C	0.84 (0.33)	0.60 (0.18)
	K-W	0.89 (0.31)	0.65 (0.18)
	K-C	0.87 (0.30)	0.67 (0.18)

Table 4.4 Analysis of Variance results on Spinal Compression Tolerance Ratio for males and females.

Independent Variable	Compression Tolerance Ratio
Gender (G)	0.0004
Weight (W)	0.0001
Asymmetry (A)	0.0001
Lift Condition (L)	0.0001
G × W	0.3222
G × A	0.0051
G × L	0.2454

The ANOVA on spinal loading indicated that the lift condition (i.e., floor to waist, floor to chest, knee to waist, knee to chest) had a significant effect on several measures of spinal

loading (Table 4.2) as well as the compression tolerance ratio (Table 4.4). This significant difference was independent of gender, and also occurred as a function of gender, depending on the dependent variable. Differences independent of gender include the generated lifting moment in the coronal and transverse plane, as well as the resultant moment and A/P shear force on the L_5/S_1 (Table 4.1). Tukey post-hoc tests found that the lifts starting near the knee resulted in greater moments in the coronal plane, whereas lifts starting near the floor resulted in greater moments in the transverse plane than those starting near the knee. Post-hoc tests for the effect of lift condition on A/P shear force found that resulting A/P shear force when starting at the knee and lifting to the chest was significantly greater than the A/P shear force from the other three conditions, with lifting from the floor to the waist resulting in the least A/P shear force.

Finally, the sagittal and resultant moment, and the compression force varies significantly as a function of gender and lift condition. Males exhibited greater sagittal and resultant moments than females for all lifting conditions, with larger differences occurring when lifting from the knee than when lifting from near the floor. Males also experienced larger compression forces than females when lifting from the knee than when starting lifts near the floor.

Discussion

The results presented in this Part of the study represent the first of its kind for assessment of spinal loading of females utilizing a female specific biomechanical model. Thus, there are no other datasets for which to compare the pattern of spinal loading predicted from this study.

The magnitudes of the spinal loading for females and males approached levels which may represent high risk for LBD from spinal compression. Lifting loads as low as 15 lbs resulted in compression forces of 3949 N and 4122 N for females and males, respectively. NIOSH (1981) states that above compression forces of 3400 N, microfractures in the vertebral endplates will begin to appear in some individuals. When subjects in this study lifted 50 lbs, mean maximum compression forces were 5940 N and 6157 N for females and males, respectively. NIOSH has estimated that at compression forces above 6400 N, most individuals will start to have microfractures of the vertebral endplates. Thus, the compression levels predicted from lifting these weights indicates that there would be an elevated level of risk of damage to the endplates. Most interesting about these results is the lack of a gender difference in compression force when

lifting 15 and 30 lbs. Males did, however, experience significantly higher compression forces when lifting 50 lbs (6157 N vs 5940 N for males and females, respectively), however the magnitude of both values were quite when compared to estimates of tolerance. The comparable compression forces at most weight levels indicates that females may be at higher risk of LBD than males given the same task conditions, as they may be closer to their tolerance limit for damage to the intervertebral discs. This is also reflected in the compression tolerance ratios shown in Table 4.3. The general trend was that females experienced about 20% to 30% higher tolerance ratios depending on the weight lifted. Thus, females were closer to the tolerance limit than males for the same tasks.

A gender effect was also present for the prediction of compression forces as a function of asymmetry of the starting position of the lift. As shown in Figure 4.3, females exhibited significantly less compression force than males for sagittally symmetric lifts (4402 N vs. 4929 N for females and males, respectively). However, lifting from an asymmetric position (60 degrees asymmetry), there was no difference in compression force between females and males (5151 N vs 5221 N for females and males, respectively). Thus, while females may already be at an elevated risk for LBD when exposed to similar loads to males, they also exhibit a disproportionate increase in compression force when compared to males when going from sagittally symmetric lifts to asymmetric lifts. This increase in risk of injury is also reflected when comparing the compression tolerance ratios as a function of gender and asymmetry (Figure 4.4). Females exhibited a greater tolerance ratio at both levels of asymmetry, however, they also experienced a larger increase than males when going from sagittally symmetric lifts to asymmetric lifting.

For both lateral and A/P shear force, the females had similar loads as the males with only minor differences resulting in the sagittally symmetric conditions. A difference of about 90 N was found during the sagittally symmetric lifts. However, no difference was found between the genders during the asymmetric lifts. Thus, the shear forces would increase the risk of LBD for females as compared to males.

As expected, lateral and A/P shear forces were significantly effected by the other experimental conditions. The asymmetric lifts had significantly more higher spine loads than the sagittally symmetric lifts. Also, a increase in weight corresponded to increases in spinal loads

for both males and females. It would appear that lifting from the floor would be less risky. However, the trunk moments were also lower, indicating that the subjects lifted differently during these conditions, thus, explaining why the difference exists. Further evaluation of these conditions is needed to determine the nature of the difference.

Conclusions

This part of the study provides the results from the first of its kind assessment of spinal loading of females utilizing a female specific biomechanical model. Females were found to be at an elevated risk for LBD when exposed to similar loads to males when considering compression force. The only difference found between the genders for the shear forces (A/P shear) was during the sagittally symmetric conditions. While these results provide some indication of the risk of LBD for females during various lifting conditions, these results should be considered to be preliminary. The current results are based on 35 female subjects and 17 male subjects with the remaining subjects being collected in a timely manner. Although the results are preliminary, there is no reason to expect that the few remaining subjects to be collected would alter the general results found in this part of the study.

REFERENCES

1. Adams, M.A. and Hutton, W.C., (1983), The effect of fatigue on the lumbar intervertebral disc, *J. Bone Joint Surg*, 65-B, 199-203.
2. Adams, M.A., McNally, D.S., Wagstaff, J., and Goodship, A.E., (1993), Abnormal stress concentration in lumbar intervertebral discs following damage to the vertebral bodies: A cause of disc failure? *European Spine Journal*, 1, 214-221.
3. Adams, M.A., Green, T.P. and Dolan, P., (1994), The strength in anterior bending of lumbar intervertebral discs, *Spine*, 19, 2197-2203.
4. Army Safety Center Annual Report (1992).
5. Army Times, Aug. 8, 1994, 13-15.
6. Bigland, B. and Lippold, O.C.L., (1954), The relation between force, velocity and integrated electrical activity in human muscle, *J. Physiology*, 123, 214-224.
7. Chaffin, D.B., Redfern, M.S., Erig, M. and Goldstein, S.A., (1990), Lumbar muscle size and locations from CT scans of 96 women of age 40 to 63 years, *Clin. Biomech.*, Vol. 5, 9-16.
8. Cooper, R.D., Hollis, S. and Jayson, M.I.V., (1992), Gender variation of human spinal and paraspinal structures, *Clin Biomech*, 7, 120-124.
9. Davis, K.G., Marras, W.S. and Waters, T.R., (1998), Evaluation of the spinal loading during lowering and lifting, *Clinical Biomechanics*, 13, 141-152.
10. Fathallah, F.A., Marras, W.S., Parnianpour, M. and Granata, K.P., (1997), A method for measuring external spine loads during unconstrained free-dynamic lifting, *J. Biomechanics*, 30, 975-978.
11. Granata, K.P., (1993), An EMG-assisted model of biomechanical trunk loading during free-dynamic lifting, *Unpublished Ph.D. Dissertation*, The Ohio State University, Columbus, OH.
12. Granata, K.P. and Marras, W.S., (1993), An EMG-assisted model of loads on the lumbar spine during asymmetric trunk extensions, *J. Biomechanics*, 26, 1429-1438.
13. Granata, K.P. and Marras, W.S., (1995), An EMG-assisted model of trunk loading during free-dynamic lifting, *J. Biomechanics*, 28, 1309-1317.
14. Granata, K.P., Marras, W.S. and Fathallah, F.A., (1995), A method for measuring external trunk loads during dynamic lifting exertions, *J. Biomechanics*, 29, 1219-1222.
15. Hill, A.V., (1938), The head of shortening and the dynamic constants of muscle, *Proceedings of the Royal Society of Biology*, 126, 136-195.
16. Jager, M., Luttmann, A. and Laurig, W., (1991), Lumbar load during one-handed bricklaying, *Int J Ind Ergon*, 8, 261-277.
17. Jones B.H., Bovee, M.W., Harris, J.M. and Cowan, D.N., (1988), Intrinsic risk factors for exercise-related injuries among male and female Army trainees, *Am. J. Sports Med.*, 21(5), 705-710.
18. Kirking, B.C., (1997), An assessment of muscle, passive, and connective tissue forces acting at L₅/S₁, during lifting, *Unpublished Masters Thesis*, The Ohio State University, Columbus, OH.

19. Komi, P.M., (1973), Measurement of the force-velocity relationship in human muscle under concentric and eccentric contractions, *Medicine and Sport*, 8, 224-229.
20. Kumar, S., (1988) Moment arms of spinal musculature determined from CT scans, *Clin. Biomech.*, Vol. 3, 137-144.
21. Marras, W.S. and Sommerich, C.M., (1991a), A three-dimensional motion model of loads on the lumbar spine: I. Model structure, *Human Factors*, 33, 123-137.
22. Marras, W.S. and Sommerich, C.M., (1991b), A three-dimensional motion model of loads on the lumbar spine: II. Model validation, *Human Factors*, 33, 139-149.
23. Marras, W.S., Fathallah, F.A., Miller, R.J., Davis, S.W. and Mirka, G.A., (1992), Accuracy of a three-dimensional lumbar motion monitor for recording dynamic trunk motion characteristics, *Int J Ind Erg*, 9, 75-87.
24. Marras, W.S., Lavender, S.A., Leurgans, S.E., Rajulu, S.L., Allread, W.G., Fathallah, F.A. and Ferguson, S.A., (1993), The role of dynamic three-dimensional trunk motion in occupationally-related low back disorders, *Spine*, 18, 617-628.
25. Marras, W.S., Lavendar, S.A., Leurgans, S.E., Fathallah, F.A., Ferguson, S.A., Allread, W.G., and Rajulu, S.L., (1995), Biomechanical risk factors for occupationally related low back disorders, *Ergonomics*, 38, 337-410.
26. Marras, W.S. and Granata, K.P., (1995), A biomechanical assessment and model of axial twisting in the thoracolumbar spine, *Spine*, 20, 1440-1451.
27. Marras, W.S. and Granata, K.P., (1997a), Spine loading during trunk lateral bending motions, *J. Biomechanics*, 30, 697-703.
28. Marras, W.S. and Granata, K.P., (1997b), The development of an EMG-Assisted model to assess spine loading during whole-body free-dynamic lifting, *J Electromyogr Kinesiol*, 4, 259-268.
29. McGill, S.M. and Norman, R.W., (1986), Partitioning of the L₄/L₅ dynamic moment into disc, ligamentous, and muscular components during lifting, *Spine*, 11, 666-678.
30. McGill, S.M., Patt, N. and Norman, R.W., (1988), Measurements of the trunk musculature of active males using CT scan radiography: Implications for force and moment generating capacity about the L4/L5 joint, *J. Biomechanics*, 21(4), 329-341.
31. McGill, S.M., Santiguada, L. and Stevens, J., (1993), Measurement of the trunk musculature from T5 to L5 using MRI scans of 15 young males corrected for muscle fiber orientation, *Clin. Biomech.*, Vol. 8, 171-178.
32. McGill, S.M. The biomechanics of low back injury: Implications on current practice in industry and the clinic. *J Biomech* 1997; 30:465-475.
33. Mirka, G.A. and Marras, W.S., (1993), A stochastic model of trunk muscle coactivation during trunk bending, *Spine*, 18, 1396-1409.
34. National Institute for Occupational Safety and Health, (1981), *Work Practices Guide for Manual Lifting*, NIOSH Technical Report DHHS(NIOSH) Publication No. 81-122.
35. Neter, J., Wasserman, W., and Kutner, M.H., (1985), Applied Linear Statistical Models, 2nd Edition, Richard D. Irwin, Inc., Homewood IL.
36. Pheasant, S., (1988), Bodyspace: Anthropometry, Ergonomics and Design, Taylor & Francis, N.Y.

37. Raschke, U. and Chaffin, D.B., (1996), Support for a linear length-tension relation of the torso extensor muscles: an investigation of the length and velocity EMG-force relationships, *J. Biomechanics*, 29, 1597-1604.
38. Reid, J.G. and Costigan, P.A., (1987), Trunk muscle balance and muscular force, *Spine*, 12, 783-786.
39. Sharp, M.A. and Vogel, J.A., (1992), Maximal lifting strength in military personnel, *Adv. Ind. Ergon. Safety IV*, Proceedings of the Annual Int'l. Ind. Ergon. Safety Conference, Denver CO., S. Kumar ed., Taylor & Francis, Washington, D.C.
40. Sharp, M.A. (1994), Physical fitness, physical training and occupational performance of men and women in the U.S. Army: A review of literature, *U.S. Army Research Institute of Environmental Medicine*, Natick, MA.
41. Tischauer, E.R., (1978), The Biomechanical Basis of Ergonomics: Anatomy Applied to the Design of Work Situations, John Wiley & Sons, N.Y.
42. Weis-Fogh, T. and Alexander, R.M., (1977), The sustained power output from striated muscle. *Scale Effects in Animal Locomotion*, pp. 511-525. Academic Press, London.
43. Wilkie, D.R., (1950), The relation between force and velocity in human muscle, *J. Physiology*, 110, 249-280.



DEPARTMENT OF THE ARMY
US ARMY MEDICAL RESEARCH AND MATERIEL COMMAND
504 SCOTT STREET
FORT DETRICK, MARYLAND 21702-5012

REPLY TO
ATTENTION OF:

MCMR-RMI-S (70-1y)

21 JUN 2001

MEMORANDUM FOR Administrator, Defense Technical Information
Center (DTIC-OCA), 8725 John J. Kingman Road, Fort Belvoir,
VA 22060-6218

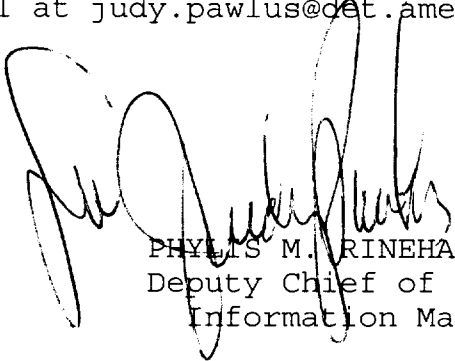
SUBJECT: Request Change in Distribution Statement

1. The U.S. Army Medical Research and Materiel Command has reexamined the need for the limitation assigned to technical reports. Request the limited distribution statement for reports on the enclosed list be changed to "Approved for public release; distribution unlimited." These reports should be released to the National Technical Information Service.

2. Point of contact for this request is Ms. Judy Pawlus at DSN 343-7322 or by e-mail at judy.pawlus@det.amedd.army.mil.

FOR THE COMMANDER:

Encl


PHYLLIS M. RINEHART
Deputy Chief of Staff for
Information Management

Reports to be changed to "Approved for public release;
distribution unlimited"

<u>Grant Number</u>	<u>Accession Document Number</u>
DAMD17-94-J-4147	ADB221256
DAMD17-93-C-3098	ADB231640
DAMD17-94-J-4203	ADB221482
DAMD17-94-J-4245	ADB219584
DAMD17-94-J-4245	ADB233368
DAMD17-94-J-4191	ADB259074
DAMD17-94-J-4191	ADB248915
DAMD17-94-J-4191	ADB235877
DAMD17-94-J-4191	ADB222463
DAMD17-94-J-4271	ADB219183
DAMD17-94-J-4271	ADB233330
DAMD17-94-J-4271	ADB246547
DAMD17-94-J-4271	ADB258564
DAMD17-94-J-4251	ADB225344
DAMD17-94-J-4251	ADB234439
DAMD17-94-J-4251	ADB248851
DAMD17-94-J-4251	ADB259028
DAMD17-94-J-4499	ADB221883
DAMD17-94-J-4499	ADB233109
DAMD17-94-J-4499	ADB247447
DAMD17-94-J-4499	ADB258779
DAMD17-94-J-4437	ADB258772
DAMD17-94-J-4437	ADB249591
DAMD17-94-J-4437	ADB233377
DAMD17-94-J-4437	ADB221789
DAMD17-96-1-6092	ADB231798
DAMD17-96-1-6092	ADB239339
DAMD17-96-1-6092	ADB253632
DAMD17-96-1-6092	ADB261420
DAMD17-95-C-5078	ADB232058
DAMD17-95-C-5078	ADB232057
DAMD17-95-C-5078	ADB242387
DAMD17-95-C-5078	ADB253038
DAMD17-95-C-5078	ADB261561
DAMD17-94-J-4433	ADB221274
DAMD17-94-J-4433	ADB236087
DAMD17-94-J-4433	ADB254499
DAMD17-94-J-4413	ADB232293
DAMD17-94-J-4413	ADB240900